UNIVERSITY OF COPENHAGEN
DEPARTMENT OF DRUG DESIGN AND PHARMACOLOGY

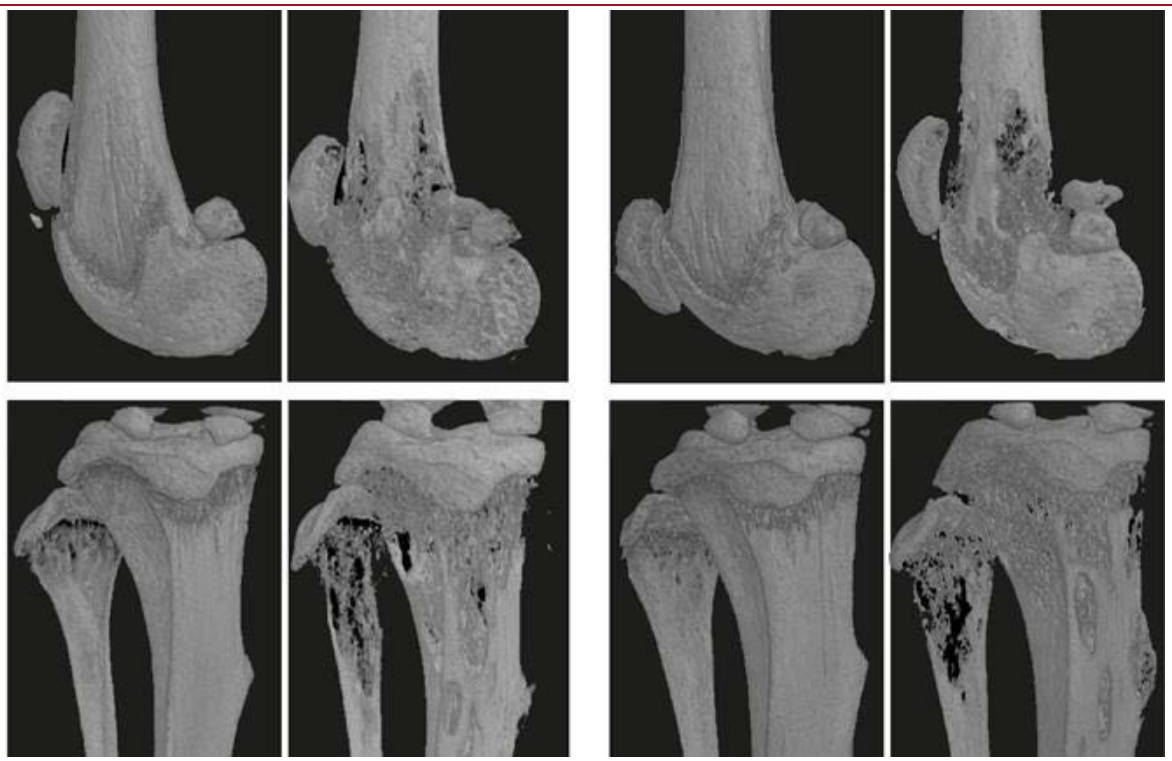

PhD Thesis

Chelsea Hopkins

Bone Pain in Fibrous Dysplasia: Nociceptive Behaviours and Mechanisms in a Preclinical Model

Bone Pain in Fibrous Dysplasia

Supervisor: Anne-Marie Heegaard, MD, PhD

This thesis has been submitted to the Graduate School of Health and Medical Sciences, University of Copenhagen on 31 December 2022.

Name of department:	Department of Drug Design and Pharmacology
Author(s):	Chelsea Hopkins (JFW664)
Title and subtitle:	Bone Pain in Fibrous Dysplasia: Nociceptive Behaviours and Mechanisms in a Preclinical Model (Bone Pain in Fibrous Dysplasia)
Topic description:	Investigation of bone pain in a murine model of fibrous dysplasia, a painful bone disorder. A translationally relevant mouse model of fibrous dysplasia was investigated to ascertain pain-like behaviour and the underlying nociceptive mechanisms. Novel pain-like behavioural tests were identified.
Supervisor:	Anne-Marie Heegaard, MD, PhD Associate Professor University of Copenhagen Denmark
Co-supervisors:	Kim Henriksen, PhD Director of Endocrinology Nordic Bioscience Denmark Paul Karila, PhD Head of Drug Discovery Cellectricon Sweden
Assessment committee:	Chairperson: Bolette Hartmann, PhD Associate Professor University of Copenhagen Denmark Reviewers: Chantal Chenu, PhD Professor Royal Veterinary College United Kingdom Christian Bjerggaard Vægter, PhD Associate Professor Aarhus University Denmark
Submitted on:	31 December 2022

Divine is the task to relieve pain.
- Hippocrates

Table of contents

Acknowledgements

I have three incredible “mothers” in my life who are responsible for getting me through my PhD studies and enriching my life. The first is Work Mom 1, my supervisor – Anne-Marie Heegaard. I cannot express my gratitude enough to Anne-Marie for choosing me for this project and supervising me so well and so thoughtfully. Approximately six months after I arrived in Denmark, the world shut down and we were forced inside for two years. It was an extremely challenging time in my life, and if I had been in any other team I wouldn’t have made it to the finish line. Anne-Marie promotes a team filled with fun, support, and kindness because she herself is bursting with those qualities. She has been there with a hug in my lowest points and cheered me on through my highest points. I have never regretted my decision in 2019 to uproot my life and move to Denmark and I will remain forever in Anne-Marie’s debt for the amazing opportunities she has given me.

Work mom 2 – Camilla Skånstrøm Dall is a warm and welcoming presence, not just in my workplace, but in my life. Camilla reminds me very much of my own mom – kind, supportive, funny, warm, and protective. Camilla was the first person who greeted me on my first day with a huge smile and radiating friendliness! She made sure that I was included in every event, took a break for lunch, and made it to Friday bar. Camilla helped me through the pandemic, welcoming me into her personal life and ensuring I had a friend when I wasn’t allowed outside to make new friends. She is the first person to help me when I need it, doing so with energy, exuberance, and brilliant ideas. My life is made richer for knowing her and I will be forever grateful for her presence.

And finally, my own mom – Megan Hopkins – the most important woman in my life! My mom has been my guiding light and supportive influence my entire life. There was never a moment where she scoffed at my dreams or said I couldn’t do something – she only asked how we could make it happen. During my early school years, my mom helped me make the most incredible school projects, in primary school and high school she would stay up until the early hours of the morning quizzing me on my work to prepare me for tests and exams. When I decided to study in Hong Kong, she made sure I had everything I needed to move there and succeed. And when I had health issues at the end of my Bachelor studies, she dropped everything to fly to Hong Kong

to support me through it – and in doing so, once again helped me study for my exams. I will be the first in my family to get a PhD and I owe it all to my mom.

I would also like to acknowledge my sister, Tiffany Hopkins, who has probably already started complaining about how far down she is on this page. My sister is probably the only person who has actually read all my work, because she has the horrid task of editing it. From removing the liberal commas I sprinkle in my work, to telling me bluntly that something makes no sense, I would like to tell her thank you, and I genuinely appreciate the help you give me! My sister is also the only person I can rant to about small inconveniences and who shares my love of dogs, dinosaurs, mugs, dogs, Doctor Who, and dogs. Thank you for helping me through this and I promise to return the favour in a few years!

I would like to thank my wonderful friends who have supported me over the last few years, but particularly Alexandra Zisser, Khaled Elhady Mohamed, Anna Odland, and Pravallika Manjappa – my PhD buddies! Also, all the other BonePainII and IVP PhD students who I am sure I will continue working with in the future.

I owe a lot to all the people I have worked with over the years: Marta Díaz del Castillo and Rie Bager Hansen (incredible mentors and teachers), Ulla Kløve Jakobsen (my problem solver), Juan Miguel Jimenez Andrade (a rockstar researcher and kind helper), Mathilde Caldara, Helena Skourup Larsen, and Natascha Synnøve Olsen (the fierce and fabulous animal technicians), and finally Cecilie Thomsen, Ida Buur Kanneworff, and Julie Benthin (my Master's student minions and friends).

I would also like to acknowledge the funding I received for my PhD studies, from the European Union's Horizon 2020 research and innovation programme under the Marie Skłodowska-Curie grant agreement No 814244.

Finally, I would like to acknowledge the 100s of mice I used in my projects. Pain is a huge problem in society, one that is not easily solved – we owe a lot of our progress in this field to them.

Summary in English

Fibrous dysplasia (FD) is a rare genetic bone disorder that commonly results in deformity, fractures, and pain. The aetiology of FD is well-characterised; it is caused by a postzygotic missense mutation in the *GNAS* gene encoding the $G\alpha_s$ subunit of G proteins, leading to accumulation of cAMP and activation of downstream pathways in bone marrow stromal cells. FD is a mosaic disorder, where lesions can develop in one or multiple bones in a highly individualistic manner. Pain is a key problem for patients, but the underlying mechanisms of pain development are unknown and treatment is often ineffective. The overall aim of this thesis is to identify a translationally relevant mouse model of FD that develops a pain-like phenotype and investigate the underlying mechanisms that contribute to this phenotype.

Manuscript 1 is a systematic review analysing and comparing different animal models of FD. The Preferred Reporting Items for Systematic Reviews and Meta-Analyses was utilised to identify animal models of FD. Seven unique causative animal models of FD were identified that expressed the causative genetic mutation of FD. These models were assessed for FD features and how closely they resembled observations in patients. Mechanistic models (no causative mutation) that developed FD-like lesions were also assessed. This review may assist researchers in identifying suitable models for their research on FD. It also facilitated the selection of a mouse model for the study conducted in Manuscript 2.

Manuscript 2 aims to identify mechanisms of FD pain in a translationally relevant mouse model of the disorder. A previously established site-specific, inducible model of FD was implemented for this study. Male and female mice with FD lesions displayed pain-related behaviours. This was indicated by decreased burrowing (recovery after ibuprofen treatment), grid hanging (partial recovery after morphine treatment), home cage activity, and wheel running. Tissue harvested from the mice demonstrated the presence of osteoclasts, immune cells, sensory nerve fibres, and increased vascularity within the FD lesion. Dorsal root ganglia demonstrated markers of nerve damage, suggesting the development of neuropathic-like pain. *In vitro* analysis demonstrated increased production of cAMP and inflammatory markers associated with painful bone diseases. In summary, the mouse model demonstrated FD development with subsequent pain-like development that suggests inflammatory and neuropathic pain components.

Manuscript 3 seeks to establish if home cage activity and wheel running in novel Digital Ventilated Cages® were affected by cancer-induced bone pain. As cancer developed, well-established pain tests – gait analysis and weight bearing – were affected, with a corresponding decline in wheel running, but not cage activity. Digital Ventilated Cages® could be a useful tool to assess spontaneous pain-like behaviour in mice, particularly wheel running. This supports the notion that the reduced wheel running described in Manuscript 2 was due to the development of pain-like behaviour.

In conclusion, a translationally relevant animal model of FD was identified and implemented. Pain-like behaviour developed, which was reversed by analgesics and underlying mechanisms corresponding to inflammatory and neuropathic pain were characterised. This model can be used to assess novel analgesic treatments for FD.

Dansk Resumé

Fibrøs dysplasi (FD) er en sjælden genetisk knoglesygdom, der ofte resulterer i deformitet, frakturer og smerte. Ætiologien af FD er velkarakteriseret, forårsaget af en postzygotisk missense-mutation i *GNAS*-genet, der koder for $G\alpha_s$, en G-protein subunit. Mutationen medfører akkumulering af cAMP og aktivering af signaleringsveje i stromale knoglemarvsceller. FD er en mosaiksygdom, hvor læsioner kan udvikles i en enkelt knogle eller flere knogler. Smerte er et stort problem for patienterne, men de mekanismer, som fører til smerterne, er ukendte, og behandlingen er ofte ineffektiv. Det overordnede formål med denne afhandling var at identificere en translationel relevant FD-musemodel, som udviklede en smertelignende fænotype, samt at undersøge de underliggende mekanismer bag denne fænotype.

Manuskript 1 havde til formål at analysere og sammenligne forskellige FD-dyremodeller i et systematisk review. The Preferred Reporting Items for Systematic Reviews and Meta-Analyses blev anvendt til at identificere FD-dyremodeller. Syv unikke FD-dyremodeller med den udløsende genetiske mutation for FD blev identificeret. Disse modeller blev vurdereret i forhold til FD-karakteristika og lighed med observationer i patienter. Mekanistiske modeller (uden udløsende mutation) med udvikling af FD-lignende læsioner blev også vurderet. Dette review kan hjælpe forskere med at identificere passende modeller til forskning i FD og faciliterede valget af musemodel til studiet udført i Manuskript 2.

Manuskript 2 havde til formål at identificere FD-smertemekanismer i en translationelt relevant FD-musemodel. En tidligere etableret inducerbar FD-model blev implementeret i dette studie. Mus af begge køn med FD-læsioner udviste smertelignende adfærd. De udviste nedsat graveadfærd (bedring efter ibuprofen behandling), nedsat evne til at hænge i gitter (delvis bedring efter morfin behandling), samt nedsat buraktivitet og løbehjulsaktivitet. Analyse af væv fra musene viste tilstedeværelse af osteoklaster, immunceller, sensoriske nervefibre og øget vaskularisering i FD-læsionerne. Dorsalrodsganglierne udtrykte markører for nerveskade, som kunne tyde på en mulig neuropatisk smerte komponent. *In vitro* analyser viste øget produktion af cAMP og inflammatoriske markører, der associeres med smertefulde knoglesygdomme. Overordnet set demonstrerede musemodellen udvikling af FD med efterfølgende udvikling af smertelignende adfærd med inflammatoriske og neuropatiske elementer.

Manuskript 3 havde til formål at undersøge om buraktivitet og løbehjulsaktivitet i ”Digitial Ventilated Cages®” (DVC®) påvirkedes af cancer-inducerede knoglesmerter (CIBP). I takt med udviklingen af CIBP, blev etablerede smertetests – analyse af gang og vægtdistribution - påvirket med en tilsvarende reduktion i løbehjulsaktivitet, men ikke buraktivitet. DVC’er®, især løbehjulsaktivitet i et kendt miljø kan være et brugbart værktøj til at vurdere spontan smertelignende adfærd i mus. Dette understøtter, at den nedsatte løbehjulsaktivitet i Manuskript 2 afspejlede smertelignende adfærd.

En translationel relevant dyremodel for FD blev identificeret og implementeret. Smertelignende adfærd, der kunne behandles med smertestillende lægemidler, udvikledes. Efterfølgende analyser af knogle- og nervevæv tyder på, at smertemekanismerne kunne involvere både af inflammatoriske og neuropatiske komponenter. Denne model kan være relevant til at undersøge nye smertestillende lægemidler til behandling af FD.

Abbreviations

ALP	Alkaline phosphatase
ANOVA	Analysis of variance
ASIC	Acid-sensing ion channels
ATF3	Activating transcription factor 3
ATP	Adenosine triphosphate
BMD	Bone mineral density
BMSC	Bone marrow stromal cell
BV/TV	Bone volume fraction
cAMP	Cyclic adenosine monophosphate
CCL	C-C motif ligand
CD68	Cluster of differentiation 68
cDNA	Complementary deoxyribonucleic acid
CGRP	Calcitonin gene-related peptide
CIBP	Cancer-induced bone pain
CNS	Central nervous system
CT	Computed tomography
CXCL	C-X-C motif chemokine
DAPI	4′,6-diamidino-2-phenylindole
DRG	Dorsal root ganglion
DVC®	Digital Ventilated Cage®
EF1α	Elongation factor 1-α
FD	Fibrous dysplasia

FGF23	Fibroblast growth factor 23
G protein	Guanine nucleotide-binding protein
GDP	Guanosine diphosphate
GFP	Green fluorescent protein
GLB1	Beta-galactosidase gene
GM-CSF	Granulocyte-macrophage colony-stimulating factor
GNAS	Guanine nucleotide-binding protein alpha subunit gene
GPCR	G protein-coupled receptor
GRO	Growth-regulated oncogene
GTP	Guanosine triphosphate
$G\alpha_s$	Alpha subunit of the guanine nucleotide-binding protein
IASP	International Association for the Study of Pain
IHC	Immunohistochemistry
IL	Interleukin
IRES	Internal ribosome entry site
KC	Keratinocyte chemoattractant
L4/L5/L6 DRG	Lumbar 4/5/6 dorsal root ganglion
Luc2	Luciferase gene
MAS	McCune-Albright syndrome
MCP-1	Monocyte chemoattractant protein-1
M-CSF	Macrophage colony-stimulating factor
MIP-1α	Macrophage inflammatory protein 1-alpha
MIP-1β	Macrophage inflammatory protein 1-beta
NF200	Neurofilament 200 kDa

NGF	Nerve growth factor
NMDAR	N-methyl-D-aspartate receptors
NSAID	Non-steroidal anti-inflammatory drugs
OA	Osteoarthritis
OPG	Osteoprotegerin
PGK	Phosphoglycerate kinase-1
PGP9.5	Protein gene product 9.5
PKA	Protein kinase A
PRISMA	Preferred Reporting Items for Systematic Reviews and Meta-Analyses
Prrx1	Paired related homeobox 1
Q227L	Glutamine to leucine mutation
R201C	Arginine to cysteine mutation
R201G	Arginine to glycine mutation
R201H	Arginine to histidine mutation
R201S	Arginine to serine mutation
RA	Rheumatoid arthritis
RANK	Receptor activator of nuclear factor kappa-B
RANKL	Receptor activator of nuclear factor kappa-B ligand
rtTA	Reverse tetracycline transactivator
SDF-1	Stromal cell-derived factor 1
Sox9	Sex-determining region Y-Box Transcription Factor 9
SYRCLE	Systematic Review Centre for Laboratory Animal Experimentation
Tb.N	Trabecular number
Tb.Sp	Trabecular spacing

Tb.Th	Trabecular thickness
TH	Tyrosine hydroxylase
TNF-α	Tumour necrosis factor alpha
TRAP	Tartrate-resistant acid phosphatase
TrkA	Tropomyosin receptor kinase A
TRPM8	Transient receptor potential cation channel subfamily M member 8
TRPV1	Transient receptor potential vanilloid subtype 1
VEGF	Vascular endothelial growth factor
Wnt	Wingless Int-1

Introduction

Fibrous Dysplasia

Fibrous dysplasia (FD) is a rare genetic bone disorder characterised by woven, fibro-osseous tissue that replaces normal bone. FD is not a hereditary disorder, but rather a mosaic disorder due to a post-zygotic mutation. This phenomenon results in FD lesions that can develop in different parts of the skeleton, affect part of or the whole bone, and affect one or more bones. As such, this can be a highly individualistic disease with different presentations and severity. FD is associated with multiple complications including deformity, disability, fractures, and pain [1, 2].

Cause

FD is caused by a missense mutation in the guanine nucleotide-binding protein alpha subunit gene (*GNAS*) located on chromosome 20q13.3 [2]. This change occurs in position 201 on exon 8 of the gene where the codon for arginine is substituted for a cysteine or histidine codon (95% of cases); as such, the mutation is denoted as R201C or R201H, respectively. Rarely, other mutations will occur such as arginine replaced with serine (R201S) or arginine replaced with glycine (R201G) in exon 8, or glutamine to leucine (Q227L) in exon 9 [3, 4]. There is currently no evidence that different mutations result in different FD phenotypes.

Although FD is a genetic disorder, it is mosaic rather than hereditary. If a spontaneous postzygotic mutation occurs in one cell, then all cells in that lineage will carry the mutation (Figure 1.1) [2].

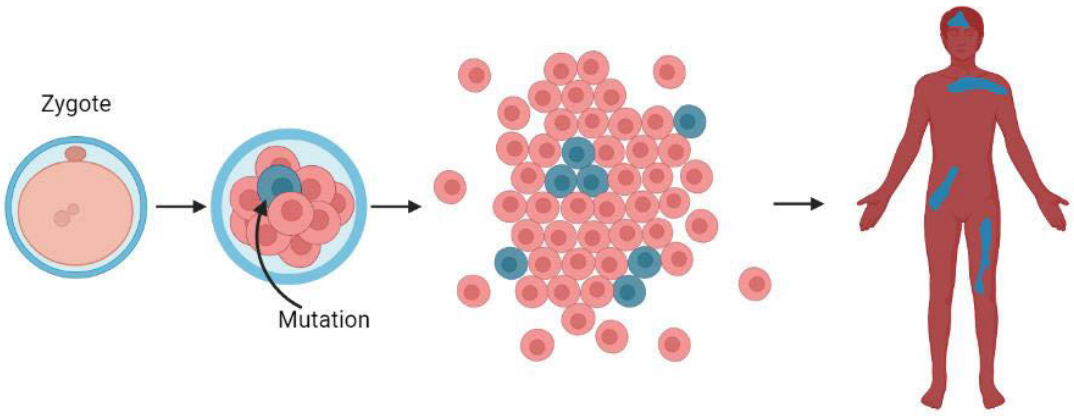

Figure 1.1 Mosaic mutation and phenotype development (created in BioRender).

Mosaicism is essential to FD development. Happle was the first to postulate this in 1986 [5], describing how cells carrying the mutation can only survive when mixed with normal cells (i.e. those not carrying the genetic mutation). This has since been confirmed in *in vivo* studies where a colony of pure FD cells was transplanted into a mouse and failed to develop, whereas a mixture of FD cells and normal cells formed a lesion in the implanted graft [6]. *In vivo* studies have also demonstrated that activating the *GNAS* mutation in early embryonic stem cells is lethal [7]. However, when the mutation is expressed in committed somatic cells it does not produce an FD phenotype, but rather a hyperostotic phenotype [8]. As such, Riminucci et al. [9] have characterised FD as a stem cell disease, where expression of the mutated gene is necessary in stromal stem cells and within a mixture of normal cells.

GNAS encodes the gene for the alpha subunit ($G\alpha_s$) of the guanine nucleotide-binding protein (G protein). G proteins are important protein units that facilitate extracellular signalling within the cell through G protein-coupled receptors (GPCRs). G proteins comprise an alpha, beta, and gamma subunit; in an inactive state they are bound together on a GPCR with guanosine diphosphate (GDP) attached to $G\alpha_s$ (Figure 1.2A). When an extracellular ligand binds to the GPCR, GDP is replaced by guanosine triphosphate (GTP) and $G\alpha_s$ separates from the other subunits, thus turning it into an active state. In a normal cell (no $G\alpha_s$ mutation), $G\alpha_s$ will bind to adenylyl cyclase, which catalyses adenosine triphosphate (ATP) to cyclic adenosine monophosphate (cAMP) and a diphosphate (Figure 1.2B). At this stage, GTP is exchanged for GDP and $G\alpha_s$ will bind to the beta and gamma subunits on a GPCR until another ligand binds [10-12]. However, in FD, the causative mutations prevent $G\alpha_s$ from binding back to the beta and gamma subunits and therefore $G\alpha_s$ remains in a constitutively active state. In this state it will continue to facilitate adenylyl cyclase activity and cAMP will accumulate in the cell (Figure 1.2C) [2, 13].

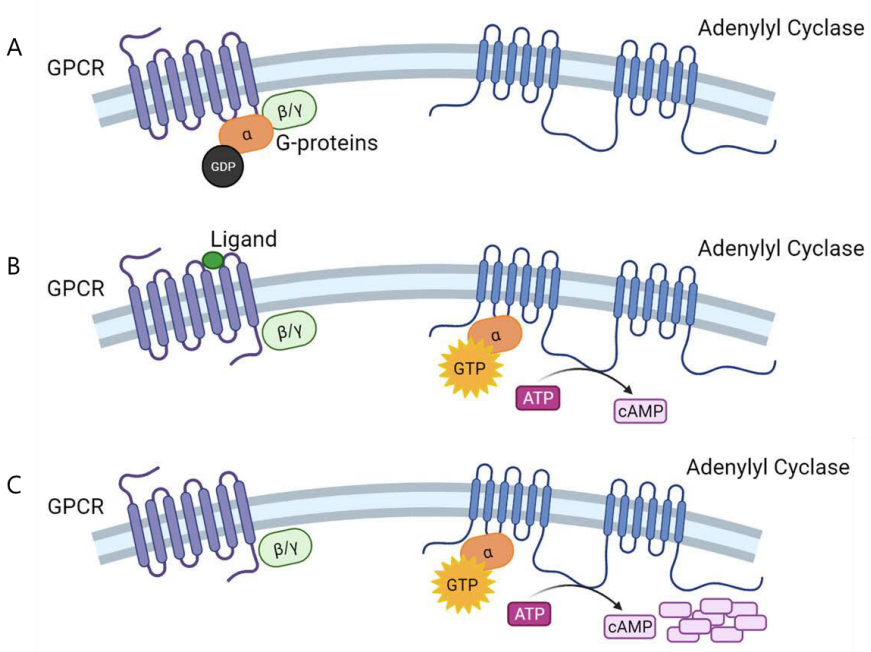

Figure 1.2 GPCR activity in an A) inactive state, B) active state in normal cells, and C) constitutively active state in FD (created in BioRender).

cAMP is a universal secondary messenger that promotes many downstream pathways and mechanisms. Protein kinase A (PKA) is considered to play a significant role in FD as a downstream mechanism of cAMP. cAMP phosphorylates PKA, facilitating phosphorylation (and activation) of further downstream mechanisms [14]. Several animal models have also demonstrated that increased expression of PKA led to FD-like lesions in mice, supporting the notion that the $G\alpha_s$/AC/cAMP/PKA pathway plays a role in FD development [15-20]. However, the exact downstream pathways that lead to the observed FD pathology have yet to be elucidated.

Epidemiology

It is difficult to determine the prevalence of FD due to 1) its rarity, 2) asymptomatic patients, and 3) diagnostic difficulty. However, studies have estimated the prevalence to be approximately 1 in 30,000 [21]. Recent questionnaire studies conducted on adult FD patients revealed that the respondents were predominantly female (60.6-82.3%; some studies may be due to more females responding [22, 23]) [21-25], although previous publications have stated that sex distribution is equal [26, 27].

Due to mosaicism, FD may present as monostotic (affecting one bone), polyostotic (affecting more than one bone), or panostotic (affecting the whole skeleton). Studies typically report that monostotic FD is most common; however, individuals identified with one lesion may not be fully assessed to identify more lesions or endocrine diseases (information about McCune-Albright syndrome below), so that monostotic FD may be overdiagnosed [2]. Nevertheless, larger cohort studies have enrolled FD patients with a diagnosis of monostotic FD (34.5-76%) and polyostotic FD (20-45.8%; including panostotic) [2, 21, 23, 28].

FD lesions begin to appear at a young age, with craniofacial lesions most likely detected at a younger age than those in the axial skeleton or extremities. Most lesions will be established by 15 years old and it is less likely for new lesions to form after this age; however, it is not uncommon for FD lesions to be identified in adulthood. As such, bone lesions tend to form and become progressively worse earlier in life, but in later life (approximately late teens to early twenties) disease progression plateaus [25].

Pathology and Symptoms

Clinical features of FD include deformity, fractures, pain, and a loss of vision (craniofacial FD affecting the optic canal), hearing (craniofacial FD affecting the temporal bone), or ambulation. These features may present in combination, although patients could be asymptomatic. However, before patients can be diagnosed with FD, it is necessary to perform a differential diagnosis to eliminate other disorders [29]. Radiological imaging is standard practice to diagnose FD due to the characteristic ground-glass appearance of lesions (Figure 1.3, Reuse permission obtained – Appendix 1) [2, 29].

Radiological images may also provide information about deformities, fractures, expansile lytic lesions (i.e. bone expansion with bone mineral loss), and other asymptomatic lesions. Many diagnosed cases of monostotic FD are incidentally discovered through non-related radiographic imaging [29, 30].

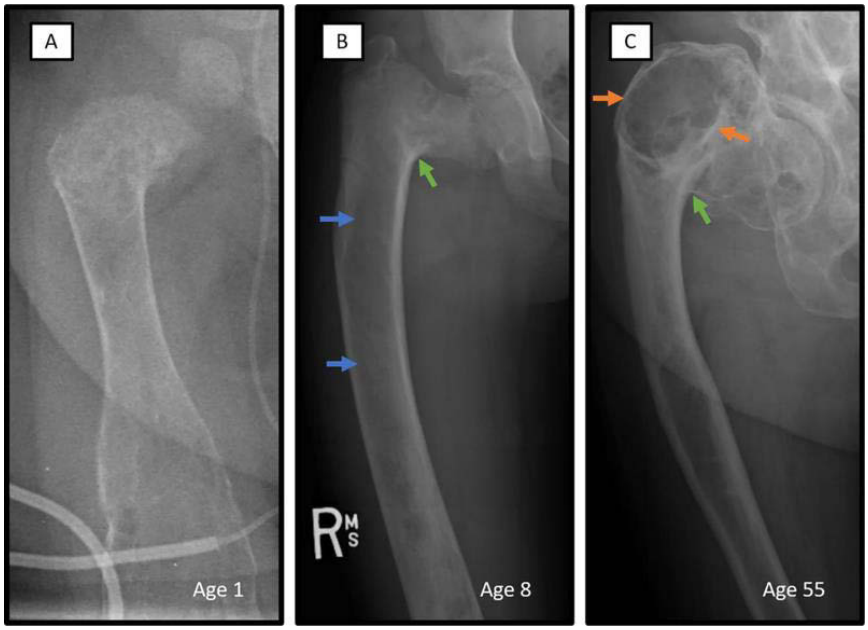

Figure 1.3 Common x-ray features of FD lesions in the right femur at age 1, 8, and 55. A) Radiograph of infant with FD, B) Child with an FD lesion demonstrating typical ground glass appearance (blue arrows) and deformity (green arrow), C) Sclerotic appearance (orange arrow) of FD lesion in an adult. Reused from Hartley et al. with permission [2].

Computed tomography (CT) scans, magnetic resonance imaging, and fluorine 18-fluorodeoxyglucose positron emission tomography/CT scans can be used to diagnose FD, particularly for differential diagnoses. A bone biopsy of the lesion for histological and genetic testing is rarely conducted, but may be done in challenging cases to confirm the diagnosis [29, 31, 32].

The histopathology of FD is unique. Normal bone structure (see below) is replaced with the characteristic woven fibro-osseous tissue – fibrous tissue interspersed with calcified regions (Figure 1.4, Reuse permission obtained – Appendix 1). Osteoblasts and osteocytes become abnormally shaped with a stellate appearance, and an increased number of osteoclasts develop at the surface of the osseous areas [2]. Sharpey's fibres (collagen fibre bundles) may also be present. Bone samples can be stained for tartrate-resistant acid phosphatase (TRAP; osteoclast staining), alkaline phosphatase (ALP), and receptor activator of nuclear factor kappa-B ligand (RANKL; bone turnover marker) [2, 29, 33].

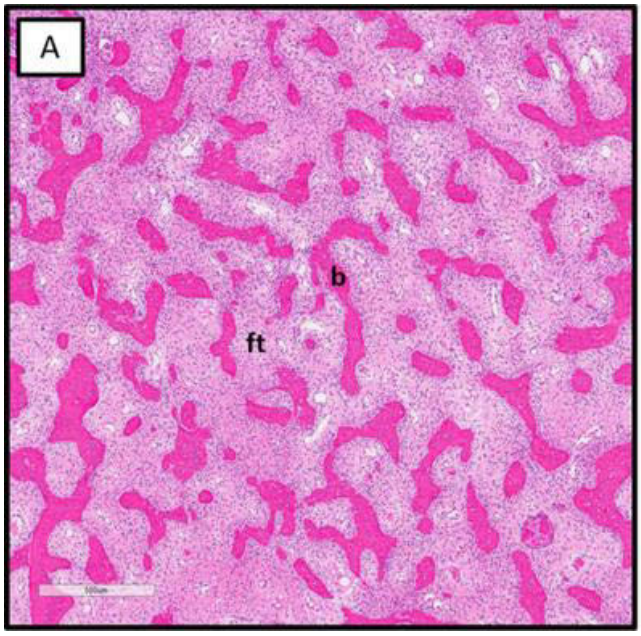

Figure 1.4 Haematoxylin and eosin staining of FD bone demonstrating the histological pathology. (b: bone, osseous tissue; ft: fibrous tissue). Reused from Hartley et al. with permission [2].

Finally, patients are recommended to undergo blood tests for renal phosphate wasting (fibroblast growth factor 23 (FGF23)), which can indicate the severity of FD [34, 35], as well as tests for ALP (bone turnover marker), procollagen type I N-terminal propeptide, and C-terminal telopeptide. Other bone turnover biomarkers may also be assessed – in particular, RANKL and bound RANKL/osteoprotegerin (OPG) [29, 35].

Pain

Kelly et al. [24] demonstrated that 81% of adults and 49% of children reported pain, with adults reporting more severe pain than children – significantly more so when lesions occurred in the lower extremity or spine. Of FD patients asked to complete a survey regarding their pain, 46% of respondents reported FD-associated pain [28]. Additionally, previous studies found that pain was more prevalent and more severe in patients with polyostotic FD than monostotic FD [23, 28].

FD is a physically disabling condition, with bodily pain significantly worse in FD patients (adults and children) than the general population, but it is not known how pain contributes to disability. FD-related physical disability is similar to that reported in cancer-affected bone, osteoarthritis (OA), and rheumatoid arthritis (RA) [22].

A recent study involving patients responding to a questionnaire on their pain demonstrated that 45.4% and 31.3% of patients reported features of nociceptive and neuropathic-like pain, respectively (pain types detailed below). Patients exhibiting neuropathic-like pain scored higher in pain severity and tended to be women. Furthermore, patients with higher pain severity reported significantly poorer mental health, general health, and sleep scores than those with lower pain severity [23].

There is currently no research that demonstrates the cause of FD pain and – despite the impact on physical disability, mental health, general health, and sleep – FD pain treatment is often ineffective [24]. Non-steroidal anti-inflammatory drugs (NSAIDs) were used in a majority of FD patients (57%), but their efficacy at producing pain relief was 56%. Opioids and bisphosphonates (anti-resorptive agent, not classified as an analgesic) were used in 26% of patients with 47% and 73% of these patients experiencing pain relief, respectively. Previous publications have speculated that bone remodelling, the possible presence of sensory nerve fibres, and increased interleukin-6 (IL-6) contribute to FD pain, but there are currently no published studies to demonstrate this [36, 37].

Experts within the FD field have developed a treatment plan for FD pain management that suggests beginning with physiotherapy and analgesics (first NSAIDs, progressing to opioids if necessary) and progressing to intravenous bisphosphonates if initial treatment fails. Surgery is considered a last resort [29].

At present, there is little information on FD pain that can be used to further benefit patient care. Studies on FD pain are primarily on cohort studies relying on questionnaire feedback. As such, there is little information on effective pain management in FD and the information on the fundamental cause of pain has not been elucidated. Further research on this aspect of FD is essential.

Treatment

FD treatment is challenging, as it is difficult to treat multiple lesions without treatment affecting normal skeletal regions. There is no standard treatment or cure for FD, with current treatment guidelines established by expert clinicians [29]. FD is a highly individualistic disorder, so it is necessary to develop personalised treatments.

In general, patients are advised to alter lifestyle factors such as diet and exercise, as well as limit smoking and alcohol intake. Patients may also be advised to undergo physiotherapy to maintain mobility and reduce pain. Patients with hypophosphatemia should be prescribed vitamin D supplements and should have regular follow-ups with their physician. For patients with McCune-Albright syndrome (see below), endocrinopathy management may be necessary alongside regular tests for gastrointestinal complications, malignancies, and medication side effects [29, 38-40]. Surgery may be considered to debride FD tissue and correct deformities. Craniofacial FD requires unique care and surgical correction to prevent deformity, vision and hearing loss, and dental problems [29]. Recent studies have indicated that denosumab, an anti-RANKL treatment, may effectively reduce osteoclast function and bone turnover, but increase the risk of hypercalcaemia after cessation [33]. In short: FD treatment requires specialised care and constant monitoring to reduce symptoms.

Fibrous Dysplasia/McCune-Albright Syndrome

As mentioned previously, endocrinopathies may accompany FD and when this occurs it is called McCune-Albright syndrome (MAS). MAS is defined either as FD combined with one or more extracellular features (FD/MAS) OR two or more extraskeletal features without FD (MAS). Mazabraud Syndrome is related to MAS and is defined as intramuscular myxomas (connective tissue within muscle) with FD. Extracellular features include skin hyperpigmentation and endocrinopathy (e.g. sex hormone dysregulation, precocious puberty, thyroid lesions, increased growth hormone, increased cortisol). The same genetic mutation responsible for FD occurs in epithelial and endocrine tissues to generate these extraskeletal features [1, 29]. FD is commonly addressed separately as it can occur without MAS, but the effect of hormones on bone homeostasis and bone pain cannot be ignored.

There are no studies that investigate the effect of MAS endocrinopathies on FD. However, inferences from studies on the effect of hormones on bone homeostasis may be useful. Bone mass is acquired during puberty and the increase in bone mineral density (BMD) at this stage is important for future bone health [41, 42]. MAS may result in precocious puberty, which can be treated with gonadotropin-releasing hormone agonists [29]. However, this treatment may significantly affect bone mineral acquisition during puberty and affect skeletal development. FD is characterised by reduced BMD and – coupled with treatment that further reduces BMD – could theoretically exacerbate FD development [43]. MAS affecting the thyroid commonly

results in hyperthyroidism, which is highly correlated with osteoporosis and is associated with higher bone turnover, lower BMD, and increased risk of fracture [44, 45]. Due to the aforementioned nature of FD, hyperthyroidism in an FD/MAS patient may exacerbate FD lesion development. FD/MAS patients may also develop acromegaly due to increased growth hormone [46]. Growth hormone also affects bone development, and studies on acromegaly demonstrate changes that may occur. Although there is more bone growth, bones may become fragile, which could be attributed to increased cortical and decreased trabecular BMD [47]. There is currently no information on how these bone changes influence FD development. In addition, acromegaly can be painful, which may be difficult to discern from FD-related pain and treatment for either may vary [48]. However, there are no studies to confirm this. Finally, hypercortisolism can occur in FD/MAS and this endocrinopathy is the cause of Cushing's syndrome. Cortisol also affects bone homeostasis by increasing bone resorption, increasing osteocyte and osteoblast apoptosis, and reducing BMD [49, 50]. Ultimately, this may further exacerbate FD development if both are present.

Endocrinopathies of MAS have been shown to influence bone health and homeostasis in other diseases; thus it can be assumed that endocrinopathies of FD/MAS should be considered when assessing FD both alone and in combination with endocrinopathies.

Animal Models

Animal models of FD are an invaluable tool in the study of FD mechanisms and treatment options. Given the rarity of the disease, it is difficult to establish large patient cohorts, obtain tissue samples, or develop tissue banks. This is made more challenging by mosaicism, which creates an individualistic phenotype in patients. However, animal models provide an opportunity to develop large sample sizes in a homogenous model that can be used to study mechanisms in many tissues and test novel treatments. Despite being a rare disease, several animal models of FD have been developed, these models have been thoroughly described and compared in Section 1.

Animal models of disease are commonly judged by their validity: face validity, predictive validity, construct (target) validity. Face validity refers to the similarity of symptoms observed in the animal model compared to that in human patients. In animal models of FD, ground glass appearance in x-ray images, deformity, increase in ALP, etc. would all signify good face

validity. Additionally, features such as time of onset may also describe face validity in a model [51, 52]. Predictive validity refers to how closely an animal model is able to mimic the action of a treatment in patients. Predictive validity has been demonstrated in two models of FD, demonstrating the efficacy of anti-RANKL in halting FD progression [33, 53-55]. This is an important feature of a model in order to assess treatment efficacy and safety before applying it to humans [51]. Construct validity (or target validity) refers to how closely the cause of the disease in humans is mimicked *in vivo* [51]. In FD, the cause is well-established and has been suitably reproduced *in vivo* [7, 52, 56-59]. For different studies, one type of validity may be more important than another. For example, if the role of the study is to further elucidate the causative and downstream mechanisms of FD, a model with high construct validity with human gene insert may be favourable [52, 58]. However, if the study concerns testing a novel treatment, the use of models that have already demonstrated good predictive validity would be more favourable [54-56, 58].

Bone

Bone Homeostasis

Bone is a highly complex tissue with a specific hierarchical structure and function. Bones are made up of dense cortical bone that encapsulates trabecular bone, and bone marrow. Surrounding the bone is a thin tissue layer – the periosteum (Figure 1.5) [60, 61].

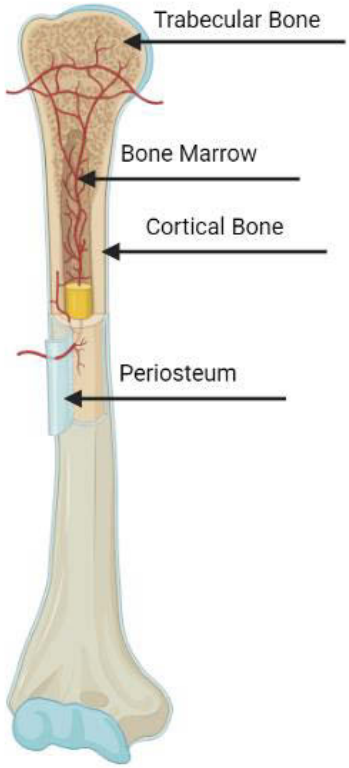

Figure 1.5 Healthy bone structure with primary bone regions (created in BioRender).

Cortical bone is dense and makes up approximately 80% of total bone mass. This tissue carries mechanical load and force for muscles and is therefore very strong and highly mineralised. Mature osteocytes are embedded in lacunae within the cortical bone. Osteocytes have thin cytoplasmic extensions through canaliculi, allowing cells to communicate with one another [60, 62, 63]. Thus, osteocytes can regulate the function of osteoblasts and osteoclasts to alter bone remodelling and release regulators such as FGF23 to regulate phosphate (see above). Osteocytes respond to mechanical and biochemical factors to regulate activity [64].

Trabecular bone makes up approximately 20% of total bone mass, but encompasses a greater volume than cortical bone due to its high porosity. Trabecular bone is made up of trabeculae, which are small, mineralised, interconnected rods that form the sponge-like structure. Porosity facilitates easy fluid exchange in the bone marrow and aids in transporting waste and nutrients within the bone. Although cortical bone is the primary strength structure, trabecular bone provides support to the cortical bone [60, 62, 63]. Trabecular degradation occurs in osteoporosis, making the bone more fragile, and increases the risk of fracture [60, 65].

The mineral micro-structure of FD can be quantified through micro-CT analysis. Different measures of the bone micro-architecture can provide information on structural changes and bone health. BMD provides information on the mass of inorganic mineral content per unit volume, with reduced BMD may indicate increased bone resorption, a common pathology of bone disease, including FD [1, 2]. As previously mentioned, cortical bone provides strength; cortical thickness and area are measures indicating whether bone resorption is reducing the cortical bone – thus decreasing the strength of the bone and making it more fragile to increased loads [60, 66]. Trabecular bone provides support to the cortical bone, and this network helps prevent fragility and therefore, fractures. The bone volume fraction (BV/TV) is described as the mineralised bone volume (BV), divided by the total volume of the sample (TV). Reduced BV/TV indicates loss of mineralised trabecular bone which could increase bone fragility [60, 66]. Finally, trabecular bone can also be described in terms of trabecular thickness (Tb.Th; thickness of the mineralised bone trabeculae), trabecular number (Tb.N; number of trabeculae), and trabecular spacing (Tb.Sp; the distance between trabeculae) [60, 66].

Bone marrow is situated within the trabecular bone and in the long bones it also fills the medullary cavity. Bone marrow contains blood vessels, mesenchymal stem cells (progenitor cells of adipocytes, myocytes, chondrocytes, osteoblasts), macrophages, adipocytes, fibroblasts, osteoblasts, osteoclasts, sympathetic nerves, blood vessels, and hematopoietic stem cells (progenitor of blood cells) [60, 67, 68].

The periosteum is a thin tissue layer surrounding the cortical bone and is composed of osteoprogenitor cells and fibroblasts. It is highly vascularised and innervated, communicating with the osteocytes in the cortical bone [60, 61, 67].

In a normal, healthy individual, bone structure and physiology remain regular and stable, responding to mechanical loads and biochemical signals. Bone homeostasis is maintained by osteoblasts (responsible for bone formation), osteoclasts (responsible for bone resorption), and osteocytes (Figure 1.6) [63, 69]. Osteoblasts are responsible for bone formation by depositing organic material and hydroxyapatite amongst collagen fibres to form mineralised bone. Osteoblasts mature into osteocytes when the cell mineralises the microenvironment around itself and encases it within its own lacuna [60, 63, 70]. Contrary to this, osteoclasts resorb bone. Monocytes are attracted to the bone where RANKL and macrophage colony-stimulating factor

(M-CSF) that are produced by osteoblasts stimulate monocytes to differentiate into pre-osteoclasts. Pre-osteoclasts fuse to form multinucleated osteoclasts capable of attaching to bone and resorbing bone. Osteoclasts attach to the bone surface, then secrete hydrogen and chloride ions, and enzymes (e.g. cathepsin K) to acidify and dissolve the bone mineral and biological matter, respectively [60, 63, 71]. In a healthy bone, formation and resorption are balanced and there is no net bone loss or formation. However, bone diseases – including FD – are characterised by dysregulated bone homeostasis and in the case of FD, bone resorption dominates [60, 63]. Osteocytes are the most abundant cell type and are responsible for regulating osteoblast and osteoclast function. They are capable of detecting mechanical stress and sensing regulatory factors from the periosteum, bone marrow, and through gap junctions with other osteocytes. Osteoblasts and osteocytes secrete RANKL and OPG, which affect bone homeostasis [63, 70, 71].

There are many bone turnover markers and regulatory factors that maintain bone homeostasis and may be affected by or contribute to bone disease. RANKL and OPG are two important factors that maintain homeostasis and are highly upregulated in FD [53, 70]. RANK is a receptor on the surface of both osteoclast precursor cells and mature osteoclasts. In osteoclast precursor cells, RANKL binds to RANK, activating downstream pathways in order to facilitate osteoclast differentiation and fusion. In mature osteoclasts, the binding of RANKL with RANK induces the expression of cathepsin K and TRAP, both of which assist in bone resorption [70]. OPG is a RANKL inhibitor; it is secreted by osteoblasts and osteocytes, preventing RANKL binding to RANK [70]. This is not to say that RANK/RANKL/OPG system is solely responsible for bone remodelling and resorption, but it is an important system, particularly in the development of FD [33, 53, 54, 63].

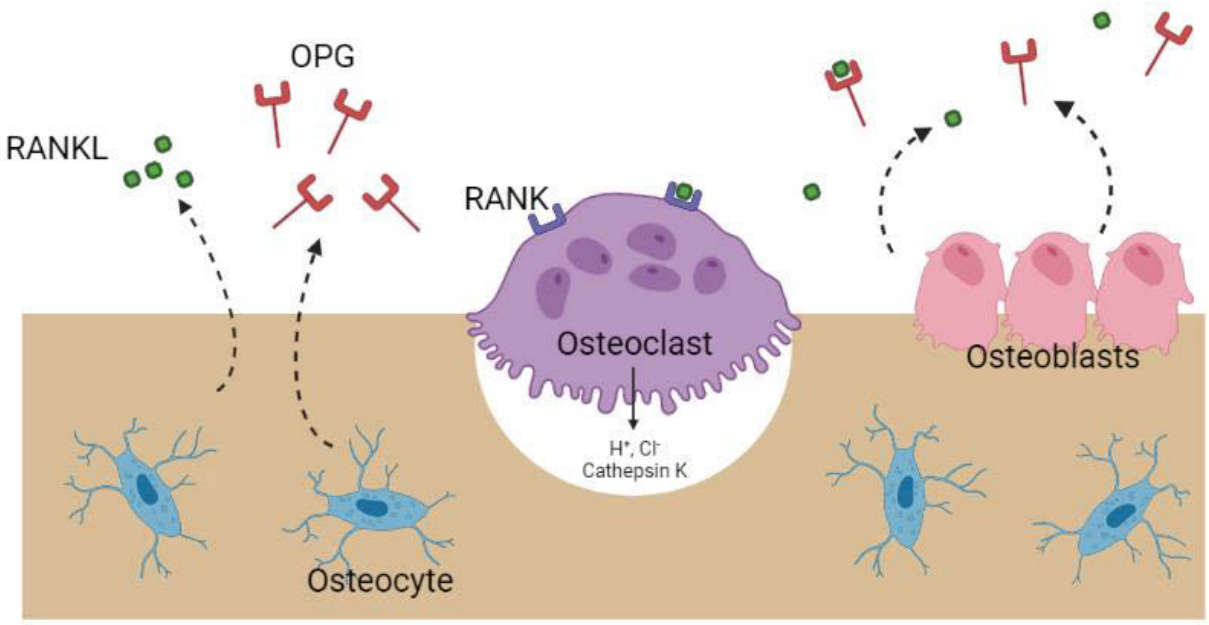

Figure 1.6 Cell populations and function in bone (created in BioRender). (RANKL: receptor activator of nuclear factor kappa-B ligand; OPG: osteoprotegerin; H^+: hydrogen ion; Cl^-: chlorine ion; RANK: receptor activator of nuclear factor kappa-B)

Bone Innervation

Bone undergoes constant change due to stimuli facilitated, in part, by neuronal signalling within the bone. Bone is highly innervated, particularly with sympathetic neurons (tyrosine hydroxylase (TH) positive) that regulate the bone microenvironment, controlling bone turnover and haematopoiesis. Nerve fibres may be myelinated or unmyelinated and commonly appear alongside blood vessels [72-74]. Sensory neurons associated with nociceptive signalling (see below) have also been shown to be present in the periosteum, bone marrow, and cortical bone, with a high volume of Substance P-positive and calcitonin gene-related peptide (CGRP)-positive sensory nerve fibres (Aδ- and C-fibres), and thickly myelinated nerve fibres (A β-fibres), but not peptide-poor C-fibres [75, 76].

Painful Bone Disorders

Little information has been generated on the pathogenesis of FD pain, primarily owing to the rarity of the disease, the difficulty of establishing large patient cohorts, and tissue samples are normally only available following surgical debridement, which is not common. However, other

painful bone diseases have similar features of FD and could guide research directions to better understand FD pain.

FD lesions are not malignant, but rapid bone turnover, pain, and bone fragility are common features of both FD and metastatic tumours in bone [2, 23, 77]. Breast cancer metastases are presented here as an example. When breast cancer metastasises to the bone it disrupts bone homeostasis, creating a 'vicious cycle'. Cancer cells secrete cytokines and chemokines that enhance osteoclast maturation (e.g. parathyroid hormone-related protein, vascular endothelial growth factor, macrophage colony-stimulating factor, IL-6, etc.) and reduce OPG secretion from osteoblasts. Mature osteoclasts resorb bone and release growth factors (e.g. transforming growth factor-beta, insulin-like growth factor, fibroblast growth factor, etc.) and calcium ions that promote tumour growth. Hence, the vicious cycle continues with further bone resorption and tumour growth [78]. The RANK/RANKL mechanism has been implicated in metastatic breast cancer. Breast cancer cells express RANK, which attracts these cells to the bone and OPG is reduced in this environment [70, 79, 80]. The secreted factors involved in this vicious cycle, rapid bone turnover, and the RANK/RANKL pathogenesis may be similar to that in FD. Cancer-induced bone pain (CIBP) is complex as there is evidence to demonstrate that pain can be nociceptive (tissue damage due to bone degradation and tumour invasion) and neuropathic (damage to sensory nerve fibres in the bone), with cancer-specific mechanisms [81, 82]. Nerve growth factor (NGF) has been shown to be produced by breast cancer cells *in vitro*, which in turn was able to upregulate expression of CGRP (a neuropeptide) [83]. Interestingly, anti-RANKL antibody or bisphosphonate treatments are suggested for metastatic breast cancer in the bone and FD, and attenuated pain is observed in both types of patients [24, 33, 84]. Additionally, a study on quality of life factors in FD patients demonstrated that FD and cancer patients exhibit a similar decrease in physical quality of life [22]. As such, understanding mechanisms of CIBP such as secreted factors, changes in the bone microenvironment, and shift in bone homeostasis to favour osteoclastogenesis may reveal commonalities with FD.

OA is another disorder with bone-related pain. OA is not strictly a bone disorder, but rather a painful joint disorder where changes in the subchondral bone may contribute to pain [85, 86]. OA is a degenerative joint disease affecting all tissue within the joint. Tissue damage of the synovium, periosteum, cartilage and subchondral bone leads to the release of inflammatory mediators (e.g. cytokines, chemokines) that cause pain. IL-1β, IL-6, and tumour necrosis factor

alpha (TNF-α) have been suggested as key inflammatory cytokine mediators in OA [87-90]. More recent studies have also demonstrated the role of chemokines in OA pain, with monocyte chemoattractant protein-1 (MCP-1) shown to be upregulated in OA, which has been shown to enhance the density of transient receptor potential vanilloid subtype 1 (TRPV1) receptors [91]. NGF expression was also shown to be increased in a mouse model of OA during periods of increased nociception, demonstrating a role of NGF in OA [92]. The joint is highly innervated, with sensory nerve fibres innervating the synovium, periosteum, and subchondral bone. The presence of these sensory neurons, coupled with increased inflammation, tissue damage, and NGF can lead to pain development [93]. Neuropathic pain has been suggested to play a role in OA pain, with increased expression of activating transcription factor 3 (ATF3) in dorsal root ganglia (DRGs) in a mouse model of OA [94]. Central sensitisation has also been assessed in OA, suggesting that advanced OA leads to hyperalgesia and activation of central mechanisms [95]. Finally, subchondral bone remodelling increases during OA due to the abnormal load bearing and bone degradation, facilitated in part by the RANK/RANKL/OPG pathway [86, 96, 97]. OA is a common disease and highly researched, in contrast to FD, which is rare and the underlying mechanisms (including that of pain) are still being elucidated. Identifying common mechanisms between FD, metastatic cancer, and OA in the bone may help to identify novel treatments for FD pain.

Pain

The International Association for the Study of Pain (IASP) describes pain as an "an unpleasant sensory and emotional experience associated with, or resembling that associated with, actual or potential tissue damage". In 2020, IASP expanded upon the definition to provide further context (paraphrased) [98]:

1) pain is a personal experience influenced by internal and external factors,

2) pain and nociception are different phenomena,

3) through life experiences, pain is learned,

4) report of pain from an individual should be respected,

5) pain plays an adaptive role, but can have adverse effects, and

6) inability to communicate does not indicate absence of pain .

In preclinical studies, these expanded definitions are important, particularly items 2 and 6 as animals cannot describe their pain experience and researchers infer pain from adverse behaviour. This is not to say that animals do not experience pain despite their inability to communicate their emotional response; however, scientific convention indicates the use of the term “pain-like” as only the observable sensory response can be measured [99, 100].

Nociceptive pain refers to actual or perceived damage to non-neuronal tissue, due to the activation of nociceptive neurons, while neuropathic pain is caused by damage or disease of the nervous system [101]. Inflammation (described below) is a complex factor in pain and is commonly considered nociceptive pain, but may also play a significant role in neuropathic pain as well [102, 103]. Nociplastic pain refers to an altered nociceptive response despite no clear tissue damage [101].

The nervous system can be broadly divided into the central and peripheral systems that are interconnected, but each plays specific roles in nociceptive signalling. Changes in either system may provide information about pain development in diseases [104].

Pain Transmission

The interplay between the peripheral nervous system and the central nervous system (CNS) and how individuals perceive pain is categorised into four steps: 1) transduction, 2) transmission, 3) modulation, 4) perception [105]. Transduction occurs when receptors in sensory neurons react to noxious stimuli (e.g. TRPV1 reacting to thermal stimulus) leading to the development of an action potential. Transmission refers to the relay of the nociceptive signal to the CNS projection neurons of the spinal cord. Descending neurons (from the hypothalamus, insular cortex, and the amygdala) synapse with neurons in the dorsal horn and release neurotransmitters (e.g. serotonin, norepinephrine) to inhibit further nociceptive transmission to the brain. Finally, the signal is processed in the somatosensory cortex where the emotional response to pain is developed and the neurochemical modulation is processed [105, 106].

Pain in the Peripheral Nervous System

The peripheral nervous system is comprised of different nerve fibres, each with specific functions related to their unique structures and receptors. Aα nerve fibres are skeletal motor neurons responsible for muscle contraction and Aβ nerve fibres are sensory neurons with sensitive mechanoreceptors that are capable of detecting light touch. Both these fibres are

heavily myelinated allowing for rapid signal transmission. Aβ receptors are sensory neurons, but due to the low threshold necessary for signal transduction, they are not commonly associated with detecting noxious stimuli. However, modulation within the spinal cord (see below) may produce sensitisation leading to hyperesthesia, where non-noxious stimuli are perceived as painful [107-109]. Aδ fibres (myelinated) and C fibres (unmyelinated) are typically associated with detecting noxious stimuli (termed 'nociceptive neurons') due to the presence of gated ion channels triggered by noxious stimuli (Table 1.1). Myelination of Aδ fibres produces a fast pain signal creating a well-localised response; meanwhile, C fibres generate a slow pain signal with poor localisation [109]. Both Aδ and C fibres can contain receptors that detect different stimuli. Receptors respond to different stimuli at different thresholds; 43°C heat, capsaicin, and low pH (e.g. TRPV1), mechanical pressure (e.g. Piezo1, Piezo2), cold and menthol (e.g. TRPM8; transient receptor potential cation channel subfamily M member 8), acid/low pH (e.g. ASIC; acid-sensing ion channel), and mechanical and chemical irritants (TRPA1; transient receptor potential ankyrin 1). Notably, sustained noxious stimuli can sensitise nociceptive neurons leading to hyperalgesia, where a less intense noxious stimuli produces a high nociceptive response [109, 110]. C fibres are classed as either peptidergic or non-peptidergic. The former express tropomyosin receptor kinase A (TrkA), which is a high-affinity receptor of NGF. TrkA activation leads to hypersensitivity to heat and mechanical stimuli. This occurs by activating downstream pathways that sensitise receptors (particularly TRPV1), promoting the expression of substance P, TRPV1, and Nav1.8 voltage-gated sodium channels. Alternatively, non-peptidergic C fibres express c-Ret neurotrophin receptors that bind to glial-derived neurotrophic factor and promote neuron survival [107, 109].

Table 1.1 Nociceptive neuron subtypes and features. Summarised from Basbaum et al. [109].

Nociceptive Neuron	Sub-type	Features
Aδ Fibre (myelinated)	Type I	• High mechanical threshold • High heat threshold (>50°C)
	Type II	• Very high mechanical threshold • Lower heat threshold (~43°C)
C Fibre (unmyelinated)	Peptidergic	• Express TrkA receptor
	Non-peptidergic	• Express c-Ret neurotrophin receptor

DRGs contain the cell bodies of peripheral sensory neurons and are located alongside the spinal cord, with peripheral and central axons. Expression of ATF3 in the DRGs is an indication of neuronal damage, and potentially neuropathic pain [111], and has been observed in CIBP and OA [94, 112]. Furthermore, the presence of sympathetic neurons in the DRGs occurs in neuropathic injury models [113, 114].

Many of these features have been observed in bone pain. Ordinarily, bone is highly innervated, with highest innervation observed in the periosteum, then bone marrow, and then cortical bone. Sympathetic neurons and sensory nerve fibres are present in all three bone structures. As such, noxious stimuli can be detected and transduced in the bone [76]. These nociceptive neurons within the bone possess TRPV1 that could contribute to increased sensitivity in painful bone disorders [115]. TRPA1 has been implicated in both metastatic breast cancer in the bone and bone cancer CIBP models [116, 117]. As previously mentioned, osteoclasts produce an acidic microenvironment, which degrades the mineralised extracellular matrix. However, when bone turnover increases, acidosis may occur which could activate ASIC receptors in the bone [118]. Finally, NGF has been implicated in painful OA [119], RA [120], and CIBP [83].

Central Sensitisation

Central sensitisation occurs when nociceptive neurons in the (CNS) demonstrate increased responsiveness and hyperexcitability compared to their normal state [101, 109]. Central sensitisation may occur when intense or prolonged stimulation activates N-methyl-D-aspartate glutamate receptors, if signal modulation by GABA and glycine are reduced or if glial cells are activated [109]. Additionally, changes in central mechanisms may also indicate the types of pain being produced; Honore et al. [121] conducted a study investigating neurochemical changes in the spinal cord in an inflammatory, neuropathic, and osteosarcoma mouse model. This study demonstrated the development of distinct neurochemical profiles for the different pain types. These profiles may be applied to FD animal models to determine the type of pain that FD produces and the neurochemical changes that occur, which may indicate treatment targets.

The spinal cord also contains glial cells – microglia and astrocytes. Microglia function as macrophages of the CNS. Their role is to protect the CNS against injury and infection, but activation or increase of microglia results in an increase of inflammatory factors which induces central sensitisation [109, 122]. Astrocytes maintain homeostasis in the CNS and assist with

tissue healing. Even though astrocytes outnumber neurons in the brain and have been shown to interact with neighbouring neurons, blood vessels, and one another, there is little information on the role they play in pain and central sensitisation. Yet, there is evidence that astrocytes maintain central sensitisation and that glial fibrillary acidic protein is upregulated in the spinal cord in neuropathic and osteosarcoma pain models [121, 123].

Inflammatory Factors in Painful Disorders

Tissue damage causes inflammation through the release of inflammatory cytokines either by the tissue itself, or immune cells (e.g. macrophages, mast cells) that are attracted to the damaged tissue by chemokines. However, inflammatory cytokines and chemokines may be upregulated in certain diseases without overt tissue damage occurring. Nevertheless, the presence of inflammatory cytokines is associated with a chemical response that acts upon nociceptive neurons. Proinflammatory factors activate the synthesis of proalgesic agents such as prostaglandins, NGF, and bradykinins. Prostanoid and bradykinin receptors (GPCRs) are present on the surface of sensory nerve fibres and when prostaglandin and bradykinin, respectively, bind to the receptors, they can sensitise TRPV1 and activate P2X3 receptors (ATP receptor; activated through PKA pathway) [107, 109, 124, 125].

Inflammation is also modulated by cytokines – including interleukins, interferons, tumour necrosis factors, and chemokines – which have pro- and anti-inflammatory effects [126]. Different diseases may be associated with and modulated by many different cytokines, but this is not fully elucidated for every cytokine or disease. Here, pro-inflammatory cytokines, anti-inflammatory cytokines, and chemokines associated with painful disorders and investigated in this thesis will be introduced.

TNF-α is a pro-inflammatory cytokine that is involved in numerous bone diseases, such as OA [90], RA [127], cherubism [128], and multiple myeloma [129]. TNF-α has also been shown to impact the RANK/RANKL/OPG pathway [130, 131]. IL-6 has been implicated in FD [36] as it is a downstream effector of cAMP and is a pro-inflammatory cytokine associated with RA [132]. Even though IL-6 antibody treatment did not produce an analgesic effect in FD patients [133] it remains an important inflammatory cytokine associated with the disorder. IL-1β is a common pro-inflammatory cytokine that is primarily associated with infection, but regarding bone it has been associated with osteoblast inhibition [134] and bone resorption [135]. Interferon-gamma

(IFN-γ) has also been shown to stimulate bone resorption in osteoporosis [136] and multiple myeloma [137]. IL-2 and IL-5 are associated with hypersensitivity [138], but there is no information on their association with painful bone disorders. In contrast, IL-4 is an anti-inflammatory cytokine that promotes B- and T-cell proliferation and tissue healing [139]. It has been shown to be reduced in chemotherapy-induced neuropathic pain [140] and sensory neuropathy [141], but its function in bone disorders is unknown. Finally, GM-CSF is secreted by inflammatory cells and functions as a cytokine. It has been associated with pain in RA [142] and cancer [143, 144], as well as neuropathic pain [145].

Chemokines are factors that induce movement of inflammatory cells to specific target tissues. MCP-1 (C-C motif ligand 2 (CCL2)) regulates migration and infiltration of monocytes and macrophages into the target tissue [146]. It is associated with CIBP [147, 148] and osteolytic processes [149, 150]. Additionally, MCP-1 has been implicated in nociceptor sensitisation through TRPV1 activation [151]. Macrophage inflammatory proteins (MIP) 1-alpha (CCL3) and 1-beta (CCL4) are both responsible for leukocyte attraction in response to inflammation [152] and have been implicated in back pain conditions [153, 154]. Stromal cell-derived factor 1 (SDF-1, C-X-C motif chemokine 12 (CXCL12)) is ubiquitously expressed in many cell types and attracts leukocytes to sites of inflammation. SDF-1 has been associated with osteoclastogenesis and osteolytic action in RA [155] and multiple myeloma [156], as well as hyperalgesia through N-methyl-D-aspartate receptors (ion channel in neurons) [157]. Keratinocyte chemoattractant (KC)/human growth-regulated oncogene (GRO) chemokines (CXCL1) attract neutrophils and have been associated with hypersensitivity in CIBP [158] and hypersensitivity in general [159]. Eotaxin (CCL11) has been implicated in osteoporosis [160] and chemotherapy-induced pain [161], but has not been investigated in painful bone disorders.

Angiogenesis itself is not an inflammatory mechanism, but it is closely coupled with inflammation, either by contributing to or responding to inflammation [162]. Angiogenesis (stimulated by vascular endothelial growth factor (VEGF)) is associated with painful bone and joint conditions such as OA [163, 164], ankylosing spondylitis [165], and CIBP [161, 166].

It is important to note that despite these chosen factors being associated with pain and/or osteolytic disorders, they may contribute indirectly and/or with other mechanisms. Therefore, targeting these factors alone may not resolve the disorder. They may also be just one factor

amongst a host of regulatory factors that contributes to a disease. However, they do provide information about underlying mechanisms of bone destruction and pain that may also be relevant in FD.

Pain in Animal Models

As previously mentioned, it is not possible to assess an emotional response to pain in animals, but there are methods to assess the sensory component. These may be broadly defined as evoked and non-evoked (spontaneous) tests [100].

Evoked tests include the Von Frey test (mechanical hypersensitivity) [167, 168], the Randall-Selitto test (mechanical hyperalgesia) [169], heat sensitivity tests (e.g. Hargreaves test [170], hot plate [171], thermal probe [172]), and cold sensitivity tests (e.g. acetone evaporation test [173]). These tests rely on experimenters applying a stimulus (e.g. mechanical, thermal) to the region of interest where a nociceptive response is likely to occur, and recording the response. These tests are highly subjective, variable, require extensive training, and are difficult to replicate. Some have suggested that these tests are reflexive behaviours that can be observed in decerebrated animals and do not register learned pain responses [100, 174].

Non-evoked (spontaneous) tests are considered to be more indicative of the human pain experience, but given that they are different species, different behaviours need to be assessed. Burrowing [175, 176], for example, is an innate and ethologically relevant behaviour in rodents. However, it is highly sensitive to analgesics, which often inhibit burrowing behaviour. For example, in sham or naïve rodents, morphine, tramadol, ibuprofen (increased in corresponding disease model, pregabalin, and gabapentin all reduced burrowing in a dose dependent manner. This is not to say that burrowing cannot be used to assess analgesic efficacy, as ibuprofen and celecoxib increased burrowing behaviour in disease models (in contrast to their sham/naïve counterparts) in a dose dependent manner [176]. Weight bearing (static and dynamic) and gait analysis are used to assess changes in movement and weight distribution [177-179]. These tests are not suitable for ubiquitous or bilateral models where a disease affects both sides of the body. These tests are best suited to models with a lateral bias where the disease is isolated to one side. Pain is an aversive experience and analgesic relief is a motivational experience, both of which are associated with the emotional aspect of pain. Conditioned place preference has been employed in rodent models to assess these features, which tend to be highly sensitive and

challenging to reproduce [180]. Wheel running is a motivational activity that has been observed in wild mice and although the motivational basis for the behaviour in rodents is not understood, laboratory mice will engage in the behaviour as well. However, sex, strain, and model type can greatly influence the outcome of the study [181-185]. Wheel running has previously been used to assess pain-like development in models of prostate CIBP [183], inflammatory pain [181, 182], and neuropathic pain (significant difference only in female mice) [182]. Home cage monitoring has been used to assess pain-like behaviour, demonstrating reduced activity (pain-like behaviour) in mice with a chronic constriction injury compared to naïve mice [186].

When working with animals, great effort must be made to ensure the highest ethical standards are maintained. The '3 R principle' proposes that animal experiments should aim to Replace, Reduce, and Refine experiments to use the fewest number of animals possible, while maintaining high experimental standards [187]. The experiments described herein considered these principles when designing animal experiments and were adjusted accordingly. The ARRIVE (Animal Research: Reporting of In Vivo Experiments) guidelines were also considered when conducting and reporting experiments to guarantee the necessary details were reported ensuring greater reproducibility opportunities in the future [188].

Objectives

Objective 1 (Manuscript 1): Describe and compare different animal models of FD that express the causative $G\alpha_s^{R201C/H}$ mutation in order to identify a suitable animal model to assess FD pain-like behaviour and mechanisms.

Objective 2 (Manuscript 2): Identify bone pain in a translationally relevant mouse model of FD and determine underlying nociceptive mechanisms.

Objective 3 (Manuscript 3): Develop a method to use Digital Ventilated Cages® with in-cage wheels to assess pain-like behaviour in a defined cancer-induced bone pain model.

Chapter 1

Fibrous dysplasia animal models: A systematic review

Introduction

Although FD is rare, numerous animal models have been developed to study the disease [7, 56-59]. Translationally relevant animal models of rare diseases are essential, as they provide a large, homogeneous sample of animals that can be used to understand underlying pathological mechanisms, or test novel treatments. That said, it is imperative to understand the model development, underlying mechanisms, and phenotypic development prior to conducting further studies.

Available FD models have been developed using different mutations, transgenes, driving promoters, constitutive and inducible modes of onset, different cells where the gene is expressed, and different skeletal sites. Furthermore, different aspects of the disease were assessed in each model. A total of 38 features of FD observed in patients that could be assessed in animals was compiled; however, it is impractical for a single study to investigate all these features [2, 29, 31, 53, 189-202]. Thus, for further research to be conducted in an *in vivo* model of FD, researchers should be aware of the features of different models and how they can be assessed.

For this thesis, it was vital to identify if an animal model of FD had been established that demonstrated pain-like development, and if not, which model would be best suited to conduct such studies. Therefore, the objective of this study was to describe and compare different animal models of FD that express the causative $G\alpha_s^{R201C/H}$ mutation in order to identify a suitable animal model with which to assess FD pain-like behaviour and mechanisms.

Methodology

The Preferred Reporting Items for Systematic Reviews and Meta-Analyses (PRISMA) was used to find, analyse, and compare different animal models of FD [203]. The following term was used in Scopus, PubMed, and Web of Science to retrieve relevant studies: "((in vivo) OR model OR transgenic OR animal) AND (fibrous dysplasia)" [52].

First, duplicate studies were removed. The remaining records were analysed and some were excluded based on the following criteria: not in English, complete article was inaccessible, not original research articles (e.g. review articles, case studies/series), did not have a relevant

negative control that did not develop FD, investigation was on human patients, no animal model development (e.g. only *in vitro*, pharmacological, imaging, etc.), and skeletal disorders closely related to FD (e.g. fibrodysplasia ossificans progressiva, cherubism, Carney complex, etc.).

Having excluded non-relevant studies, the remaining studies were categorised as causative FD models, mechanistic FD models, or implant models. Causative FD models are animal models expressing the causative $G\alpha_s^{R201C/H}$ FD mutation and developing FD phenotypical characteristics. Mechanistic models do not express the causative mutation but instead report the development of FD-like lesions. Implant models are those that were implanted or injected with allogeneic or xenogeneic FD cells. The features of causative models were assessed based on those reported in FD patients that could also be assessed in animal models. The categories of assessment were: clinical features, imaging, histology and histomorphometry, histochemical and cellular markers, and blood/urine markers.

Lastly, the Systematic Review Centre for Laboratory Animal Experimentation (SYRCLE) risk of bias tool was utilised to analyse the risk of bias of the included studies [204].

Results and Discussion

Seven unique transgenic mouse models expressing the causative R201 mutation of FD were identified [7, 54, 56-59, 205] and these were assigned names based on the driving promoter and the name of the lead investigator. Two models used promoters (EF1α – elongation factor 1 α and PGK – phosphoglycerate kinase 1) allowing for ubiquitous gene expression of the $G\alpha_s^{R201C}$ cDNA (complementary deoxyribonucleic acid) construct. These models developed slowly, with FD lesions developing at 2-3 months of age, first appearing in the tail (distal region) and eventually affecting the entire skeleton [56].

Three models were developed using Prrx1 (paired related homeobox 1) as the expression promoter, limiting mutated gene expression to skeletal stem cells. The first Prrx1-driven model was developed by Zhao et al. where human $G\alpha_s^{R201C}$ cDNA was expressed in a site-specific, tetracycline-inducible model. These lesions developed in the long bones and parietal bone [58]. The second model altered the endogenous $Gnas^{R201H}$ gene on one allele with exon 7-12 floxed (flanked by loxp), so that when Cre recombinase was present, the mutated allele would be expressed in skeletal stem cells. These mice were bred with Prrx1-Cre mice to develop the Prrx1-Yang model. Additionally, the mice with the endogenous $Gnas^{R201H}$ gene were bred with

Osx-Cre (tetracycline inducible) mice to develop the Osx-Yang model and Sox9-Cre (tamoxifen inducible) mice to develop the Sox9-Yang model [7, 59]. The Prrx1-Bastepe model was developed by inserting a floxed $G\alpha_s^{R201C}$ gene into a mouse and that mouse bred with a Prrx1-Cre mouse. This final model was overall poorly defined in the literature with minimal reporting of the physiology. The only feature assessed (which was not assessed in other models), was the increase of c-fos expression [57]. Further discussion excludes this model due to the lack of information provided in the study.

All models reported the development of FD lesions, which were assessed using either x-ray and/or micro-CT to image the skeleton. Histological analysis revealed characteristic woven fibro-osseous bone lesions, but the Osx-Yang model demonstrated hyperostotic lesions, which are not characteristic of FD [7, 56, 58, 59]. An increased number of osteoclasts were observed in four of the models, which also investigating features of increased bone turnover, such as ALP presence and RANKL and RANKL/OPG expression [7, 56, 58, 59]. However, none of the models investigated the presence of pain or the influence of extraskeletal features of MAS. IL-6 and FGF23 are also commonly associated with FD, but neither of these factors was assessed in any models.

Two models attempted to establish FD in different cell types, namely mature osteoblasts and embryonic stem cells. Expression of $G\alpha_s^{R201C}$ in mature osteoblasts resulted in a hyperostotic phenotype with highly mineralised bone lesions, which is not characteristic of FD [8]. Meanwhile, expression of $Gnas^{R201H}$ in embryonic stem cells was lethal and embryos died during foetal development [7].

A risk of bias analysis was conducted for these causative model studies, which revealed that their reporting methods for the included studies were generally unclear. For many features, such as blinding, randomisation, and reporting of incomplete data, there was insufficient detail to judge whether there was a low or high risk of bias. This could be considered a flaw in these studies and makes reproducibility a challenge.

Overall, only four models demonstrated high face validity, reporting features that closely resemble FD observed in patients. Only the Prrx1-Gutkind model demonstrated good construct validity, utilising a human $G\alpha_s^{R201C}$ cDNA construct [58], while the Prrx1-, Osx-, and Sox9-Yang models utilised the endogenous mouse gene, which preserves the natural physiology and

may prevent genetic disturbance [7, 59, 206]. The EF1α- and PGK-Riminucci models have the ability to develop MAS due to ubiquitous expression of $G\alpha_s^{R201C}$, but this was not reported [56]. The EF1α-Riminucci model has been used in two previous studies to assess the efficacy of anti-RANKL antibody treatment and zoledronic acid (anti-resorptive medication) [54, 205].

Eight unique mechanistic models were identified. One model was generated using an engineered serotonin receptor that could only be activated using a synthetic ligand. However, expression occurred in mature osteoblasts, resulting in a hyperostotic phenotype, similar to that produced in when $G\alpha_s^{R201C}$ was expressed in mature osteoblasts [8]. Although not FD, this mechanism, when expressed in skeletal stem cells, could be highly advantageous for further studies if such a model was developed [207-212]. Other mechanistic models explored alteration of the PKA [15-18, 20, 213] and parathyroid hormone pathways [214, 215], which have both been implicated as FD mechanisms, as well as the Wnt (wingless Int-1)/β-catenin pathway [216, 217]. Very early studies on FD mechanisms assessed the role of c-fos expression, which is indirectly induced by cAMP, but there was limited reporting on the physiological changes [218, 219].

Seven studies reported the use of implants to assess FD *in vivo*. Six of the studies demonstrated that FD cells require wild type cells for FD to develop, otherwise the physiological environment becomes lethal [6, 215, 220-224]. Two other studies reported the treatment and pathway targets of FD; however, further study in more advanced transgenic models would be beneficial [221, 223].

Animal models are an invaluable tool to study and understand FD. Although several causative FD models have been developed and established, only three models demonstrate good face validity and have been highly characterised to fully understand the models and their respective features: EF1α-Riminucci [56], Prrx1-Yang [7, 59], and Prrx1-Gutkind [58]. As such, these models are best suited for further studies, particularly to investigate pain-like development. The EF1α-Riminucci model demonstrates excellent face validity in a mosaic-like fashion, it has the potential to develop MAS which may influence FD-associated pain, and it has been used in previous studies to assess FD treatment. However, it has a long time of onset, where initial lesions first occur in the tail at 2-3 months and lesion development in the rest of the skeleton occurs at 9 months [54, 56, 205]. The Prrx1-Yang and Prrx1-Gutkind models both demonstrate excellent face validity with a mosaic-like phenotype. The Prrx1-Yang model is a relatively

simpler model to establish than the Prrx1-Gutkind model as there are fewer transgenes and it is not inducible [7, 58, 59]. However, the inducible element of the Prrx1-Gutkind model is highly beneficial, allowing for greater control over FD induction in a relatively fast progression (2-3 weeks). It also presents unique opportunities for induction at different life stages, from pre-term development to older mice [58].

Conclusion

The established models have unique features which is beneficial to FD research as a whole, with more tools to investigate different aspects of a complicated disorder. For purposes of further research of pain in FD, the Prrx1-Gutkind model is highly beneficial from both a scientific and practical viewpoint [58].

This review was important for further studies for this thesis project, and may be beneficial for other researchers investigating FD. This study established areas of FD research that are lacking, such as the impact of MAS and hormonal perturbations on the development of FD. This review will assist researchers in selecting an *in vivo* model most relevant to their own research requirements and identify gaps in current research.

Bone 155 (2022) 116270

Contents lists available at ScienceDirect

Bone

journal homepage: www.elsevier.com/locate/bone

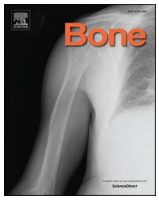

Full Length Article

Fibrous dysplasia animal models: A systematic review

Chelsea Hopkins [a], Luis Fernandez de Castro [b], Alessandro Corsi [c], Alison Boyce [d], Michael T. Collins [b], Mara Riminucci [c], Anne-Marie Heegaard [a,*]

[a] Department of Drug Design and Pharmacology, University of Copenhagen, Copenhagen, Denmark
[b] Skeletal Disorders and Mineral Homeostasis Section, National Institute of Dental and Craniofacial Research, National Institutes of Health, Bethesda, MD, USA
[c] Department of Molecular Medicine, Sapienza University of Rome, Rome, Italy
[d] Metabolic Bone Disorders Unit, National Institute of Dental and Craniofacial Research, National Institutes of Health, Bethesda, MD, USA

ARTICLE INFO

Keywords:
Fibrous dysplasia
In vivo
Animal

ABSTRACT

Background: Fibrous dysplasia (FD) is a rare genetic bone disorder resulting in an overproduction of cAMP leading to a structurally unsound tissue, caused by a genetic mutation in the guanine nucleotide-binding protein gene (*GNAS*). In order to better understand this disease, several animal models have been developed with different strategies and features.
Objective: Conduct a systematic review to analyze and compare animal models with the causative mutation and features of FD.
Methods: A PRISMA search was conducted in Scopus, PubMed, and Web of Science. Studies reporting an *in vivo* model of FD that expressed the causative mutation were included for analysis. Models without the causative mutation, but developed an FD phenotype and models of FD cell implantation were included for subanalysis.
Results: Seven unique models were identified. The models were assessed and compared for their face validity, construct validity, mosaicism, and induction methods. This was based on the features of clinical FD that were reported within the categories of: macroscopic features, imaging, histology and histomorphometry, histochemical and cellular markers, and blood/urine markers.
Limitations: None of the models reported all features of FD and some features were only reported in one model. This made comparing models a challenge, but indicates areas where further research is necessary.
Conclusion: The benefits and disadvantages of every model were assessed from a practical and scientific standpoint. While all published reports lacked complete data, the models have nonetheless informed our understanding of FD and provided meaningful information to guide researchers in bench and clinical research.

1. Introduction

Fibrous dysplasia (FD) is a rare bone disorder that results in fibro-osseous tissue replacing normal bone. The structurally unsound tissue leads to deformity, fractures, and often pain that reduces the patient's quality of life and may cause significant disability [1–9]. The FD etiology is due to post-zygotic substitution mutations of the *GNAS* gene, specifically the stimulatory alpha-subunit of the guanine nucleotide-binding protein ($G\alpha_s$); the arginine residue at the 201 codon in exon 8 is usually replaced by a cysteine or histidine (R201C/H). Rarely, a mutation at

Abbreviations: FD, fibrous dysplasia; GNAS, guanine nucleotide-binding protein gene; PRISMA, Preferred Reporting Items for Systematic Reviews and Meta-Analyses; cAMP, cyclic adenosine monophosphate; MAS, McCune-Albright syndrome; Gαs, alpha-subunit of the guanine nucleotide-binding protein; ALP, alkaline phosphatase; FGF23, fibroblast growth factor-23; GPCR, G protein-coupled receptor; CT, computed tomography; μCT, micro-CT; PKA, Protein Kinase A; CREB, cAMP responsive element binding protein; RANKL, Receptor activator of nuclear factor kappa-B ligand; OPG, osteoprotegerin; Wnt, Wingless Int-1; β-Catenin, beta-catenin; IL-6, Interleukin 6; Runx2, Runt-related transcription factor 2; TRAP, Tartrate-resistant acid phosphatase; P1NP, Procollagen type 1 N-terminal Propeptide; NR, not reported; SYRCLE, Systematic Review Centre for Laboratory Animal Experimentation; Cre, Cre recombinase; rtTA, reverse tetracycline transactivator; cDNA, complementary DNA; WT, wild type; mRNA, messenger RNA; BMSC, bone marrow-derived stem/stromal cell; SSC, skeletal stem cell; PTH, parathyroid hormone; PTHrP, PTH-related protein; PTH1R, PTH receptor 1; EF1α, elongation factor-1 alpha; PGK, phosphoglycerate kinase-1; Prrx1, paired related homeobox-1; Sox9, sex determining region Y-box 9; Osx, osterix; KI, knock-in; IHC, immunohistochemistry; IF, immunofluorescence; qRT-PCR, quantitative real-time polymerase chain reaction; pCREB, phosphorylated CREB; WB, western blot; ELISA, enzyme-linked immunosorbent assay; Tet, tetracycline; Tam, Tamoxifen.

* Corresponding author at: Department of Drug Design and Pharmacology, University of Copenhagen, Universitetsparken 2, 2100 Copenhagen, Denmark.
E-mail address: amhe@sund.ku.dk (A.-M. Heegaard).

https://doi.org/10.1016/j.bone.2021.116270
Received 15 September 2021; Received in revised form 22 November 2021; Accepted 25 November 2021
Available online 4 December 2021

codon 227 (in exon 9; Q227) will result in FD as well [2]. These mosaic mutations result in the dysregulated overproduction of cyclic adenosine monophosphate (cAMP) [10].

The mutation responsible for FD can also result in extraskeletal disease and the combination of FD and one or more extraskeletal feature is termed McCune-Albright syndrome (FD/MAS). The most commonly involved extraskeletal sites are the skin (hyperpigmented macules referred to as café-au-lait skin spots), multiple endocrine tissues (including precocious puberty, hyperthyroidism, or growth hormone excess), and occasionally skeletal muscles (intramuscular myxomas, also known as Mazabraud's syndrome). Due to the mosaic nature of the disease and that $G\alpha_s$ is so broadly expressed, the spectrum of phenotypic possibilities is wide and the presentation of FD/MAS is therefore unique in each individual patient [2].

Key clinical features of FD include bone deformity and fractures, which in severe cases may lead to functional impairment such as loss of vision, hearing, and ambulation [1,2,9,11]. Patients might also experience pain, with a higher prevalence and intensity in adults [7,8]. FD exhibits an age-related phenotype: lesions become clinically apparent over the first few years of life and expand to reach final disease burden in late adolescence. In adulthood, lesions become less metabolically active and fracture rates decline [4,12]. X-rays of the lesion have a "ground-glass" appearance due to the replacement of bone and marrow by fibro-osseous tissue [13]. However, imaging techniques (including computed tomography and magnetic resonance imaging), deformity, and fractures are not suitable on their own to diagnose FD. A complete clinical assessment for skeletal and extraskeletal features of FD/MAS needs to be conducted to confirm the diagnosis, and in uncertain cases a molecular diagnosis of the affected tissues may be required [14]. Hematoxylin and eosin staining will reveal woven bone with the presence of Sharpey fibers, and Von Kossa staining will display undermineralization of the bone and the absence of bone marrow. Elevated levels of bone turnover markers support the diagnosis of FD, with alkaline phosphatase (ALP) being the minimum recommended biomarker in FD; the greater the burden of disease, the greater the elevation in bone turnover markers [14–16]. FD also influences the generation of the phosphate- and vitamin D-regulating hormone, fibroblast growth factor-23 (FGF23) and in patients with extensive FD, FGF23 is elevated and patients are hypophosphatemic [14].

FD/MAS is currently incurable and reduces the quality of life in patients [7,17]. Care of these patients is symptomatic and sometimes ineffective, as in the case of pain [7]; although, some case studies suggest that denosumab may be a promising treatment of pain in FD patients [18–20]. The rarity of the disease makes it challenging to investigate its pathology and progression as well as establish an appropriate sample size for clinical studies. Nonetheless, an international consortium of dedicated clinicians, researchers, and patients' advocates has developed clinical guidelines for the definition, diagnosis, staging, treatment, and monitoring for FD/MAS [14]. However, it is imperative that appropriate animal models of FD are established. Animal models are an invaluable tool to study the pathogenesis and progression of the disease and provide the means to test novel treatment options that may help patients. To date, several groups have proposed FD models using the principal causative *GNAS* R201 mutations and have reported features that are similar to human FD, demonstrating both the construct and face validity of the models. These models, however, have been created using different approaches and exhibit unique features, each with its advantages and disadvantages, making it challenging for researchers to determine which model is best-suited to model specific aspects of this complex disease. Moreover, some transgenic mouse models have been developed that do not express FD-associated *GNAS* mutations, but cause G protein-coupled receptor (GPCR)/$G\alpha_s$/cAMP pathway activation to mimic some aspects of the FD phenotype. Lung et al. [21] reviewed key clinical presentations of FD/MAS, the current status of mouse models targeting the G_s GPCR signaling pathway, and human cellular models. However, there exists no systematic comparisons of available animal models or information to identify gaps in current research and what further studies may be needed.

The aim of this systematic review is to analyze and compare current animal models of FD that exhibit a causative *GNAS* R201 substitution mutation and compare the pathology of FD in patients to that experimentally assessed in animal models. Studies including any laboratory animal species with the FD-associated *GNAS* R201 substitution mutation were considered, but only if the model included an appropriate control that did not express the FD-associated *GNAS* mutation.

2. Methodology

The Preferred Reporting Items for Systematic Reviews and Meta-Analyses (PRISMA) approach was applied to conduct a systematic review on *in vivo* studies that reported the generation of an FD phenotype by way of the FD-associated *GNAS* mutation. Studies had to have included an appropriate control that did not exhibit the FD-associated *GNAS* mutation, or which did not induce expression of the mutated *GNAS* R201 gene. Models that exhibited FD-like lesions, but did not contain the FD-associated *GNAS* mutation were excluded from the main analysis of this study because they lacked the causative mutation of the disease, as were studies that transplanted cells from FD-like lesions into an animal host.

The term "((in vivo) OR model OR transgenic OR animal) AND (fibrous dysplasia)" was used in Scopus, PubMed, and Web of Science to collect all papers related to *in vivo* FD articles (search conducted on 8 February 2021). Other articles were collected by assessing the references of those that appeared in the database search (these articles were collected from 9 to 15 February 2021). Articles were not limited or excluded by year, access type, publication stage, source title, country of publication, or funding body. Publications were excluded if they were not published in English, if the complete article could not be accessed, or if they were not original research articles.

Original articles that reported an *in vivo* model of FD-associated *GNAS* mutations were included for further analysis as causative models. Studies were excluded if they presented a case study or case series of animals with FD or FD-like phenotype, if the study was investigating human patients, if the work was solely an *in vitro*, biomaterial, pharmacological, imaging, surgical study, with no animal model development, and any non-osseous disorder. Skeletal disorders and syndromes not related to the FD-associated *GNAS* mutation were excluded. These include: cherubism, fibrodysplasia ossificans progressiva, Carney complex, Albright hereditary osteodystrophy, and osteogenesis imperfecta. McCune-Albright Syndrome (including Mazabraud Syndrome) was included, as FD is a condition of this disease.

Previous review articles and book chapters were evaluated to determine the clinical and pathological features of FD that could be assessed *in vivo* [2,12,14,16,17,22–34]. These features were grouped according to how they were analyzed; they include:

Clinical features:

- Deformity
- Pain
- Fracture
- Loss of vision, hearing, ambulation

Bone imaging - appearance, density, and microarchitecture:

- Poly/monostotic FD
- Ground glass appearance
- Undermineralized bone and/or low bone mineral density
- Cortical thinning
- Expansile deformity
- Computed tomography (CT)/micro-CT (μCT) appearance of lesions

Histology and histomorphometry:

- Fibrous-osseous tissue
- Loss of hematopoiesis
- Woven bone
- Abnormal curvilinear trabeculae
- Sharpey's fibers
- Abnormally shaped (stellate, retracted) osteoblasts
- Increased number of osteoclasts in fibro-osseous tissue

Histochemical and cellular markers:

- cAMP (increased; including assessment *via* Protein Kinase A (PKA)/cAMP responsive element binding protein (CREB) pathway)
- Alkaline phosphatase (ALP; increased)
- Receptor activator of nuclear factor kappa-B ligand (RANKL; increased)
- RANKL/osteoprotegerin (OPG) ratio (increased)
- Wnt signaling/β-Catenin (Wingless Int-1/beta-catenin; increased)
- Interleukin 6 (IL-6; increased)
- Runt-related transcription factor 2 (Runx2; increased)
- Osteocalcin (increased)
- c-fos expression (increased)
- Tartrate-resistant acid phosphatase (TRAP; increased)

Blood and/or urine markers:

Bone Formation Markers
- ALP (increased; blood)
- Osteocalcin (increased; blood)
- Procollagen type 1 N-terminal Propeptide (P1NP) (increased; blood)

Bone Resorption Markers
- Hydroxyproline (increased; blood or urine)
- Deoxypyridinoline (increased; urine)
- C-telopeptide (increased; blood)
- N-telopeptide (increased; blood)
- RANKL (increased; blood)
- RANKL/OPG ratio (increased; blood)

Other Markers
- FGF23 (increased; blood)
- IL-6 (increased; blood)

Manuscripts that met the inclusion criteria were assessed to determine which features of FD (listed above) were reported in the animal model. The results of this assessment were tabulated for comparison. Three responses were tabulated for every item: yes (the phenotypic feature was expressed); no (the phenotypic feature was not expressed), and not reported (NR; feature not reported in model). For quantitative data, only significant differences from the control were recorded as demonstrating the phenotype. The results were then qualitatively assessed. No quantitative assessment was conducted.

Lastly, the risk of bias for included articles was assessed using the Systematic Review Centre for Laboratory Animal Experimentation (SYRCLE) assessment method – a tool similar to the Cochrane risk of bias tool, adjusted for reporting animal studies [35].

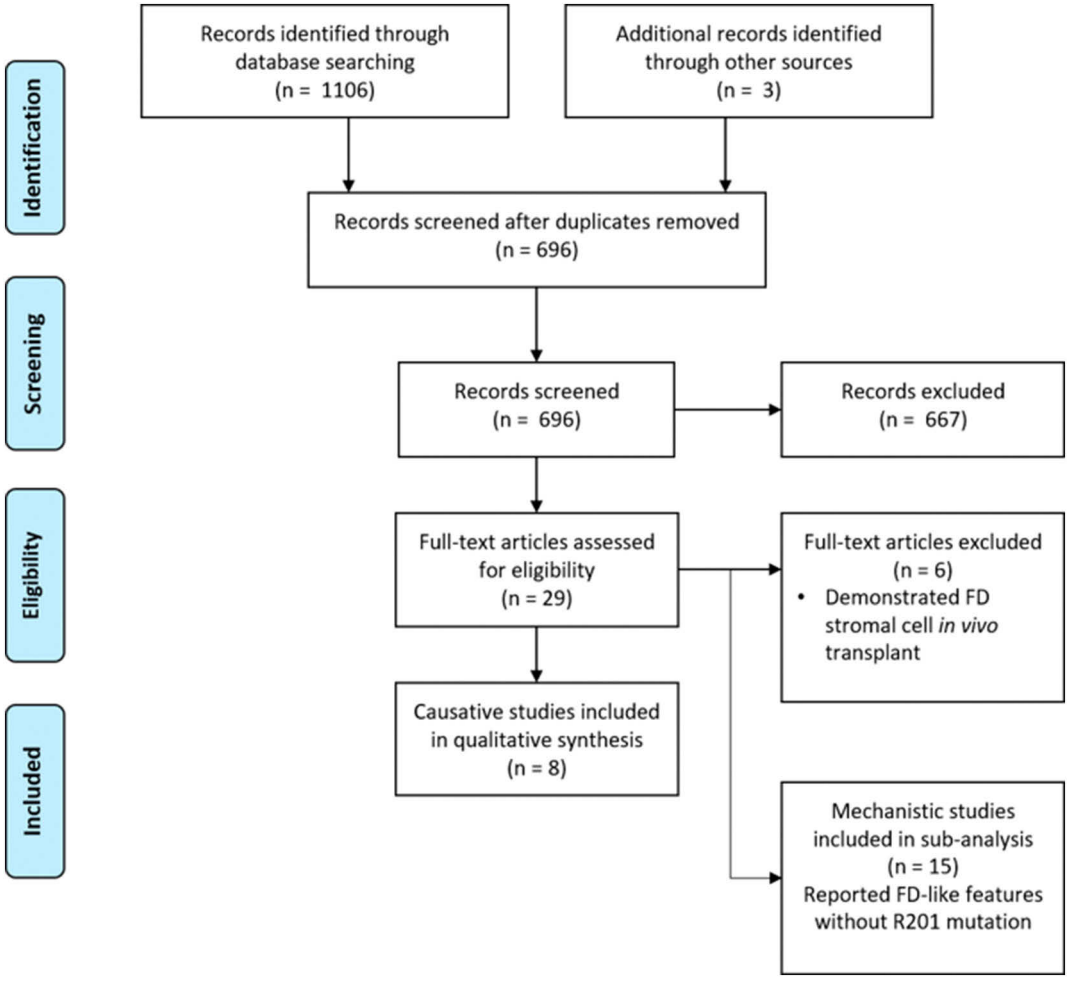

Fig. 1. PRISMA flow chart demonstrating search results and articles included for qualitative synthesis.
(FD = fibrous dysplasia; n = number; R201 = arginine in position 201 of the *GNAS* gene).

3. Results

The search yielded 696 unique articles, 667 of which were excluded based on the exclusion criteria, and the remaining 29 were assessed for potential inclusion for qualitative assessment. Eight studies were included for qualitative assessment, based on the inclusion and exclusion criteria (Fig. 1).

During the search, 15 studies were identified as mechanistic studies that did not meet the inclusion criteria of exhibiting a *GNAS* mutation; however, they reported FD-like lesions and were included in a subanalysis given the information they could yield about mechanisms that may contribute to the FD phenotype. Six studies were excluded as they established a model in which cells derived from human FD lesions were transplanted into mice, and therefore the animal itself did not carry a causative or mechanistic mutation. The classification of these models is demonstrated in Fig. 2 in order to establish a standardized nomenclature of the models assessed in this review.

Seven unique causative mouse models were identified. None of the studies of these seven models assessed or reported the development of the extra-skeletal findings associated to MAS. Two additional models (Col1a1-Bianco and Sox2-Yang models) [36,37] did not develop an FD phenotype, but were analyzed for the information they might yield about FD.

3.1. Qualitative analysis of causative models

Table 1 summarizes the details of the seven models of FD included in the qualitative synthesis.

The causative models were developed using a wide variety of genetic strategies to drive the expression of mutant $G\alpha_S$. The promoters used allowed for ubiquitous or tissue-specific expression through cell type or developmental stages. Some models were developed to allow inducible expression of the mutated gene, but others developed constitutively. The gene mutation was inserted randomly in most models or using the homologous GNAS replacement in others. Finally, different models used GNAS from different species with either the R201C or R201H mutation.

The EF1α-Riminucci and PGK-Riminucci models were developed by randomly inserting rat $G\alpha_S^{R201C}$ cDNA under EF1α and PGK promoters, respectively, in the genome of a fertilized embryo [38,39]. This resulted in a ubiquitous and constitutive expression of the gene and subsequent FD development.

The Prrx1-Gutkind model involved three transgenic constructs. The first transgene consisted of a Cre recombinase (Cre) controlled by the promoter of Prrx1, transiently expressed in embryogenesis in the budding mesenchyme, which gives rise to the appendicular skeleton and some areas of the parietal bones. The second transgene encoded a tetracycline-inducible transcription factor (reverse tetracycline transactivator, rtTA) driven by a constitutive ROSA26 promoter, but repressed by a floxed STOP codon. During embryogenesis, this codon would be removed in Prrx1-expressing cells, allowing the constitutive expression of rtTA in these cells and their progeny. The third transgene was human $G\alpha_S^{R201C}$ cDNA, controlled by a tetracycline inducible element. Upon postnatal administration of doxycycline to these mice, $G\alpha_S^{R201C}$ is expressed and lesions form in the appendicular skeleton and some areas of the parietal bones [40,41].

All models by the Yang group were developed using a mouse strain in which one endogenous *Gnas* allele contains the R201H mutation, and the wild type exons 7–12 floxed upstream of exon 8 of the mutated endogenous gene. In the absence of Cre, this *Gnas* allele expresses the WT gene, and when Cre is present, the mutated gene is expressed [36]. This strain was crossed with different Cre strains to obtain different $Gnas^{R201H}$ expression patterns, although still regulated by its endogenous promoter. They used a mouse in which Cre is expressed under a tetracycline-regulated Osx promoter [42] (Osx-Yang model), Prrx1 promoter [43] (Prrx1-Yang model), and a tamoxifen-inducible Cre expressed under the control of Sox9 (Sox9-Yang) [36].

Finally, the Prrx1-Bastepe model was generated by randomly inserting a floxed rat $G\alpha_S^{R201H}$ cDNA construct into the mouse genome under a constitutive promoter [44]. These mice were then bred with Prrx1-Cre mice to ensure that the gene was only expressed in skeletal stem cells [45].

The time of onset – defined as the initial presentation of the FD phenotype, either from induction (*i.e.* tetracycline induction) or from fertilization/birth (*i.e.* constitutive expression) – varied greatly between models. Some models demonstrated a FD phenotype within two weeks of induction (Prrx1-Gutkind and Prrx1-Yang) [36,40,46] and others developed it in 2–3 months (EF1α- PGK-Riminucci models) [38,47,48] postpartum.

The manifestation of the expression of $G\alpha_s^{R201H}$ also varied among the mouse models. Although both Riminucci models [38,47,48] allow a ubiquitous expression of $G\alpha_s^{R201H}$, they are reported to first appear in the distal tail (at 2–3 months) and then progress to later include the long

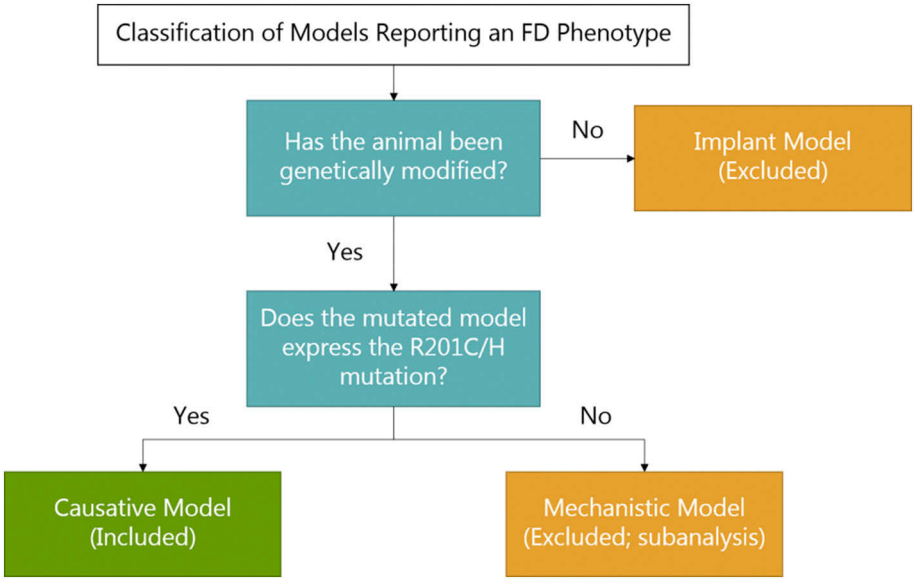

Fig. 2. Flow diagram classifying the different animal models of FD that the systematic search yielded. (FD = fibrous dysplasia; R201C/H = arginine replaced by cysteine/histidine at codon position 201).

Table 1
Features of FD assessed and reported in causative models that reported the development of an FD phenotype (EF1α = elongation factor-1 alpha; PGK = phosphoglycerate kinase-1; Prrx1 = paired related homeobox-1; Sox9 = sex determining region Y-box 9; Osx = osterix; $G\alpha_S^{R201C}$ = arginine replaced by cysteine at position 201 of the G-alphaS protein; $G\alpha_S^{R201H}$ = arginine replaced by histidine at position 201 of the G-alphaS protein; SSC = skeletal stem cell; Yes = phenotypic feature observed in model; No = phenotypic feature not observed in model; NR = not reported; KI = knock-in; Time of onset = from birth/induction to FD phenotype development; CT = computed tomography; μCT = microCT; ALP = alkaline phosphatase; RANKL = receptor activator of nuclear factor kappa-B ligand; cAMP = cyclic adenosine monophosphate; Runx2 = runt-related transcription factor 2; P1NP = procollagen type 1 N-terminal propeptide; OPG = osteoprotegerin; FGF23 = fibroblast growth factor-23; BT = bone tissue; mRNA = messenger ribonucleic acid; Pr = protein; IHC = immunohistochemistry; IF = immunofluorescence; qRT-PCR = quantitative real-time polymerase chain reaction; pCREB = phosphorylated response element-binding protein; WB = western blot; US = unclear source; ELISA = enzyme-linked immunosorbent assay). The Sox2-Yang and Col1a1-Bianco model are not described here as they do not develop an FD-like phenotype, but they are considered for full analysis.

		Models						
Model moniker		EF1α-Riminucci[38,47,48]	PGK-Riminucci[38]	Prrx1-Gutkind[40]	Prrx1-Yang[36,46]	Sox9-Yang[36]	Osx-Yang[33,46]	Prrx1-Bastepe[45]
Transgene species and type		Rat $G\alpha_S$ cDNA	Rat $G\alpha_S$ cDNA	Human $G\alpha_S$ cDNA	Mouse *Gnas* KI	Mouse *Gnas* KI	Mouse *Gnas* KI	Rat $G\alpha_S$ cDNA
GNAS mutation		R201C	R201C	R201C	R201H	R201H	R201H	R201H
$G\alpha_S$/*Gnas* promoter		EF1α	PGK	tetO7	Endogenous	Endogenous	Endogenous	CAG
Targeted expression promoter				Prrx1	Prrx1	Sox9	Osx	Prrx1
Type of onset		Constitutive	Constitutive	Doxycycline inducible	Constitutive	Tamoxifen inducible	Doxycycline inducible – Tet-off gene silencing	Constitutive
Target cells		Ubiquitous expression	Ubiquitous Expression	SSCs and progeny (Dox-dependent)	SSCs and progeny	Multipotent BMSCs and progeny	Immature osteoblasts and progeny	SSCs and progeny
Phenotype expression site		Whole skeleton, prominently in tail, femur, tibia, spine, humerus, short bones, cranium, ribs, pelvis	Whole skeleton, prominently in tail, femur, tibia, spine, humerus, short bones, ribs, pelvis	Appendicular skeleton, parietal bone areas	Appendicular skeleton, parietal bone areas	Only reported in humerus (whole skeleton targeted)	Only reported in humerus (whole skeleton targeted)	Appendicular skeleton, parietal bone areas
Mouse strain		FVB	C57BL/6	FVB ⚭ C57BL/6	Unclear	Unclear	Unclear	C57BL/6 ⚭ 129
Time of onset (from birth/induction to FD phenotype development (approximate)		2–3 months	2–3 months	2 weeks	10–16 days	4 weeks	4 weeks	Within 21 days
Mosaicism reported		No	No	No	No	Yes	No	No
Sex		• NR [35] • Male and female [44] • Female only [45]	NR	Male and female	NR	Embryonic/neonatal – male and female Weaned - NR	Embryonic/neonatal – male and female Weaned - NR	Male and female
Clinical	Bone deformity	Yes	Yes	Yes	Yes	Yes	Yes	Yes
	Fracture	Yes	NR	Yes	NR	NR	NR	NR
Bone X-ray appearance, density, and microarchitecture	Poly/monostotic	Polyostotic	Polyostotic	Polyostotic	Polyostotic	Polyostotic	Polyostotic	Polyostotic
	Ground glass appearance	Yes	Yes	Yes	NR	NR	NR	NR
	Undermineralised bone/low bone mineral density	Yes	Yes	Yes	Yes	NR	NR	NR
	Cortical thinning	Yes	NR	Yes	Yes	NR	NR	NR
	Expansile deformity	NR	NR	Yes	Yes	NR	NR	NR
	CT/μCT appearance of lesions	NR	NR	Yes	Yes	Yes	Yes	NR
Histology/histomorphometry features	Woven Bone	Yes	Yes	Yes	Yes	NR	NR	NR
	Abnormal curvilinear trabeculae	Yes	Yes	Yes	Yes	NR	NR	NR
	Loss of hematopoiesis	NR	NR	Yes	NR	NR	NR	NR
	Presence of fibrous-osseous tissue	Yes	Yes	Yes	NR	NR	NR	NR
	Sharpey's fibers	Yes	NR	Yes	Yes	NR	NR	NR
	Abnormally shaped (stellate, retracted) osteoblasts	NR	NR	Yes	NR	NR	NR	NR
	Increased number of osteoclast in fibro-osseous tissue	Yes	Yes	Yes	Yes	NR	NR	NR
	TRAP	Yes	No	Yes	Yes	NR	NR	NR
Histochemical and cellular markers	Increased cAMP	Yes (cells, cAMP assay)	Yes (cells, cAMP assay)	Yes (BT, Pr, pCREB, WB); (cells, cAMP assay)	NR	NR	NR	NR
	Increased ALP		NR			NR		NR

(*continued on next page*)

Table 1 (*continued*)

		Yes (BT, Pr, IHC)		Yes (BT, Pr, IHC, IF)	Yes (BT; mRNA; qRT-PCR)		Yes (BT; mRNA; qRT-PCR)	
	Increased RANKL	Yes (BT, Pr, IHC)	NR	Yes (BT, Pr, IF)	Yes (BT; mRNA; qRT-PCR)	NR	NR	NR
	Increased RANKL/OPG ratio	NR	NR	Yes (BT, mRNA, qRT-PCR)	Yes (US; mRNA; qRT-PCR)	NR	NR	NR
	Increased β-Catenin	NR	NR	NR	Yes (BT; Pr; IHC)	Yes (BT; Pr; IF)	NR	NR
	Increased osteocalcin	NR	NR	No (BT, Pr, IF, IHC)	NR	NR	No (BT; mRNA; qRT-PCR)	NR
	Increased Runx2	NR	NR	Yes (BT, Pr, IF)	NR	NR	Yes (BT; mRNA; qRT-PCR)	NR
	Increased c-fos	NR	NR	NR	NR	NR	NR	Yes (cells; mRNA; qRT-PCR)
	Increased P1NP	No (no change) (serum, Pr, ELISA)	NR	NR	NR	NR	NR	NR
Blood/urine marker	Increased C-telopeptide	No (no change) (serum, Pr, ELISA)	NR	NR	NR	NR	NR	NR
	Increased RANKL	NR	NR	Yes (serum, Pr, ELISA)	NR	Yes (BT; mRNA; qRT-PCR)	NR	NR
	Increased FGF23	NR	NR	NR	NR	NR	NR	NR

bones, spine, short bones, cranium, ribs, and pelvis (eventually affecting the entire skeleton; Fig. 3A). Prrx1 is expressed in skeletal stem cells (in early limb bud mesenchyme and in a subset of craniofacial mesenchyme). Accordingly, the Prrx1-controlled models [36,40,45,46] reported FD-like lesions in the appendicular skeleton. Prrx1-Bastepe and Prrx1-Gutkind also developed lesions in the calvaria region (Fig. 3B) and the Prrx1Yang model displayed affected parietal and inter-parietal regions. Osx promoter allows for expression in osteoblast progenitor cells, throughout the skeleton; however, it remains unclear exactly where lesions appeared as the humerus and cranial bones were the only regions examined in the articles [36,46]. Sox9 promoter ensures expression in mesenchymal precursor cells in the bone marrow region; however, in the article, we only know that it was assessed in humerus [36].

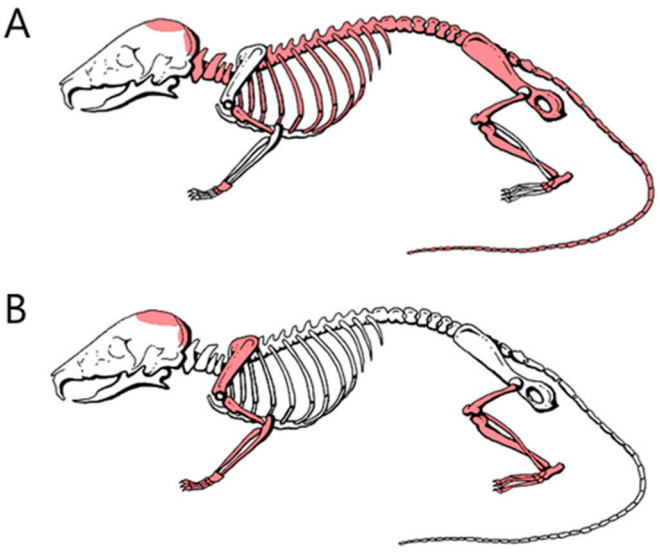

Fig. 3. Illustrative diagrams demonstrating site of reported FD-like lesions in the (A) EF1α- and PGK-Riminucci models, (B) Prrx1-Gutkind and Prrx1-Yang models. Other models are not shown as their full phenotypic expression was not described.

Studies inconsistently reported the sex of the mice (Table 1). Studies using the PGK-Riminucci model and the study on the development of the EF1α-Riminucci model did not report the sex of the mice [36,38,46]. However, the following studies using the EF1α-Riminucci model [47,48], Prrx-Gutkind [40], and the Prrx1-Bastepe model [45] reported the sex of the mice. The studies conducted on embryonic and neonatal mice by the Yang group described that the sex was not determined and both males and females were used in those studies [36,46]; however, the sex of the weaned mice was not reported.

3.1.1. *Clinical features*

All models resulted in deformity due to abnormal bone growth and "FD-like lesions". None of the models assessed whether the induction of FD led to pain in the animal, either due to the disease development or resultant fractures. Microfractures were observed in x-rays and μCT in the EF1α-Riminucci model [38] and the Prrx1-Gutkind model [40].

3.1.2. *Bone imaging - appearance, density, and microarchitecture*

All models developed a polyostotic phenotype of FD. The "ground glass" appearance of FD in x-rays was observed in the EF1α- and PGK-Riminucci models [38], as well as the Prrx1-Gutkind model [40]. Other studies made no mention of this; however, x-ray images of the Prrx1-Yang model [36] demonstrate ground glass opacity. An under-mineralized bone phenotype was presented in the EF1α- and PGK-Riminucci models (as assessed by quantitative backscattered electron microscopy) [38], the Prrx1-Gutkind model (μCT) [40], and the Prrx1-Yang model (μCT) [36]. Cortical bone loss was reported in the EF1α-Riminucci model [38,47,48], the Prrx1-Gutkind model [40], and the Prrx1-Yang model [36]. The Prrx1-Gutkind [40] and Prrx1-Yang model [36] also reported expansile deformity of the FD lesions. The Prrx1-Gutkind [40], Prrx1-Yang, and Osx-Yang [36,46], models all used μCT scans to image skeletal lesions, though the appearance of the lesions by μCT in the Osx-Yang model was not typical of what is seen clinically in FD, instead it showed increased bone mass similar to the Col1a1-Rs1 model described below.

3.1.3. Histology/histomorphometry

Apart from the Prrx1-Bastepe model [45], all models developed lesions with woven bone and variably dense fibrotic tissue, characteristic of human FD, without clear marrow and trabecular regions. These models also demonstrated abnormal curvilinear trabeculae. Only the Prrx1-Gutkind model [40] reported the loss of hematopoiesis. The Prrx1-Gutkind model [40] and EF1α- and PGK-Riminucci models [38] both demonstrated presence of fibro-osseous tissue in the FD lesions. Sharpey's fibers (collagen bundles perpendicularly oriented to the bone surface, characteristic of FD histology) were present in the EF1α-Riminucci model [38], the Prrx1-Gutkind model [40], and the Prrx1-Yang model [36,46]; the Prrx1-Gutkind model [40] also displayed abnormally shaped (stellate, retracted) osteoblasts. The EF1α- and PGK-Riminucci [38,47,48], Prrx1-Gutkind [40], and Prrx1-Yang [36,46] models exhibited an increased number of osteoclasts, confirmed by TRAP staining and histomorphometric analyses. The Osx-Yang model [36] demonstrated hyperostosis in histological images, a finding not typical of FD tissue.

3.1.4. Histochemical and cellular markers

Fibroblast-like FD cells demonstrated a localized, increased ALP protein expression in the EF1α-Riminucci [38] and the Prrx1-Gutkind [40] models. Increased ALP mRNA expression was reported in the Osx-Yang and Prrx1-Yang models [36,46]. The EF1α- and PGK-Riminucci models [38] and the Prrx1-Gutkind model [40] demonstrated an increase of cAMP in cultured bone marrow stromal cells (BMSCs) from their models and the Prrx1-Gutkind model also demonstrated phosphorylated-CREB protein, consistent with increased cAMP signaling. Runx2 protein expression was increased in the Prrx1-Gutkind model and Runx2 mRNA expression in the Osx-Yang model [36,40,46]. The Prrx1-Bastepe model demonstrated increased c-fos gene expression in cultured BMSCs [45]; however, no other studies assessed for c-fos expression in the models. Osteocalcin protein expression was reported as decreased in the Prrx1-Gutkind [40] model BMSCs, and osteocalcin mRNA expression decreased in humerus bone tissue in the Osx-Yang model [36,46], in spite of the fact that serum osteocalcin levels are consistently and often significantly elevated in patients with FD. The EF1α-Riminucci [47] and Prrx1-Gutkind [40] models demonstrated an increased localized protein expression of RANKL in the fibroblast-like FD cells. RANKL and RANKL/OPG mRNA expression was increased in tissue harvested from the Prrx1-Gutkind [40] and Prrx1-Yang (only RANKL) [36,46] models. The Prrx1-Yang and Sox9-Yang models [36,46] demonstrated increased localized protein expression of β-Catenin, which indicates activation of the Wnt/β-Catenin pathway. Finally, the EF1α- and PGK-Riminucci [38,47,48], Prrx1-Gutkind [40], and Prrx1-Yang [36,46] models also demonstrated an increased number of osteoclasts through TRAP staining.

3.1.5. Blood and/or urine markers

Circulating RANKL was increased in the Prrx1-Gutkind [40]. The EF1α-Riminucci model reported no changes in the serum protein of P1NP or C-telopeptide [38,47,48]. None of the studies used urine to test for biomarkers.

3.1.6. Features not investigated

Notably, a number of features observed clinically in FD were not investigated or observed in these models. None of the studies investigated extraskeletal features associated with MAS. In particular, the Riminucci models that exhibit constitutive, ubiquitous expression of the FD-associated *GNAS* mutation might have these extraskeletal features. None of the studies assessed whether the appearance of FD led to pain in the animal, either due to the normal disease development or microfractures. IL-6 was not investigated in any of the *in vivo* models, through histochemical or biomarker analysis. None of the studies reported changes in FGF23 serum levels in their models. Similarly, many of the bone turnover markers were not assessed, nor was the loss of vision, hearing, or ambulation assessed where relevant.

3.2. Models with causative GNAS mutation, but not FD

3.2.1. Col1a1-Bianco model

Remoli et al. [37] developed a model in which $G\alpha_s^{R201C}$ was expressed under the control of the Col1a1 promoter (expressed in differentiating and mature osteoblasts). The model developed a high bone mass phenotype, but not FD. This Col1a1-Bianco model [37] did not demonstrate a reduction of mineralization (quantitative backscattered electron microscopy); instead hyperostosis throughout the whole skeleton was observed. The skeletal architecture observed using μCT did not resemble that observed in FD and hematopoiesis was preserved. There was also a notable absence of fractures and Sharpey's fibers in the model contrary to what is observed in FD patients. However, several features that are also seen in, but are not specific to FD were observed in this model. There was increased, localized ALP protein expression and cultured, mature osteogenic cells from the affected animals demonstrated increased cAMP. Furthermore, BMSCs isolated from affected animals demonstrated a decreased expression of osteocalcin mRNA. Lastly, this model demonstrated that circulating FGF23 increased; however, the mechanism leading to increased FGF23 seems to be different from that in FD.

3.2.2. Sox2-Yang model

The Sox2-Yang model developed by Khan et al. [36] was embryonic lethal and therefore does not develop an FD phenotype. This model was developed in order to express the R201H mutation in embryonic stem cells under the Sox2 promoter to demonstrate that the mutation causes embryonic lethality. The expression of $GNAS^{R201H}$ occurred 5–10 days post fertilization and embryos died between embryonic day 12.5 and 15.5. Further investigation demonstrated an increase in Wnt/β-catenin signaling in the embryo.

3.3. Risk of bias assessment

Most of the studies demonstrated an unclear risk of bias due to a lack of reporting of experimental features of the studies (Fig. 4).

In most of the studies, the method of assigning animals to groups was not defined, particularly regarding which animals were assigned to treatment and control groups. Similarly, it was difficult to assess whether studies included a baseline assessment and whether further measurements were adjusted in line with a baseline assessment. Most studies did not discuss the housing of the animals and whether this occurred randomly or if the test and control subjects were housed together. Only two studies reported using random animals for outcome assessments. Most studies had a low risk of bias with regard to outcome reporting; reporting key outcomes, figures, and significance values. One study failed to report the significance values as calculated, preferring to report when differences were significant, leading to a higher risk of bias.

None of the studies reported blinding of the case and control groups to the assessor, therefore it was unclear if this occurred. Similarly, none of the studies reported blinding the assessor to the intervention used. One study reported that assessors were blinded during outcome assessments, reducing the risk of bias. None of the studies reported attrition bias based on animals not being used for assessments or in the final results. There was no indication that further bias may have occurred, but this was not explicitly stated and remains unclear.

4. Discussion

4.1. Causative model comparison

Although the causative models all contain one of the *GNAS* mutations in FD/MAS under various conditions (*i.e.* promoters, R201C/H mutation, strain, *etc.*), different features have been studied and every

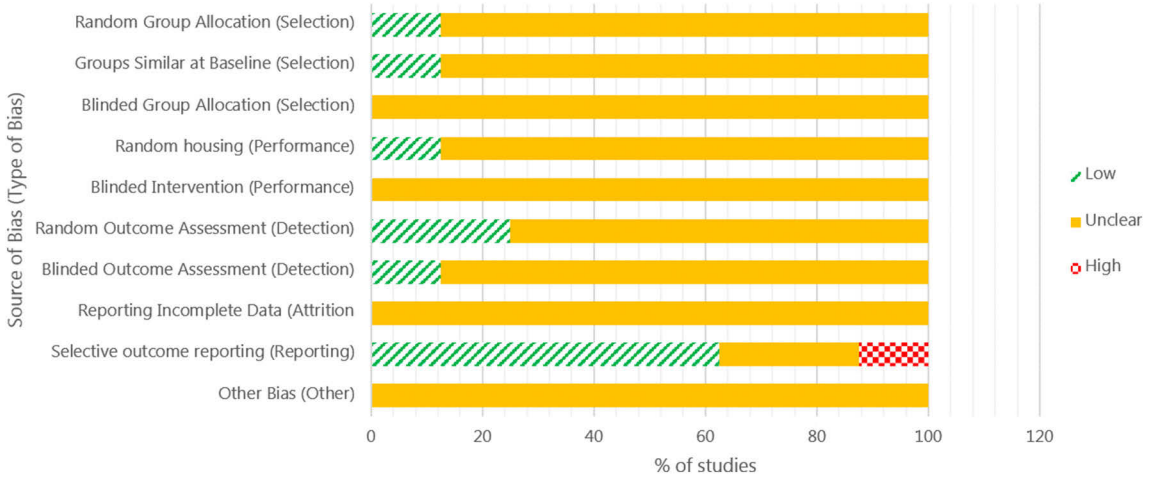

Fig. 4. SYRCLE risk of bias assessment of the included studies. (green = low risk of bias; yellow = unclear risk of bias; red = high risk of bias). (For interpretation of the references to colour in this figure legend, the reader is referred to the web version of this article.)

model presents its own advantages and disadvantages. In order to aid researchers in assessing the model best suited to one's own research, the advantages and disadvantages of these models have been compared in Table 2.

How closely an FD mouse model resembles the observations made in FD patients (*i.e.* face validity) varied among the models. Generally, all models assessed some of the major features of FD, such as deformity, radiographic ground glass appearance, bone undermineralization, and elevated ALP levels. However, some features were only explored in one model, providing greater information about the model and its face validity. Except for the Prrx1-Bastepe, Sox2-Yang, and Col1a1-Bianco models, all the models reported good face validity, producing many of the same features of FD that are observed in patients. The Prrx1-Bastepe model [45] assessed few features of FD, assessing only c-fos expression and deformity. The Sox2-Yang model [36] expressed the *GNAS*^{R201H} mutation in early embryonic stem cells in order to determine if the mutation resulted in embryonic lethality. This was successfully demonstrated as the mice did not develop to term. However, given that it did not develop to term, it is not appropriate to assess the face validity of the model as a model of FD, *per se*. The model does, however, provide valuable information about the formation of an affected individual with early expression of the mutation, but cannot be used as an appropriate model to study FD. The Col1a1-Bianco model [37] has poor face validity of FD as it failed to produce FD-like lesions. While this model would not be appropriate for further research in FD, it does yield interesting information. When mutated *GNAS* is expressed in skeletal stem cells and their progeny, an FD phenotype is produced, but when expressed in osteoblasts or committed osteoprogenitors, a high bone mass phenotype that is not representative of FD is produced (Col1a1, Osx promoters). This need for the presence of mutated SSCs to generate the characteristic fibro-osseous lesions supports the notion that FD is a stem cell disease and makes these models a valuable tool to further understand this phenomenon [49]. It is also important to note that the FD-like features observed in the Col1a1-Bianco model do not indicate that FD has developed, but rather, these features occur due to increased osteogenic activity. A notable exception to the face validity is the observed levels of osteocalcin. The literature demonstrates the blood levels of osteocalcin are elevated and that osteocalcin is increased in FD tissue (IHC) [32], but the Prrx1-Gutkind [40] (IHC, IF), Osx-Yang [36,46] (mRNA expression in tissue samples), and Col1a1-Bianco [37] (mRNA expression in cultured cells from model) models all demonstrated decreased osteocalcin. Furthermore, the EF1α-Riminucci model did not demonstrate changes in serum levels of P1NP or C-telopeptide. To determine if this may be due to age, serum may be evaluated at different developmental stages and other models may also be assessed for changes in bone turnover markers [38,47,48].

The EF1α-Riminucci model [38,47,48] was the only model used to test treatments of FD; anti-RANKL monoclonal antibody and zoledronic acid were studied in order to determine the effects of these drugs *in vivo*. The findings were impressive and consistent with early clinical reports of efficacy of anti-RANKL antibody treatment in patients. This demonstrates the ability of these models to test the mechanisms and efficacy of drugs that have been used for FD treatment [19,20]. However, FD is a highly variable disease, yet the animal models are is homogeneous and each model may only represent some aspects of the disease. The Prrx1-Gutkind model was the only model to assess and describe cell body

Table 2
Key features, advantages, and disadvantages of *in vivo* FD models (✓ = advantage of the model; × = disadvantage of the model; "-" = no advantage/disadvantage; EF1α = elongation factor-1 alpha; PGK = phosphoglycerate kinase-1; Prrx1 = paired related homeobox-1; Sox9 = sex determining region Y-box 9; Osx = osterix; GNAS = guanine nucleotide-binding protein alpha subunit; MAS = McCune-Albright Syndrome; Tet = tetracycline; Tam = tamoxifen).

		EF1α-Riminucci[35,44,45]	PGK-Riminucci[35]	Prrx1-Gutkind[37]	Prrx1-Yang[33,43]	Sox9-Yang[33]	Osx-Yang[33,43]	Prrx1-Bastepe[42]
Face validity		✓	✓	✓	✓	?	?	–
Time of onset – practical application		×	×	✓	✓	✓	✓	✓
Mouse strain purity		×	×	×	×	×	×	×
Construct validity (GNAS Source)		×	×	✓	×	×	×	×
Mosaicism	Mosaic-like gene expression	–	–	✓	✓	✓	?	✓
	Mosaic-like phenotype	✓	✓	✓	✓	✓	✓	✓
Tamoxifen/tetracycline-dependent *GNAS* expression		–	–	✓ (Tet)	–	✓ (Tam)	✓ (Tet)	–
Potential induction of MAS		✓	✓	×	×	×	×	×

retraction in osteoblasts and lining cells (sometimes described as absence of bone rimming cells). FGF23 elevation is an important marker of disease severity, as well as a contributor to morbidity through renal phosphate wasting, which could further impact bone health. Berosumab (a human recombinant monoclonal antibody to FGF23) has been assessed in an FD/MAS case study, demonstrating a possible treatment option for FD/MAS patients. However, FGF23 was only reported in the Col1a1-Bianco model, but given the poor face validity of the model it would not be appropriate to further study this marker in this model. Nevertheless, animal models provide a great advantage in that they provide a large homogenous sample size to assess safety and efficacy. Thus the models demonstrating good face validity of FD may be suitable to further assess FGF23, its impact, and possible treatments.

The difference in time to onset of the FD phenotype in the different FD mouse models may be accompanied by both practical and validity concerns. The Riminucci group models have a relatively [38,47] long time to onset, reporting FD in the tail at approximately 2–3 months post-partum and are fully expressed at 1 year. This long natural history may be beneficial if wanting to perform long term tests. However, in order to develop and maintain these models in a laboratory and to use them for long-term tests, significant time and resources would be necessary. This may not be practical for some researchers. The other seven models [36,37,40,45,46] have a relatively fast time of onset, which is practically beneficial and if induced early during development, may better mimic what is observed in patients with FD [4].

In the Prrx1-Gutkind [40], the expression of $G\alpha_s^{R201C}$ is tetracycline-dependent, allowing the phenotype to be turned on and off at different stages of development, or stop the expression of the gene to assess FD lesion regression. This allows not only a better control of the phenotype, but also the pathogenic gene cessation, which leads to the regression of the lesions. This could be used to serve as a positive control to assess the therapeutic effect of drugs under investigation.

Inbred mouse strains have a defined genetic background that does not vary widely between animals within the strain, thus leading to a replicable phenotype. However, as is often the case for transgenic mice, most of the causative FD mouse models have a mixed strain backgrounds, which leads to variability in the findings [50]. This can be remedied by backcrossing into one strain. The Yang group's models [36,46] did not clearly state the strains used and how they were bred. Not only does this make it more difficult to assess which strains were used and the phenotype they would contribute to the model, but also makes it challenging for other investigators to replicate the same mouse model.

It is an open question as to whether the host's native mutated gene or a human construct provides better fidelity to the human disease and thus greater construct validity. When using the mouse gene, the native physiology can be preserved, but the true nature of the mutated gene might not be revealed and *vice versa* [51]. The construct validity is best established in the Prrx1-Gutkind model [40], which uses a mutated human $GNAS^{R201C}$ construct in the transgenic mouse. This human construct could be advantageous for testing drugs that specifically target the human protein *in vivo*. The Yang group's models [36,46] use a mouse $Gnas^{R201H}$ knock-in. Notably, *GNAS* is highly conserved between mice and humans (>90% identity). Using a model with the endogenous promoter and gene maintains the normal gene site, regulatory elements and minimizes the number of genes inserted into the mouse. This could favor the normal physiological features of the mouse and not introduce genetic disturbance. In transgenic models of human diseases this conflict will always present itself and it is not possible to say with the current data, which construct is best suited to creating an FD model.

Sex differences were not reported in any of the studies. Three studies reported the use of both male and female mice in their studies; however, sex-based comparisons were not reported [40,45,47]. FD may be influenced by hormone changes, particularly if MAS occurs in endocrine tissues. Further studies on these models should report sex differences as they may impact mechanisms of the disease and treatments.

Somatic mosaicism is a key feature of FD/MAS. Some cells harbor the *GNAS* mutation, but the remaining majority do not; as such, certain skeletal sites may develop FD due to the presence of cells with the genetic mutation. The precise cause of the post-zygotic mutations that are responsible for FD/MAS are challenging to mimic *in vivo*. However, true replication of a random post-zygotic mutation would result in variability between animals, which would be experimentally disadvantageous. Instead, a mosaic-like phenotype in which all cells have the genetic mutation, but expression of the gene is limited to certain skeletal cells or sites has been generated in several models. This feature is favorable for some reasons in a research model, such as to reduce variability and thus reduce the number of mice needed. The Sox9-Yang model [36] reported that it initially established a mosaic state, but the mosaicism could not be preserved. When Tamoxifen is administered to these mice, it generates a subset of cells that will express $Gnas^{R201H}$. When the administration is stopped the affected cells and their progeny continue to express $Gnas^{R201H}$ and unaffected cells will not. Thus, a mosaic state is generated, but cannot be sustained throughout the animal's lifetime. The three models using the Prrx1 promoter [36,40,45,46] limited $GNAS^{R201H}$ expression to certain skeletal sites (Fig. 3). The models developed by Riminucci et al. [38,47] demonstrate a mosaic-like phenotype throughout most of their development (Fig. 3), except in the very late stages in which FD affects the whole skeleton. While true somatic mosaicism was not developed in any of the reported models, all models developed some degree of phenotypic mosaicism, except the Sox2-Yang model [36,37,40,45,46]. Other mosaic-like phenotypes may be able to be generated through the creation of chimera models of FD. Mosaicism in these animal models is a complex subject that is achieved at varying levels in almost all these models. This aspect of the phenotype in these models is challenging and researchers should be aware of the features and limitations when selecting a model for their study.

Only in the Riminucci models [38,47] is the $GNAS^{R201C}$ mutation both constitutively and ubiquitously expressed. It is puzzling that the models can develop to term and not suffer embryonic lethality, which is assumed to happen if the mutation occurs very early in development, as seen with the Sox2-Yang models [36]. Due to the ubiquitous expression, further investigation of these models to assess whether endocrinopathies have developed as in MAS, would be beneficial. It might be that in the Riminucci models [38,47] only the transgenic embryos with lower expression of the transgene were *de facto* selected by being able to develop to term. Alternatively, it is possible that the lack of embryo lethality is due to the random integration of the transgene into a region of the genome allowing viability. Further studies with these models could provide insight into the mechanisms underlying the effect of the *GNAS* mutation in embryonic development.

As previously stated, the Prrx1 promoter is expressed in skeletal stem cells in early limb bud mesenchyme and a subset of craniofacial mesenchyme. This was utilized to control Cre expression in three different models, by three different teams, with different strategies; these were the Prrx1-Gutkind [40], Prrx1-Yang [36,46], and Prrx1-Bastepe [45] models. Upon expression of Cre, the Prrx1-Gutkind model [40] activated the constitutive expression of reverse tetracycline transactivator in order to establish a tetracycline-inducible model. In the Prrx1-Bastepe [45] model, expression of Cre led to a constitutive expression of $G\alpha_S^{R201H}$, and in the Prrx1-Yang [36,46] model Cre enabled the replacement of the one of the endogenous *Gnas* alleles by $Gnas^{R201H}$. The Prrx1-Gutkind model [40] used a human construct of $G\alpha_S^{R201C}$, Prrx1-Yang [36,46] used the endogenous $Gnas^{R201H}$, and Prrx1-Bastepe [45] utilized a rat $G\alpha_S^{R201H}$. The Prrx1-Gutkind [40] and Prrx1-Yang [36,46] model had a time of onset of approximately two weeks from induction and the Prrx1-Bastepe model [45] developed within the first three weeks of life. All three models developed in the appendicular skeleton and areas of the parietal bones. The Prrx1-Gutkind [40] and Prrx1-Yang model [36,46] assessed many of the same features. The Prrx1-Bastepe model [45], however, developed a very mild FD phenotype and assessed few characteristics of FD. The mild

phenotype observed in this model could be due to a weaker expression by the CAG promoter, as Karaca et al. discuss in the publication, highlighting the importance of suitable promoters to develop an *in vivo* model [45].

4.2. Mechanistic models sub-analysis

During screening, fifteen articles emerged that did not have the R201 (or rare Q227) *GNAS* mutation but reported FD or FD-like lesions in the animal model. These models do not fulfil the inclusion criteria for full qualitative assessment but do provide valuable information about the mechanisms that contribute to the FD phenotype and may reveal potential therapeutic targets. Supplementary Table 1 summarizes these models as well as the FD features they exhibit and features that indicate that a true FD phenotype may not have been generated. The mechanistic model names were generated according to the promoter used and the target gene. It is important to note that in all of the models presented here, a causal link was not established.

Of the 15 studies included, 8 unique models were reported in which FD-like lesions developed when specific transgenes were expressed. One model was reported in six studies [52–57] in which a serotonin receptor was engineered to form Rs1 that can only be activated by a synthetic ligand, avoiding activation by host ligands. This mutated gene was placed under the control of the Col1a1 promoter, limiting expression to osteoblasts. Across the six studies, various features of FD were established, such as deformity, reduced number of hematopoietic cells, increased number of bone marrow stromal cells, increased number of osteoclasts, a change in bone turnover markers, as well as an increase of RANKL and the RANKL/OPG ratio. However, the model consistently demonstrated increased bone mineral density and a high bone mass phenotype, which is remarkably different from the undermineralized fibroosseous tissue containing Sharpey's fibers in FD. Interestingly, this same phenotype was generated in the Col1a1-Bianco model [37] that used the Col1a1 promoter to express mutant *GNAS*^{R201C} in mature osteoblasts. Given its similarity to the Col1a1-Bianco model, it can be hypothesized that expression of Rs1 under a promoter that is also expressed in BMSCs/skeletal stem cells (SSCs) (*e.g.* EF1α, PGK, Prrx1, Sox9) may yield an FD-like phenotype.

Several studies have explored signaling pathways or hormones believed to be involved in the pathology of FD/MAS [58–61]. cAMP binds to regulatory subunits of PKA, releasing the activated subunits, which are then able to phosphorylate numerous other proteins [62]. A minority of patients with Carney complex – a disease due to gain-of-function mutations in PKA subunits, downstream of cAMP, develop bone lesions with some of the features of FD [63], supporting the assertion that FD lesion formation is mediated through downstream PKA activity [59–61,64,65]. A model in which one allele of protein kinase cAMP-dependent type I regulatory subunit alpha (Prkar1a) gene was deleted, led to an increased ubiquitous activation of PKA through increased cAMP-responsive PKA activity. This Prkar1a haploinsufficiency model presented skeletal deformity, showing undermineralized woven bone with persisting chondrocytes in the bone matrix, and increased number of osteoclasts. Increased levels of ALP and c-fos expression were observed. It demonstrated some features that are absent in FD, including normal osteoblast rimming of the trabeculae, increased Runx2 and decreased osteocalcin in fibroblast-like cells in the tissue lesion (immunolocalization). Further, because Prkar1a and Prkaca haploinsufficiency lead to cyclooxygenase activation and prostaglandin E2 production, inhibition of this pathway with celecoxib, a cyclooxygenase-2 inhibitor inhibited FD-like lesions [60]. Taken together, these data, support the notion that the development of FD is due on the activation of Gas/AC/PKA pathway.

Parathyroid hormone (PTH) and PTH-related protein (PTHrP) receptor 1 (PTH1R) is a GPCR that signals, at least in part, through G_S alpha, cAMP, and PKA. Mouse models of PTH1R hyperactivation (similar to Jansen's metaphyseal chondrodysplasia) partially mimic FD [66,67]. These transgenic mice demonstrated skeletal deformity, a reduced number of hematopoietic cells, an accumulation of fibrous tissue in the bone and an increased number of osteoclasts, all similar to that observed in FD. However, the model also demonstrated increased mineral apposition rate and high bone mass, which does not resemble FD, possibly due to the use of the Col1a1 promoter, that targets differentiating osteoblasts and not BMSCs/SSCs.

The Wnt/β-catenin pathway has been implicated in numerous disorders due to its function of activating the expression of transcription factors that control a wide variety of developmental processes [68]. Several animal models explored the relation of β-catenin and FD/MAS. The Col1a1-β-catenin model [69] expressed constitutively active β-catenin in osteoprogenitor cells and resulted in an increased number of fibroblasts in the bone marrow, but hematopoiesis was preserved. The Osx-β-catenin model [70] demonstrated undermineralized bone and reduced hematopoiesis. This mechanistic model may be comparable to the causative Osx-Yang model, which assessed the Wnt/β-catenin signaling pathway [36,46] and demonstrated that *Gnas*^{R201H} regulates it. Xu et al. postulate [46] that the constitutively active $G\alpha_S$ signaling increases Wnt/β-catenin, thus preventing the osteoblast maturation. The Col1a1-β-catenin model, Osx-β-catenin, Osx-Yang model, and Prrx1-Yang model may be further studied and compared to elucidate the possible role of the Wnt/β-catenin pathway.

The proto-oncogene c-fos is indirectly induced by cAMP [71], leading to the speculation that c-fos expression may play a role in the development of FD/MAS. Previous studies have demonstrated that c-fos expression is significantly higher in FD bone lesions compared to healthy subjects as well as patients with other bone disorders [72]. The hMT-c-fos model [73] with ubiquitous, increased gene expression of c-fos demonstrated an FD-like phenotype with skeletal abnormalities, including deformity, undermineralized bone, woven trabecular bone with cartilaginous areas, and increased ALP. The Col1a1-c-fos model [74] – where c-fos was expressed in osteoblasts – demonstrated an increase of periostin protein expression; however, the study conducted on these mice was limited and other features of FD were not assessed. As the hMT-c-fos model [73] was established and assessed in 1987, updated assessments and model development may be beneficial.

4.3. Implant models

Studies that conducted *in vivo* transplantation of cells into mice were ultimately excluded from qualitative assessment; however, these models have significant merit and warrant discussion as they provide the opportunity to study human FD lesions *in vivo* and in a controlled experimental setting. Briefly, seven studies reported a transplant model (of these, one article reported both a transplant and mechanistic model, so it was classified as a mechanistic study [67]) in which FD cells were transplanted into a mouse. All studies transplanted immunocompromised mice with FD cells and an osteoconductive scaffold subcutaneously in order to develop an FD-like lesion; all studies included a healthy control implant [39,67,75–79]. Apart from one study, which implanted stromal cells from a mechanistic model mouse (Col1a1-HKrKH223R model) into nude mice [67], all the studies injected implant material from human subjects [39,75–79]. In the latter studies, BMSCs were extracted from human FD tissue or healthy bone marrow and expanded *in vitro*. After 6–8 weeks following transplantation, an FD-like lesion formed in all the models in which the FD-like woven bone was observed. Bianco et al. were the first to demonstrate a transplant model of fibroblast-like FD cells and reported that an “ossicle” formed subcutaneously that resembled FD lesions observed in human patients [77] and was also confirmed in the study by Kuznetsov et al. [67]. Five studies demonstrated that FD cells need to be mixed with wild type cells from the same patient before transplantation otherwise they will not grow and form a lesion. This demonstrates that mosaicism is not only a feature of FD/MAS, but likely necessary in order for the FD/MAS phenotype to develop [39,75,76,79]. One of these studies also demonstrated that

histone deacetylase 8 (HDAC-8) may be a therapeutic target for FD, but further studies are required [78]. One study demonstrated that the CREB-Smad6-Runx2 axis may play a role in the development of the FD phenotype [76].

4.4. Current gaps and future directions

Endocrinopathies are an important feature of MAS and their impact on FD has not been addressed in any of the causative models. The literature search did not yield any animal models that generated a MAS-like phenotype, however a transgenic mouse model in which R201H was expressed in a thyroid specific manner led to hyperthyroidism [80]. Abnormal hormone production may affect the development of FD and normal bone as well as FD treatments. This has been discussed previously [81]; however, a study has not yet been reported. The Riminucci models [38,47] might have the capacity to develop additional features of MAS phenotype given the ubiquitous expression of the gene (*i.e.* endocrinopathies, skin macules). However, the global expression of GNAS is not expected to be the unique determinant involved in the development of extra-skeletal features of MAS. For instance, selective expression of an active $G\alpha_s$ mutant in cells of the limb mesenchymal bud or in skeletal stem/osteoprogenitor cells [34,39,43,49] could also be associated with a skeletal muscle phenotype.

On the other hand, hormones may be administered to the available FD models to determine how various hormonal perturbations may influence the FD phenotype. For example, Akintoye et al. demonstrated that patients with excess growth hormone exhibited more severe craniofacial FD than FD/MAS patients with normal growth hormone levels [82]. Although the treatment with exogenous hormones has poor construct validity in comparison to a *GNAS* mutation-associated endogenous production, it would facilitate elucidating the influence of hyperregulated hormones in MAS, as the composition and dosage of the hormones would be controlled and thus, more replicable between mice.

Numerous features of FD were not investigated in any of the causative models, and some features were insufficiently examined to yield conclusive information. Pain, FGF23 and cytokines production by FD lesions, extra skeletal changes indicative of MAS, and several bone turnover markers were not assessed in any of the models. Further investigation into these areas in the established causative models would be beneficial, and for treatment studies one could implement methodologies currently used in the clinic such as pre- and post-treatment 18F NaF PET/CT scans. Pain is an important, but variable feature of FD that has a remarkable impact on a patient's quality-of-life [6]. However, the widespread FD disease burden of the animal models might provide a challenge for pain behavioral testing. One should consider employing behavioral measures assessing whole body pain/well-being rather than reflexive measures and validate the findings with analgesics. Furthermore, extensive samples can be taken from these models in order to discern the mechanisms. Pre-clinical models may provide information about the disease and pain at various stages in order to elucidate alterations in the phenotype.

4.5. Limitations and conclusion

Articles were included or excluded based on whether the studies claimed to have developed an FD-like phenotype, rather than on an independent fact-based assessment of the generation of an FD-like phenotype. This demonstrates the complexity of classifying the disease: features on their own are not enough to identify the disease, but rather, numerous key features of FD in combination need to be present before it can be classified as such. Therefore, in addition to using an appropriate causative or mechanistic genetic strategy, tests at various levels, including clinical observation, imaging, histology, and serology must be done to assess a possible FD-like phenotype. Furthermore, the selected images and data presented in most studies are often insufficient to classify the disease, relying solely on the reports from the authors. The methodology and results reported in these studies led to an unclear risk of bias. This may affect the reproducibility of the work conducted in these studies, as there may be changes in conditions and environment if the study were to be conducted by an independent researcher.

This paper excluded *ex vivo* and *in vitro* studies, which would aid in highlighting the broad spectrum of the models currently available and the information they yield. A full systematic study of these models and the models discussed in this article would be vast and each area may not be thoroughly explored if combined. A similar analysis of the various mechanistic models of FD and the implications of their results on clinical applications would be beneficial.

In conclusion, there are numerous causative *in vivo* models that generate an FD phenotype. These models have various capabilities that can be used for different needs, depending on the subject under investigation. These models can be used for a wide variety of applications, including – but not limited to – investigating mechanisms that contribute to the FD phenotype, identifying therapeutic targets, understanding the mechanisms of action of current therapeutic agents, and testing new therapeutic agents for FD. Other models have also been created that do not represent an FD phenotype, but nevertheless inform the mechanisms involved in FD. FD/MAS is a rare genetic disorder that is associated with significant morbidity. The development of robust *in vivo* models of FD/MAS, such as those discussed here, will not only advance our understanding of bone biology in general, but also undoubtedly advance our understanding of the pathomechanism of FD and certainly contribute to progress in treating patients with FD so as to relieve their suffering. As DiGeorge remarked in 1975 on the topic of Albright Syndrome: “A rare disorder, yes; an unimportant one, never.” [83].

Supplementary data to this article can be found online at https://doi.org/10.1016/j.bone.2021.116270.

Funding

Anne-Marie Heegaard and Chelsea Hopkins receive funding from the European Union's Horizon 2020 research and innovation programme under the Marie Skłodowska-Curie grant agreement no. 814244.

Michael T. Collins, Alison M. Boyce, and Luis Fernandez de Castro are funded by the Division of Intramural Research of the National Institute of Dental and Craniofacial Research, National Institutes of Health, Bethesda, MD.

Mara Riminucci and Alessandro Corsi receive funding from University of Pennsylvania Orphan Disease Center in partnership with the Fibrous Dysplasia Foundation (MDBR-19-110-FD/MAS) and Sapienza University (RM11916B839074A8 to Mara Riminucci and RP11715C7C4DC57A and RM118164289636F0 to Alessandro Corsi).

CRediT authorship contribution statement

Chelsea Hopkins: Conceptualization, Data curation, Formal analysis, Methodology, Validation, Visualization, Writing – original draft, Writing – review & editing. **Luis Fernandez de Castro:** Conceptualization, Formal analysis, Validation, Visualization, Writing – original draft, Writing – review & editing. **Alessandro Corsi:** Conceptualization, Validation, Writing – original draft, Writing – review & editing. **Alison Boyc:** Conceptualization, Validation, Writing – original draft, Writing – review & editing. **Michael T. Collins:** Conceptualization, Validation, Writing – original draft, Writing – review & editing. **Mara Riminucci:** Conceptualization, Validation, Writing – original draft, Writing – review & editing. **Anne-Marie Heegaard:** Conceptualization, Funding acquisition, Project administration, Supervision, Validation, Visualization, Writing – original draft, Writing – review & editing.

Declaration of competing interest

None of the authors have conflicts of interest to declare.

References

[1] A.I. Leet, S. Wientroub, H. Kushner, B. Brillante, M.H. Kelly, P.G. Robey, M. T. Collins, The correlation of specific orthopaedic features of polyostotic fibrous dysplasia with functional outcome scores in children, J. Bone Joint Surg. Am. 88 (4) (2006) 818–823.

[2] I. Hartley, M. Zhadina, M.T. Collins, A.M. Boyce, Fibrous dysplasia of bone and McCune-albright syndrome: a bench to bedside review, Calcif. Tissue Int. 104 (5) (2019) 517–529.

[3] B.C.J. Majoor, C.D. Andela, C.R. Quispel, M. Rotman, P.D.S. Dijkstra, N.A. T. Hamdy, A.A. Kaptein, N.M. Appelman-Dijkstra, Illness perceptions are associated with quality of life in patients with fibrous dysplasia, Calcif. Tissue Int. 102 (1) (2018) 23–31.

[4] E.S. Hart, M.H. Kelly, B. Brillante, C.C. Chen, N. Ziran, J.S. Lee, P. Feuillan, A. I. Leet, H. Kushner, P.G. Robey, M.T. Collins, Onset, progression, and plateau of skeletal lesions in fibrous dysplasia and the relationship to functional outcome, J. Bone Miner. Res. 22 (9) (2007) 1468–1474.

[5] M.H. Kelly, B. Brillante, M.T. Collins, Pain in fibrous dysplasia of bone: age-related changes and the anatomical distribution of skeletal lesions, Osteoporos. Int. 19 (1) (2008) 57–63.

[6] A. Tucker-Bartley, J. Lemme, A. Gomez-Morad, N. Shah, M. Veliu, F. Birklein, C. Storz, S. Rutkove, D. Kronn, A.M. Boyce, E. Kraft, J. Upadhyay, Pain phenotypes in rare musculoskeletal and neuromuscular diseases, Neurosci. Biobehav. Rev. 124 (2021) 267–290.

[7] R.D. Chapurlat, D. Gensburger, J.M. Jimenez-Andrade, J.R. Ghilardi, M. Kelly, P. Mantyh, Pathophysiology and medical treatment of pain in fibrous dysplasia of bone, Orphanet. J. Rare Dis. 7 (Suppl 1) (2012) S3.

[8] M.H. Kelly, B. Brillante, H. Kushner, P. Gehron Robey, M.T. Collins, Physical function is impaired but quality of life preserved in patients with fibrous dysplasia of bone, Bone 37 (3) (2005) 388–394.

[9] E. Ippolito, P. Farsetti, A.M. Boyce, A. Corsi, F. De Maio, M.T. Collins, Radiographic classification of coronal plane femoral deformities in polyostotic fibrous dysplasia, Clin. Orthop. Relat. Res. 472 (5) (2014) 1558–1567.

[10] L.S. Weinstein, G(s)alpha mutations in fibrous dysplasia and McCune-albright syndrome, J. Bone Miner. Res. 21 (Suppl 2) (2006) P120–P124.

[11] A.I. Leet, A.M. Boyce, K.A. Ibrahim, S. Wientroub, H. Kushner, M.T. Collins, Bone-grafting in polyostotic fibrous dysplasia, J. Bone Joint Surg. Am. 98 (3) (2016) 211–219.

[12] P. Florenzano, K.S. Pan, S.M. Brown, S.M. Paul, H. Kushner, L.C. Guthrie, L.F. de Castro, M.T. Collins, A.M. Boyce, Age-related changes and effects of bisphosphonates on bone turnover and disease progression in fibrous dysplasia of bone, J. Bone Miner. Res. 34 (4) (2019) 653–660.

[13] M. Riminucci, L.W. Fisher, A. Shenker, A.M. Spiegel, P. Bianco, P. Gehron Robey, Fibrous dysplasia of bone in the McCune-albright syndrome: abnormalities in bone formation, Am. J. Pathol. 151 (6) (1997) 1587–1600.

[14] M.K. Javaid, A. Boyce, N. Appelman-Dijkstra, J. Ong, P. Defabianis, A. Offiah, P. Arunde, N. Shaw, V.D. Pos, A. Underhil, D. Portero, L. Heral, A.M. Heegaard, L. Masi, F. Monsell, R. Stanton, P.D.S. Dijkstra, M.L. Brandi, R. Chapurlat, N.A. T. Hamdy, M.T. Collins, Best practice management guidelines for fibrous dysplasia/McCune-albright syndrome: a consensus statement from the FD/MAS international consortium, Orphanet. J. Rare Dis. 14 (1) (2019) 139.

[15] A.I. Leet, M.T. Collins, Current approach to fibrous dysplasia of bone and McCune-albright syndrome, J. Child. Orthop. 1 (1) (2007) 3–17.

[16] A. Corsi, M.T. Collins, M. Riminucci, P.G. Howell, A. Boyde, P.G. Robey, P. Bianco, Osteomalacic and hyperparathyroid changes in fibrous dysplasia of bone: core biopsy studies and clinical correlations, J. Bone Miner. Res. 18 (7) (2003) 1235–1246.

[17] R.D. Chapurlat, P. Orcel, Fibrous dysplasia of bone and McCune-albright syndrome, Best Pract. Res. Clin. Rheumatol. 22 (1) (2008) 55–69.

[18] B.C.J. Majoor, S.E. Papapoulos, P.D.S. Dijkstra, M. Fiocco, N.A.T. Hamdy, N. M. Appelman-Dijkstra, Denosumab in patients with fibrous dysplasia previously treated with bisphosphonates, J. Clin. Endocrinol. Metab. 104 (12) (2019) 6069–6078.

[19] A.M. Boyce, W.H. Chong, J. Yao, R.I. Gafni, M.H. Kelly, C.E. Chamberlain, C. Bassim, N. Cherman, M. Ellsworth, J.Z. Kasa-Vubu, F.A. Farley, A.A. Molinolo, N. Bhattacharyya, M.T. Collins, Denosumab treatment for fibrous dysplasia, J. Bone Miner. Res. 27 (7) (2012) 1462–1470.

[20] M.E. Meier, S.N. Clerkx, E.M. Winter, A.M. Pereira, A.C. van de Ven, M.A.J. van de Sande, N.M. Appelman-Dijkstra, Safety of therapy with and withdrawal from denosumab in fibrous dysplasia and McCune-albright syndrome: an observational study, J. Bone Miner. Res. 36 (9) (2021) 1729–1738.

[21] H. Lung, E.C. Hsiao, K.L. Wentworth, Advances in models of fibrous Dysplasia/McCune-albright syndrome, Front. Endocrinol. (Lausanne) 10 (2019) 925.

[22] L.F. de Castro, A.B. Burke, H.D. Wang, J. Tsai, P. Florenzano, K.S. Pan, N. Bhattacharyya, A.M. Boyce, R.I. Gafni, A.A. Molinolo, P.G. Robey, M.T. Collins, Activation of RANK/RANKL/OPG pathway is involved in the pathophysiology of fibrous dysplasia and associated with disease burden, J. Bone Miner. Res. 34 (2) (2019) 290–294.

[23] A. Sakamoto, Y. Oda, Y. Iwamoto, M. Tsuneyoshi, A comparative study of fibrous dysplasia and osteofibrous dysplasia with regard to gsalpha mutation at the Arg201 codon: polymerase chain reaction-restriction fragment length polymorphism analysis of paraffin-embedded tissues, J. Mol. Diagn. 2 (2) (2000) 67–72.

[24] B.C.J. Majoor, C.D. Andela, J. Bruggemann, M.A.J. van de Sande, A.A. Kaptein, N. A.T. Hamdy, P.D.S. Dijkstra, N.M. Appelman-Dijkstra, Determinants of impaired quality of life in patients with fibrous dysplasia, Orphanet. J. Rare Dis. 12 (1) (2017) 80.

[25] N.D. Riddle, M.M. Bui, Fibrous dysplasia, Arch. Pathol. Lab. Med. 137 (1) (2013) 134–138.

[26] R.D. Chapurlat, P.J. Meunier, Fibrous dysplasia of bone, baillieres, Best Pract. Res. Clin. Rheumatol. 14 (2) (2000) 385–398.

[27] M.R. DiCaprio, W.F. Enneking, Fibrous dysplasia: pathophysiology, evaluation, and treatment, JBJS 87 (8) (2005) 1848–1864.

[28] M. Riminucci, B. Liu, A. Corsi, A. Shenker, A.M. Spiegel, P.G. Robey, P. Bianco, The histopathology of fibrous dysplasia of bone in patients with activating mutations of the gs alpha gene: site-specific patterns and recurrent histological hallmarks, J. Pathol. 187 (2) (1999) 249–258.

[29] K.A. Fitzpatrick, M.S. Taljanovic, D.P. Speer, A.R. Graham, J.A. Jacobson, G. R. Barnes, T.B. Hunter, Imaging findings of fibrous dysplasia with histopathologic and intraoperative correlation, AJR Am. J. Roentgenol. 182 (6) (2004) 1389–1398.

[30] R.S. Weinstein, Long-term aminobisphosphonate treatment of fibrous dysplasia: spectacular increase in bone density, J. Bone Miner. Res. 12 (8) (1997) 1314–1315.

[31] N. Bhattacharyya, M. Wiench, C. Dumitrescu, B.M. Connolly, T.H. Bugge, H. V. Patel, R.I. Gafni, N. Cherman, M. Cho, G.L. Hager, M.T. Collins, Mechanism of FGF23 processing in fibrous dysplasia, J. Bone Miner. Res. 27 (5) (2012) 1132–1141.

[32] S. Toyosawa, M. Yuki, M. Kishino, Y. Ogawa, T. Ueda, S. Murakami, E. Konishi, S. Iida, M. Kogo, T. Komori, Y. Tomita, Ossifying fibroma vs fibrous dysplasia of the jaw: molecular and immunological characterization, Mod. Pathol. 20 (3) (2007) 389–396.

[33] H. Guerin Lemaire, B. Merle, O. Borel, D. Gensburger, R. Chapurlat, Serum periostin levels and severity of fibrous dysplasia of bone, Bone 121 (2019) 68–71.

[34] J.B. Regard, N. Cherman, D. Palmer, S.A. Kuznetsov, F.S. Celi, J.M. Guettier, M. Chen, N. Bhattacharyya, J. Wess, S.R. Coughlin, L.S. Weinstein, M.T. Collins, P. G. Robey, Y. Yang, Wnt/beta-catenin signaling is differentially regulated by galpha proteins and contributes to fibrous dysplasia, Proc. Natl. Acad. Sci. U. S. A. 108 (50) (2011) 20101–20106.

[35] C.R. Hooijmans, M.M. Rovers, R.B. de Vries, M. Leenaars, M. Ritskes-Hoitinga, M. W. Langendam, SYRCLE's risk of bias tool for animal studies, BMC Med. Res. Methodol. 14 (2014) 43.

[36] S.K. Khan, P.S. Yadav, G. Elliott, D.Z. Hu, R. Xu, Y. Yang, Induced Gnas(R201H) expression from the endogenous gnas locus causes fibrous dysplasia by up-regulating Wnt/beta-catenin signaling, Proc. Natl. Acad. Sci. U. S. A. 115 (3) (2018) E418–E427.

[37] C. Remoli, S. Michienzi, B. Sacchetti, A. Di Consiglio, S. Cersosimo, E. Spica, P. G. Robey, K. Holmbeck, A. Cumano, A. Boyde, G. Davis, I. Saggio, M. Riminucci, P. Bianco, Osteoblast-specific expression of the fibrous dysplasia (FD)-causing mutation Gs(R201C) produces a high bone mass phenotype but does not reproduce FD in the mouse, J. Bone Miner. Res. 30 (6) (2015) 1030–1043.

[38] I. Saggio, C. Remoli, E. Spica, S. Cersosimo, B. Sacchetti, P.G. Robey, K. Holmbeck, A. Cumano, A. Boyde, P. Bianco, M. Riminucci, Constitutive expression of Gsalpha (R201C) in mice produces a heritable, direct replica of human fibrous dysplasia bone pathology and demonstrates its natural history, J. Bone Miner. Res. 29 (11) (2014) 2357–2368.

[39] S. Piersanti, C. Remoli, I. Saggio, A. Funari, S. Michienzi, B. Sacchetti, P.G. Robey, M. Riminucci, P. Bianco, Transfer, analysis, and reversion of the fibrous dysplasia cellular phenotype in human skeletal progenitors, J. Bone Miner. Res. 25 (5) (2010) 1103–1116.

[40] X.F. Zhao, P. Deng, R. Iglesias-Bartolome, P. Amornphimoltham, D.J. Steffen, Y. Y. Jin, A.A. Molinolo, L.F. de Castro, D. Ovejero, Q. Yuan, Q.M. Chen, X.L. Han, D. Bai, S.S. Taylor, Y.Z. Yang, M.T. Collins, J.S. Gutkind, Expression of an active G alpha(s) mutant in skeletal stem cells is sufficient and necessary for fibrous dysplasia initiation and maintenance, Proc.Natl.Acad.Sci.U.S.A. 115 (3) (2018) E428–E437.

[41] R. Iglesias-Bartolome, D. Torres, R. Marone, X. Feng, D. Martin, M. Simaan, M. Chen, L.S. Weinstein, S.S. Taylor, A.A. Molinolo, J.S. Gutkind, Inactivation of a Galpha(s)-PKA tumour suppressor pathway in skin stem cells initiates basal-cell carcinogenesis, Nat. Cell Biol. 17 (6) (2015) 793–803.

[42] S.J. Rodda, A.P. McMahon, Distinct roles for hedgehog and canonical wnt signaling in specification, differentiation and maintenance of osteoblast progenitors, Development 133 (16) (2006) 3231–3244.

[43] M. Logan, J.F. Martin, A. Nagy, C. Lobe, E.N. Olson, C.J. Tabin, Expression of cre recombinase in the developing mouse limb bud driven by a prxl enhancer, Genesis 33 (2) (2002) 77–80.

[44] Z. Liu, S. Turan, V.L. Wehbi, J.P. Vilardaga, M. Bastepe, Extra-long galphas variant XLalphas protein escapes activation-induced subcellular redistribution and is able to provide sustained signaling, J. Biol. Chem. 286 (44) (2011) 38558–38569.

[45] A. Karaca, V.R. Malladi, Y. Zhu, O. Tafaj, E. Paltrinieri, J.Y. Wu, Q. He, M. Bastepe, Constitutive stimulatory G protein activity in limb mesenchyme impairs bone growth, Bone 110 (2018) 230–237.

[46] R.S. Xu, S.K. Khan, T.F. Zhou, B. Gao, Y.X. Zhou, X.D. Zhou, Y.Z. Yang, G alpha(s) signaling controls intramembranous ossification during cranial bone development by regulating both hedgehog and Wnt/beta-catenin signaling, Bone Res. 6 (2018).

[47] B. Palmisano, E. Spica, C. Remoli, R. Labella, A. Di Filippo, S. Donsante, F. Bini, D. Raimondo, F. Marinozzi, A. Boyde, P. Robey, A. Corsi, M. Riminucci, RANKL inhibition in fibrous dysplasia of bone: a preclinical study in a mouse model of the human disease, J. Bone Miner. Res. 34 (12) (2019) 2171–2182.

[48] A. Corsi, B. Palmisano, E. Spica, A. Di Filippo, I. Coletta, M. Dello Spedale Venti, R. Labella, F. Fabretti, S. Donsante, C. Remoli, M. Serafini, M. Riminucci, Zoledronic acid in a mouse model of human fibrous dysplasia: ineffectiveness on

tissue pathology, formation of "giant osteoclasts" and pathogenetic implications, Calcif. Tissue Int. 107 (6) (2020) 603–610.
[49] M. Riminucci, I. Saggio, P.G. Robey, P. Bianco, Fibrous dysplasia as a stem cell disease, J. Bone Miner. Res. 21 (2006) P125–P131.
[50] A. Yoshiki, K. Moriwaki, Mouse phenome research: implications of genetic background, ILAR J. 47 (2) (2006) 94–102.
[51] F. Zhu, R.R. Nair, E.M.C. Fisher, T.J. Cunningham, Humanising the mouse genome piece by piece, Nat. Commun. 10 (1) (2019) 1845.
[52] K. Schepers, E.C. Hsiao, T. Garg, M.J. Scott, E. Passegue, Activated gs signaling in osteoblastic cells alters the hematopoietic stem cell niche in mice, Blood 120 (17) (2012) 3425–3435.
[53] O. Akil, F. Hall-Glenn, J. Chang, A. Li, W. Chang, L.R. Lustig, T. Alliston, E. C. Hsiao, Disrupted bone remodeling leads to cochlear overgrowth and hearing loss in a mouse model of fibrous dysplasia, PLoS One 9 (5) (2014), e94989.
[54] E.C. Hsiao, B.M. Boudignon, B.P. Halloran, R.A. Nissenson, B.R. Conklin, Gs G protein-coupled receptor signaling in osteoblasts elicits age-dependent effects on bone formation, J. Bone Miner. Res. 25 (3) (2010) 584–593.
[55] E.C. Hsiao, S.M. Millard, A. Louie, Y. Huang, B.R. Conklin, R.A. Nissenson, Ligand-mediated activation of an engineered gs g protein-coupled receptor in osteoblasts increases trabecular bone formation, Mol. Endocrinol. 24 (3) (2010) 621–631.
[56] G.J. Kazakia, D. Speer, S. Shanbhag, S. Majumdar, B.R. Conklin, R.A. Nissenson, E. C. Hsiao, Mineral composition is altered by osteoblast expression of an engineered G(s)-coupled receptor, Calcified Tissue Int. 89 (1) (2011) 10–20.
[57] E.C. Hsiao, B.M. Boudignon, W.C. Chang, M. Bencsik, J. Peng, T.D. Nguyen, C. Manalac, B.P. Halloran, B.R. Conklin, R.A. Nissenson, Osteoblast expression of an engineered gs-coupled receptor dramatically increases bone mass, Proc. Natl. Acad. Sci. U. S. A. 105 (4) (2008) 1209–1214.
[58] L. Tascau, T. Gardner, H. Anan, C. Yongpravat, C.P. Cardozo, W.A. Bauman, F. Y. Lee, D.S. Oh, H.A. Tawfeek, Activation of protein kinase a in mature osteoblasts promotes a major bone anabolic response, Endocrinology 157 (1) (2016) 112–126.
[59] K.M. Tsang, M.F. Starost, M. Nesterova, S.A. Boikos, T. Watkins, M.Q. Almeida, M. Harran, A. Li, M.T. Collins, C. Cheadle, E.L. Mertz, S. Leikin, L.S. Kirschner, P. Robey, C.A. Stratakis, Alternate protein kinase a activity identifies a unique population of stromal cells in adult bone, Proc. Natl. Acad. Sci. U. S. A. 107 (19) (2010) 8683–8688.
[60] E. Saloustros, S. Liu, E.L. Mertz, N. Bhattacharyya, M.F. Starost, P. Salpea, M. Nesterova, M. Collins, S. Leikin, C.A. Stratakis, Celecoxib treatment of fibrous dysplasia (FD) in a human FD cell line and FD-like lesions in mice with protein kinase a (PKA) defects, Mol. Cell. Endocrinol. 439 (2017) 165–174.
[61] S. Liu, E. Saloustros, E.L. Mertz, K. Tsang, M.F. Starost, P. Salpea, F.R. Faucz, E. Szarek, M. Nesterova, S. Leikin, C.A. Stratakis, Haploinsufficiency for either one of the type-II regulatory subunits of protein kinase a improves the bone phenotype of Prkar1a(+/-) mice, Hum. Mol. Genet. 24 (21) (2015) 6080–6092.
[62] P. Skroblin, S. Grossmann, G. Schäfer, W. Rosenthal, E. Klussmann, Mechanisms of protein kinase a anchoring, Int. Rev. Cell Mol. Biol. (2010) 235–330.
[63] J.A. Carney, L. Boccon-Gibod, D.E. Jarka, Y. Tanaka, R.G. Swee, K.K. Unni, C. A. Stratakis, Osteochondromyxoma of bone: a congenital tumor associated with lentigines and other unusual disorders, Am. J. Surg. Pathol. 25 (2) (2001) 164–176.
[64] S. Liu, J.M. Shapiro, E. Saloustros, C.A. Stratakis, Bone abnormalities in mice with protein kinase a (PKA) defects reveal a role of cyclic AMP signaling in bone stromal cell-dependent tumor development, Horm. Metab. Res. 48 (11) (2016) 714–725.
[65] S. Espiard, L. Drougat, N. Settas, S. Haydar, K. Bathon, E. London, I. Levy, F. R. Faucz, D. Calebiro, J. Bertherat, D. Li, M.A. Levine, C.A. Stratakis, PRKACB variants in skeletal disease or adrenocortical hyperplasia: effects on protein kinase a, Endocr. Relat. Cancer 27 (11) (2020) 647–656.
[66] L.M. Calvi, N.A. Sims, J.L. Hunzelman, M.C. Knight, A. Giovannetti, J.M. Saxton, H. M. Kronenberg, R. Baron, E. Schipani, Activated parathyroid hormone/parathyroid hormone-related protein receptor in osteoblastic cells differentially affects cortical and trabecular bone, J. Clin. Invest. 107 (3) (2001) 277–286.
[67] S.A. Kuznetsov, M. Riminucci, N. Ziran, T.W. Tsutsui, A. Corsi, L. Calvi, H. M. Kronenberg, E. Schipani, P.G. Robey, P. Bianco, The interplay of osteogenesis and hematopoiesis: expression of a constitutively active PTH/PTHrP receptor in osteogenic cells perturbs the establishment of hematopoiesis in bone and of skeletal stem cells in the bone marrow, J. Cell Biol. 167 (6) (2004) 1113–1122.
[68] A. Kikuchi, H. Yamamoto, A. Sato, S. Matsumoto, New insights into the mechanism of wnt signaling pathway activation, Int. Rev. Cell Mol. Biol. 291 (2011) 21–71.
[69] J. Yu, J. Cao, H. Li, P. Liu, S. Xu, R. Zhou, Z. Yao, X. Guo, Bone marrow fibrosis with fibrocytic and immunoregulatory responses induced by beta-catenin activation in osteoprogenitors, Bone 84 (2016) 38–46.
[70] J.B. Regard, N. Cherman, D. Palmer, S.A. Kuznetsov, F.S. Celi, J.M. Guettier, M. Chen, N. Bhattacharyya, J. Wess, S.R. Coughlin, L.S. Weinstein, M.T. Collins, P. G. Robey, Y.Z. Yang, Wnt/beta-catenin signaling is differentially regulated by G alpha proteins and contributes to fibrous dysplasia, Proc.Natl.Acad.Sci.U.S.A. 108 (50) (2011) 20101–20106.
[71] U. Moens, N. Subramaniam, B. Johansen, J. Aarbakke, The c-fos cAMP-response element: regulation of gene expression by a beta 2-adrenergic agonist, serum and DNA methylation, Biochim. Biophys. Acta 1173 (1) (1993) 63–70.
[72] G.A. Candeliere, F.H. Glorieux, J. Prud'homme, R. St-Arnaud, Increased expression of the c-fos proto-oncogene in bone from patients with fibrous dysplasia, N. Engl. J. Med. 332 (23) (1995) 1546–1551.
[73] U. Ruther, C. Garber, D. Komitowski, R. Muller, E.F. Wagner, Deregulated C-fos expression interferes with Normal bone-development in transgenic mice, Nature 325 (6103) (1987) 412–416.
[74] T.G. Kashimaa, T. Nishiyama, K. Shimau, M. Shimazaki, I. Kii, A.E. Grigoriadis, M. Fukayama, A. Kudo, Periostin, a novel marker of intramembranous ossification, is expressed in fibrous dysplasia and in c-fos-overexpressing bone lesions, Hum. Pathol. 40 (2) (2009) 226–237.
[75] S.A. Kuznetsov, N. Cherman, M. Riminucci, M.T. Collins, P.G. Robey, P. Bianco, Age-dependent demise of GNAS-mutated skeletal stem cells and "normalization" of fibrous dysplasia of bone, J. Bone Miner. Res. 23 (11) (2008) 1731–1740.
[76] Q.M. Fan, B. Yue, Z.Y. Bian, W.T. Xu, B. Tu, K.R. Dai, G. Li, T.T. Tang, The CREB-Smad6-Runx2 axis contributes to the impaired osteogenesis potential of bone marrow stromal cells in fibrous dysplasia of bone, J. Pathol. 228 (1) (2012) 45–55.
[77] M. Riminucci, M.T. Collins, A. Corsi, A. Boyde, M.D. Murphey, S. Wientroub, S. A. Kuznetsov, N. Cherman, P.G. Robey, P. Bianco, Gnathodiaphyseal dysplasia: a syndrome of fibro-osseous lesions of jawbones, bone fragility, and long bone bowing, J. Bone Miner. Res. 16 (9) (2001) 1710–1718.
[78] T. Xiao, Y. Fu, W. Zhu, R. Xu, L. Xu, P. Zhang, Y. Du, J. Cheng, H. Jiang, HDAC8, a potential therapeutic target, regulates proliferation and differentiation of bone marrow stromal cells in fibrous dysplasia, Stem Cells Transl Med 8 (2) (2019) 148–161.
[79] P. Bianco, S.A. Kuznetsov, M. Riminucci, L.W. Fisher, A.M. Spiegel, P.G. Robey, Reproduction of human fibrous dysplasia of bone in immunocompromised mice by transplanted mosaics of normal and gsalpha-mutated skeletal progenitor cells, J. Clin. Invest. 101 (8) (1998) 1737–1744.
[80] F.M. Michiels, B. Caillou, M. Talbot, F. Dessarps-Freichey, M.T. Maunoury, M. Schlumberger, L. Mercken, R. Monier, J. Feunteun, Oncogenic potential of guanine nucleotide stimulatory factor alpha subunit in thyroid glands of transgenic mice, Proc. Natl. Acad. Sci. U. S. A. 91 (22) (1994) 10488–10492.
[81] K.L. Roszko, M.T. Collins, A.M. Boyce, Mosaic effects of growth hormone on fibrous dysplasia of bone, N. Engl. J. Med. 379 (20) (2018) 1964–1965.
[82] S.O. Akintoye, C. Chebli, S. Booher, P. Feuillan, H. Kushner, D. Leroith, N. Cherman, P. Bianco, S. Wientroub, P.G. Robey, M.T. Collins, Characterization of gsp-mediated growth hormone excess in the context of McCune-albright syndrome, J. Clin. Endocrinol. Metab. 87 (11) (2002) 5104–5112.
[83] A.M. Di George, Editorial: albright syndrome: is it coming of age? J. Pediatr. 87 (6 Pt 1) (1975) 1018–1020.

Chapter 2

Pain Behaviours and Nociceptive Mechanisms in a Preclinical Model of Fibrous Dysplasia

Introduction

Pain is a common symptom of FD that significantly compromises quality of life. However, the underlying pain mechanisms of FD are unknown, treatment options demonstrate limited efficacy, and presentation of FD and associated pain is individualistic [2, 24, 25, 225]. Previous studies on patients have demonstrated that FD is likely to exhibit inflammatory and neuropathic components [23].

Manuscript 1 described the available animal models of FD. None of these models evaluates the development of pain, revealing a gap in current *in vivo* research [52]. A translationally relevant model of FD was identified that was developed and characterised by Zhao et al. This is a site-specific (Cre-loxp system) and tetracycline inducible model that develops FD due to the causative $G\alpha_s^{R201C}$ FD mutation. This model demonstrates high face validity, high construct validity, fast rate of onset, and is physiologically robust. [58].

The objective of this study was to identify bone pain in a translationally relevant mouse model of FD and determine the underlying peripheral pain mechanisms.

Methodology

A colony of the Prrx1-Gutkind model was established in our laboratory. The mice generated contained three essential genes for FD mice: *Prrx1-Cre* (expression of Cre recombinase driven by the Prrx1 promoter expressed in bone marrow stromal cells (BMSCs)), *loxp-STOP-loxp-rtTA-IRES-GFP* (expression of reverse tetracycline transactivator (rtTA) when Cre recombinase is present), and *TetO-GNAS* (expression of $G\alpha_s^{R201C}$ FD mutation when rtTA and doxycycline are present). Control mice contained only the first two genes, and not *TetO-GNAS* [58]. A reporter gene, *TetO-GLB1-Luc2,* was optionally present in both FD and control mice for behavioural studies. However, the reporter gene was included for mice used in *in vitro* studies.

Baseline behavioural analysis was conducted before mice were induced with doxycycline in their drinking water (0.08-0.1g/L). In the first study, grid hanging, burrowing, home cage activity, and wheel running were assessed once per week on male and female mice. Grid hanging was

performed by placing the mice on a metal grid, inverting the grid, and measuring latency to first fall (maximum of 2.5 minutes) [226, 227]. Burrowing was performed by placing mice in an empty cage with an inclined burrowing tube filled with 500g of sand. Mice were left alone for 2 hours and the displaced sand was weighed afterwards [228]. Home cage activity and wheel running were performed in Digital Ventilated Cages® (DVCs®) over an uninterrupted 48-hour period per week, and the behaviour was assessed in the 12-hour dark phase [229]. In the second study, female mice underwent grid hanging and burrowing assessments with morphine and ibuprofen treatment, respectively. Grid hanging was performed without treatment in the morning. In the afternoon, mice were treated with 10mg/kg morphine or vehicle and tested 45 minutes later. Mice were treated with 30mg/kg of ibuprofen or vehicle 30 minutes before the start of burrowing behaviour (performed 3 days after grid hanging). Whenever mice were handled during the studies, weight was measured and severity scoring was conducted (Appendix 2). After both behavioural studies, mice were euthanised by intracardial perfusion; both hind limbs and DRGs of the lumbar region 4 (L4), L5, and L6 were obtained (perfused with 4% paraformaldehyde with 1.2% picric acid) [230].

During both studies, x-ray imaging was conducted once per week to track FD development. Post-euthanasia, the hind limbs underwent micro-CT imaging and micro-CT analysis. Following micro-CT analysis, bones were decalcified. Both decalcified bones and DRGs were dehydrated and cryoembedded for sectioning and immunohistochemistry (IHC). After sectioning, bones were stained for all neurons (protein gene product 9.5; PGP9.5), Aδ and C sensory nerve fibres (CGRP), myelinated fibres (neurofilament 200 kDa; NF200), sympathetic nerve fibres (TH), blood vessels (endomucin), osteoclasts (cluster of differentiation 68; CD68; multinuclear), and monocytes, macrophages, preosteoclasts (CD68; mononuclear). This study only assessed the L4 DRG, which was stained for ATF3 (indicator of neuropathic pain) and sympathetic neurons (TH) [114, 231].

BMSCs were extracted from FD and control mice and cultured in 12-well plates until they reached 80% confluency [232]. Cells were activated with 10µg/ml doxycycline in culture media, or vehicle (PBS) in media for 24 hours. Afterwards, the conditioned media and cell lysate were collected. A cAMP assay was conducted on cell lysate and conditioned media and a multiplex assay was conducted to assess the expression of cytokines and chemokines associated with painful bone disorders.

All statistical analysis was conducted in GraphPad Prism 9. Parametric tests were used, either as t-tests or ANOVA (analysis of variance), with appropriate corrections for multiple comparisons.

Results and Discussion

When female and male mice were induced with doxycycline, there was a reduction in grid hanging, burrowing, home cage activity, and wheel running. The male mice progressed faster than female mice by approximately one week. This corresponded with the x-ray imaging observations, where male mice developed visible FD lesions only in the calcaneus, tibia, and fibula at one week on doxycycline, whereas females demonstrated FD lesions only in the calcaneus and, for some female mice, in the tibia. After 2 weeks on doxycycline, female mice demonstrated changes in the calcaneus, tibia, and fibula, while male mice demonstrated more advanced changes in those bones, as well as in the femur. There was no change in behaviour or skeletal appearance in any control mice over the course of the study. Morphine partially reversed the adverse behaviour in grid hanging at D11, but not D18. Burrowing behaviour was maintained during the whole experiment in FD mice treated with ibuprofen compared to mice treated with vehicle where there was a decline in burrowing behaviour from D14. Micro-CT images and analysis demonstrated that phenotypic changes occurred in the femur and tibia in both male and female mice, but the progression was more advanced in the male mice. As FD advanced there was development of pain like behaviour that was reversed when analgesics were administered. The efficacy of anti-inflammatory analgesics on pain-like behaviour suggests development of inflammatory pain. The behavioural deficits observed also corresponded with FD progression, with poorer behaviour corresponding to more advanced FD development.

IHC staining exhibited increased CD68 staining, with DAPI (4′,6-diamidino-2-phenylindole) demonstrating the presence of multinuclear (osteoclasts) and mononuclear (monocytes, macrophages, preosteoclasts) cells. Furthermore, there was increased staining of CGRP in the FD lesion, signalling the presence of Aδ and C sensory nerve fibres. The presence of many osteoclasts that are capable of producing an acidic microenvironment, with sensory nerve fibres may indicate that pain-like development may arise due to acidosis [118]. FD lesions also showed increased vascularity, which commonly accompanies inflammatory conditions (supporting the evidence of effective ibuprofen treatment described above) [162]. DRGs from male FD mice demonstrated an increased proportion of cells with ATF3 staining compared to male control

mice. There were also significantly more TH-positive neurons within the DRG in male FD mice compared to male control mice. There was no significant difference for either marker between female FD and control mice. The presence of ATF3 and TH demonstrates the development of neuropathic pain in male mice [114, 231]. This may be due to the more advanced FD observed in male mice, where neuropathic pain develops at more advanced stages of FD after an initial inflammatory response.

In vitro assays demonstrated increased cAMP production in FD cells stimulated with doxycycline compared to FD cells stimulated with vehicle and control cells stimulated with doxycycline and vehicle. This confirms that the mechanisms associated with FD develop in this model only when stimulated with doxycycline and only when the mutated *GNAS* gene is present. The NGF ELISA demonstrated that only FD cells that were stimulated with doxycycline demonstrated significantly increased NGF expression compared to control cells and unstimulated FD cells; coupled with nerve sprouting observed in the IHC analysis, this may be a nociceptive mechanism of FD in this model [81, 85]. The multiplex assay revealed upregulated expression of IL-6, VEGF, KC/GRO, and MCP-1 in FD cells stimulated with doxycycline compared to the cell and treatment controls. These are factors associated with painful bone and inflammatory conditions [36, 127, 129, 132, 135, 137, 138, 140, 142].

Conclusion

When induced with doxycycline, FD developed in male and female mice, which demonstrated pain-like behaviour. Further experiments demonstrated that inflammatory, neuropathic, acidosis-related, and nerve sprouting components may all contribute to the development of the observed pain-like behaviour.

For the first time, possible underlying mechanisms of FD pain have been described. A limitation of this study, however, is that the results cannot yet be compared to observations in human tissue.

This model has now been established as a transgenic mouse model of FD that develops a characterised pain-like phenotype. Future studies further investigating pain-like mechanisms of FD and testing novel analgesics can employ this model.

Pain Behaviours and Nociceptive Mechanisms in a Preclinical Model of Fibrous Dysplasia

Chelsea Hopkins[1], Luis Fernandez de Castro[2], Marta Diaz Del Castillo[3], Pravallika Manjappa[4], Alison Boyce[5], Ruth Elena Martinez Mendoza[6], Juan Antonio Vazquez Mora[6], Lizeth Jazmín Ponce Gomez[6], Michael T Collins[2], Juan Miguel Jimenez Andrade[6], Anne-Marie Heegaard[1]*

[1] Department of Drug Design and Pharmacology, University of Copenhagen, Copenhagen, Denmark

[2] Skeletal Disorders and Mineral Homeostasis Section, National Institute of Dental and Craniofacial Research, National Institutes of Health, Bethesda, MD, USA

[3] Department of Forensic Medicine, University of Aarhus, Aarhus, Denmark

[4] Neuroscience, Biopharmaceuticals R&D, AstraZeneca, Cambridge, UK

[5] Metabolic Bone Disorders Unit, National Institute of Dental and Craniofacial Research, National Institutes of Health, Bethesda, MD, USA

[6] Department of Unidad Académica Multidisciplinaria Reynosa Aztlan Universidad Autónoma de Tamaulipas Reynosa, Tamaulipas Mexico

*Corresponding author: Department of Drug Design and Pharmacology, University of Copenhagen, Universitetsparken 2, 2100 Copenhagen, Denmark, amhe@sund.ku.dk

Abstract

Introduction: Pain is a common symptom of fibrous dysplasia (FD), a rare genetic bone disorder that manifests as mosaic lesions. There is little information about the underlying nociceptive mechanisms in FD and pain treatment is often ineffective. The aim of this study was to identify nociceptive behaviour and mechanisms in a previously established translationally relevant, tetracycline-inducible mouse model of FD.

Method: Mice were induced to develop FD. Burrowing (ibuprofen efficacy assessed), grid hanging (morphine efficacy assessed), home cage activity, and wheel running behaviour were used to evaluate the development of pain-like behaviour. Bones and dorsal root ganglia (DRGs) were collected from the mice to identify neurochemical changes using immunohistochemistry.

Bone marrow stromal cells were isolated from mice and cultured *in vitro,* stimulated with doxycycline, and conditioned media was assessed to identify inflammatory mediators.

Results: Both male and female mice demonstrated pain-like behaviour when FD developed; burrowing and grid hanging deficits were improved after ibuprofen and morphine treatment, respectively. FD lesions of the tibia and femur demonstrated the presence of mono- and multi-nucleated CD68+ cells, CGRP+ sensory nerve fibres, and increased vascularisation. Sympathetic nerve fibres were also observed in some tissue samples. DRGs in male mice demonstrated increased staining for activating transcription factor 3 and sympathetic neurons. Conditioned media from FD cells stimulated with doxycycline demonstrated an increased concentration of inflammatory cytokines and chemokines associated with painful conditions.

Discussion and conclusion: Pain-like development was described in a pre-clinical model of FD for the first time. The efficacy of an anti-inflammatory analgesic (and morphine), presence of vascularisation, and secretion of inflammatory mediators *in vitro* suggest that there is an inflammatory component of FD pain. ATF3 staining and presence of sympathetic neurons in the DRGs suggest the development of neuropathic pain. The development of nociceptive changes in this model makes it beneficial for further mechanistic studies and analgesic testing.

Introduction

Fibrous dysplasia (FD) is a rare bone disorder in which a mosaic genetic mutation results in fibro-osseous tissue replacing normal bone. This tissue is structurally unstable, leading to deformity, fractures, and pain (both fracture and non-fracture pain), all of which diminishes patients' quality of life [1-4]. The cause of FD is well described; a post-zygotic substitution mutation occurs in the *GNAS* gene, which encodes the G-protein (guanine nucleotide-binding protein) alpha subunit ($G\alpha_S$). Here, the arginine amino acid in exon 8 is replaced by a cysteine or histidine amino acid (R201C or R201H, respectively). Rarely, FD will be caused by a mutation of codon 227 in the same gene [1]. These mutations cause the $G\alpha_S$ subunit to remain constitutively active, acting on adenylyl cyclase, which will produce excess cyclic adenosine monophosphate (cAMP) and activate downstream mechanisms [5]. McCune-Albright syndrome (MAS) is caused by the same genetic mutation that occurs in endocrine, epithelial, or osseous tissue, whereas FD only encompasses changes in the bone [1, 6].

Pain is a common feature of FD, but the underlying mechanisms are unknown, making adequate treatment a challenge [7]. Previous studies have attempted to characterise pain through questionnaire studies indicating that pain could have neuropathic and nociceptive components [2, 8]; however, there are no studies on FD tissue to confirm this supposition. FD pain is more common in lower extremity sites and adults and individuals with polyostotic FD tend to report more severe pain than individuals with monostotic FD [4, 8-10]. Bisphosphonates and anti-RANKL (receptor activator of nuclear factor kappa-B ligand) treatment are promising treatment modalities that may relieve pain to some degree, although opioids and NSAIDs (non-steroidal anti-inflammatory drugs) are effective in approximately half of patients [4]. Understanding the underlying mechanisms of pain in FD may indicate more effective pain treatment options and perhaps individualised pain treatment modalities.

In general, pain is classified as neuropathic (i.e. neuronal tissue damage) or nociceptive (i.e. non-neuronal tissue damage). Inflammatory pain is typically classed as nociceptive pain, but may also contribute to neuropathic pain, or manifest without overt tissue damage [11]. The bone environment poses a unique challenge to investigating and treating pain. The bone is highly innervated and disruption of the bone can lead to the development of debilitating pain [12, 13]. However, innervation changes within FD lesions are currently unknown. FD lesions are areas of increased bone remodelling and osteoclastogenesis [1, 14, 15] and as such, there may be pathological changes in innervation, vascularisation, acidosis, or FD-specific factors that contribute to pain development.

Seven unique animal models of FD with the causative genetic mutation have been developed with different approaches and variable translatability and validity [16]. The Prrx1-Gutkind model developed and characterised by Zhao et al. [14] is a translationally relevant mouse model with good face and construct validity; it produces a robust phenotype that is site specific and inducible. However, the development of a pain-like phenotype in this model has not been investigated.

The aim of this study is to identify pain-like behaviours and potential underlying nociceptive mechanisms in the Prrx1-Gutkind mouse model of FD.

Methods

Animals

The transgenic mouse model of FD developed by the Gutkind laboratory and described by Zhao et al. was used in this study [14, 17]. Paired related homeobox 1 *(Prrx1)-Cre*-expressing mice, where Cre recombinase expression is limited to early limb bud mesenchymal stem cells of the bone [18] were bred with *Tet-G*α_s^{R201C} mice that express the mutated *GNAS* gene responsible for FD under a tet-responsive element that can only be expressed when reverse tetracycline transactivator (rtTA) and doxycycline are present [17]. These mice were further bred with mice carrying the *TetO-GLB1-Luc2* genes. The mice established with these three gene regions (*Prrx1-Cre*, *Tet-G*α_s^{R201C}*, TetO-GLB1-Luc2*) are termed "GNAS mice". To generate mice for this study, GNAS mice were bred with mice carrying the *loxp-STOP-loxp-rtTA-IRES-GFP* gene cassette – coined "Linker mice" (B6.Cg-*Gt(ROSA)26Sor*$^{tm1(rtTA,\ EGFP)Nagy}$/J; Strain #005670; The Jackson Laboratory, USA). After genotyping, the mice were categorised according to the genes they possessed for further experiments (Table 1) while mice without any of those gene profiles were euthanised.

The experiment was conducted in accordance with the Danish Animal Experiments Inspectorate (Copenhagen, Denmark, licences 2021-15-0201-00872 and 2016-15-0202-00045). GNAS mice were obtained from the National Institute of Health and rederived by Charles River (France). Linker mice were purchased from The Jackson Laboratory. All mice were housed in a certified specific pathogen-free facility at the University of Copenhagen. The research facility maintains a temperature of 22±2°C and humidity of 55±10%. The light-dark cycle is 12-hours and light was maintained at 60% intensity during all experimental studies. Mice were housed in GM500 individually ventilated cages (Tecniplast®, USA) in groups of 2-5 mice. All cages contained wood-chip bedding material (Tapvei 2HV, Brogaarden, Denmark), two transparent red housing units (Polycarbonate Mouse Tunnel, Datesand, UK), nesting material (paper shavings, Brogaarden, Denmark), a wooden gnawing block (Aspe små klodser, Brogaarden, Denmark), and a paper rope (Diamond Twist, Envigo, USA). Standard chow (Altromin 1324, Brogaarden, Denmark) and tap water were provided ad libitum (both changed once per week). When mice were induced with doxycycline, chow was placed on the cage floor to assist mice that may have had difficulty rearing to the trough. Cages were changed every two weeks.

GNAS mice were backcrossed five times onto a C57Bl/6J (The Jackson Laboratory, USA) background strain. Control mice contained the *Prrx1-Cre* and *loxp-STOP-loxp* genes, but not the causative *GNAS*^{R201C} gene of FD, while FD mice contained all genes. For all mice, the reporter gene was optional and did not influence behavioural outcomes (Table 1). Severity scoring was conducted at least twice per week (more frequently if necessary) to assess their welfare based on coat condition, mobility, disease-specific conditions, weight-loss, etc. When mice reached the experimental or humane endpoint, they were euthanised by decapitation or intracardial perfusion. The experimental endpoint was defined at a specific time point for each study. However, for *in vitro* cell extraction, mice were euthanised by cervical dislocation. Male and female mice were used for behavioural studies and female mice were used for intervention studies. Tissue samples were taken from both male and female mice after each study. Pilot studies indicated faster progression in male mice compared to female mice, otherwise physiological characteristics and behaviour remained consistent between the two sexes. Intervention studies were conducted only on female mice due to the slower disease progression observed in pilot studies. All mice were over 10 weeks old when first induced with doxycycline, corresponding to the adult life stage of mice compared to humans [19].

Fibrous Dysplasia Induction

This mouse model of FD is a tetracycline-inducible model. Doxycycline (doxycycline hyclate; Sigma-Aldrich, USA) was administered continuously in drinking water, which was protected from light and changed twice per week. Mice were dosed with 0.1g/L in the behavioural studies and 0.08g/L in the intervention studies. Both FD and control mice received doxycycline.

Study Design

The study designs are shown in Supplementary Figure 1. The first behavioural study was conducted to assess the development of pain-like behaviour in male and female mice using burrowing, grid hanging, home cage activity, and wheel running. In the first study (Supplementary Figure 1A), mice underwent baseline training and assessment in the week prior to doxycycline administration. On D0, mice were administered doxycycline in their drinking water (0.1g/L; changed twice per week and covered in tin foil) to induce FD in FD mice for two weeks. For 48 hours each week, mice were left undisturbed in the home cages for continuous home cage activity and wheel running assessment. Burrowing was conducted once per week

after the home cage assessments. The day after burrowing, grid hanging was assessed followed by x-ray imaging. On each behaviour day, severity scoring was conducted after the behaviour assessment was conducted. The sequence of home cage assessment, burrowing, grid hanging, and imaging was maintained to ensure minimal interference of one assessment on another. The four-day period between imaging and the next home cage assessment was sufficient to allow mice to return to normal behaviour after isoflurane exposure. All of the materials and equipment used in this experiment were kept separate between male and female mice. Male and female mice were also assessed separately, with male mice tested prior to female mice. The second experiment (Supplementary Figure 1B) was conducted with female mice to assess the effect of analgesics on pain-like behaviour. Mice underwent baseline tests one week prior to doxycycline administration. Mice were administered doxycycline in their drinking water (0.08g/L) at D0 to induce FD for three weeks. Grid hanging was performed with morphine treatment on D4, D11, and D18 with one week between each assessment. Burrowing was performed on D7, D14, and D21 with ibuprofen treatment followed by x-ray imaging.

Except for home cage activity and wheel running behaviour, one mouse is categorised as one experimental unit (n). For home cage activity and wheel running, one cage is categorised as one experimental unit, where male mice were single-housed and female mice were double-housed. FD mice were excluded from the study if they did not develop FD during the course of the experiment according to the x-ray images. Blinding was not possible between the control and FD mice, due to the physiological changes that occur in FD. The experimenter (CH) was blinded to the treatment groups established by the principle researcher (AMH). The mice were randomised according to burrowing baseline data and remained in the same treatment groups throughout the study. The experimenter remained blinded until the data analysis was completed.

Behaviour

Grid hanging

The grid hanging methodology was adapted from Falk et al. [20] and the inverted screen test [21, 22].

Mice were placed on a metal grid set over a large container lined with thick bedding material. The grid was gently rocked for 2-3 seconds before being inverted. Mice freely roamed on the inverted grid. All tests were filmed for further analysis to determine the total grid hanging time,

with a maximum of 2.5 minutes. When analgesic treatment tests were conducted, mice were tested in the morning without treatment (pre-treatment timepoint) and after 2-3 hours in the afternoon (post-treatment). Prior to testing, mice were trained by completing the procedure for a total of 2 minutes (e.g. a mouse that hangs for 45 seconds, falls, and then hangs for 1.5 minutes after being placed back on the grid completes the training). Mice that were not able to complete the training and the mice in the bottom 10% of grid hanging times at baseline were excluded from data analysis.

Burrowing

Burrowing was conducted as previously described [23]. At baseline, mice were trained for three days, followed by two days of burrowing baseline assessments. On the first day of training, mice were placed in an empty burrowing box in pairs (from the same home cage) with an empty burrowing tube for 2 hours to habituate to the experimental environment. On the second and third day, mice were placed in pairs in a testing box with an inclined burrowing tube filled with 500g of sand and left alone to burrow for 2 hours. On the third day, mouse pairs were changed to pair mice with good burrowing behaviour with mice with poor burrowing behaviour. On the fourth and fifth day, mice were placed in individual boxes with a burrowing tube filled with 500g of sand and left to burrow for 2 hours. Mice were placed back in the home cage and the sand burrowed was assessed. The 10% of mice that burrowed the least in the baseline assessment were excluded from further analysis.

Cage Activity

Mice were housed in Digital Ventilated Cages® (DVCs®) by Tecniplast® (USA). The cage activity system and metrics have been described in a previous publication by Ianello [24] which demonstrated a high correlation between the acquired data and video analysis of behaviour. The home cage is set over a capacitance sensing technology board with 12 electrodes that can detect disturbance when a mouse moves over the electrodes. An electrode is activated when a mouse disturbs that electrode over a specific period. The calculated information of activity density is automatically calculated for every minute and the average cage activity in one hour of the dark phase was assessed. Male mice were single-housed and female mice were double-housed in the cages. Mice were left in their cages undisturbed for 48 hours and the activity in the dark phase was assessed.

Wheel running

Wheel running was performed in the DVCs® using electromagnetic wheels (GYM500, Tecniplast, USA) where distance, speed, and rotation are automatically tracked. Wheels are secured inside the cage to the side so that the magnetic field of the wheel can be detected on the outside of the cage. When the wheel spins, the electromagnetic field is detected and tracked. A previous study demonstrated that a cancer-induced bone pain model of metastatic breast cancer that developed pain-like behaviour also demonstrated reduced wheel running behaviour in the same system (Hopkins et al., unpublished data). The cumulative distance during each hour of the dark phase was assessed.

Analgesic Treatment

Only female mice were used for intervention assessments. Ibuprofen (Sigma-Aldrich, USA) was administered at 30mg/kg intraperitoneally 30 minutes prior to burrowing. Morphine (Abcur, Sweden) was administered at 10mg/kg subcutaneously 45 minutes prior to grid hanging. Ibuprofen and morphine were freshly diluted in 0.9% sterile saline (used as vehicle treatment) within 24 hours prior to administration. After injection and prior to behavioural studies, mice were placed back in their home cages to prevent associating the injection procedure with behavioural assessments. Half of the FD and control mice received analgesic treatment and remained in the treatment group throughout the study, and the other half of FD and control mice were treated with the vehicle.

Imaging

X-ray imaging was conducted throughout the behavioural experiments to track FD development. Micro-computed tomography (micro-CT) was conducted post-euthanasia on the hind limbs.

X-ray Imaging

X-ray imaging was conducted weekly using Lumina XR IVIS (In Vivo Imaging System) apparatus (Caliper Life Sciences, Teralfene, Belgium). Mice were sedated and maintained using 2.5% isoflurane (1000mg/g isoflurane, Attane vet, ScanVet, UK). X-ray images were obtained of the entire skeleton and the hind limbs.

Micro-Computed Tomography Imaging and Analysis

Post-euthanasia and prior to decalcification, hind limbs were imaged using computerised microtomography (Skyscan 1272, Bruker, Belgium). The scanning process was performed with a power of 60 kVp and 166 µA, with an integration time of 627 ms, a voxel size of 10 µm, aluminium filter of 0.25 mm and resolution of 2016x1344 pixels according to the guidelines for bone structure analysis in rodents. The reconstruction of the images obtained was performed using NRecon software (Bruker, Belgium) with the following settings: the ring reduction parameters were adjusted to 5.0, high-energy photon increment was set at 30%, and a histogram of a minimum value of 0.00 and a maximum value of 0.15 was established. Subsequently, images were analysed using Bruker computed tomography software (Bruker, Belgium), where the parameters to be evaluated were the following: bone mineral density (BMD), bone volume fraction (BV/TV), trabecular thickness (Tb.Th), number of trabeculae (Tb.N), and trabecular spacing (Tb.Sp) in both the distal femur and proximal tibia. The cortical bone parameters evaluated were: BMD, cortical thickness (Ct.Th), and cortical area (Ct.Ar) in both the distal femur and proximal tibia.

Trabecular bone was analysed by defining the region of interest, taking the reference point 0.2 mm from the growth plate and taking a vertical axis of 1 mm from the reference point. An automatic segmentation algorithm was performed to isolate the trabecular bone from the cortical bone.

The cortical bone was assessed in the mid-diaphysis of the tibia and femur. The region of interest was selected with a volumetric band of 1 mm to 4 mm from the growth plate. Hydroxyapatite calibrators with values of 250 and 750 mg/cm^3 were used to calibrate the bone mineral density parameter, which were processed under the same conditions performed on the samples.

Tissue Collection and Embedding

Serum was collected from mice treated with analgesics during euthanasia at 15-20 weeks old. Mice were sedated during final x-ray imaging and decapitated. Whole blood was collected and kept at room temperature for 30 minutes. Samples were centrifuged at 4°C for 10 minutes at 2000g. The serum portion was collected and stored at -80°C.

Remaining mice were euthanised by intracardial perfusion similar to previous literature at 15-20 weeks old [25]. Mice were anaesthetised with xylazine/ketamine cocktail (85.5mg/kg ketamine,

MSD Animal Health, AN Boxmeer, the Netherlands; 12mg/kg xylazine, Rompun vet, Bayer, Germany). When reflexes ceased, the mouse was fixed with needles in a supine position. An incision was made through the skin and ribcage to expose the heart. A small incision was made in the right atrium and a needle attached to a tube (connected to a pump) was placed in the left ventricle. Phosphate buffered saline (PBS; 4°C) was pumped through the tube for 4 minutes, corresponding to approximately 50ml, followed by 4% paraformaldehyde (PFA; Sigma Aldrich, USA; 37% diluted in PBS) with 1.2% picric acid (VWR, Denmark) in 4°C PBS for 4 minutes. The L4, L5, and L6 dorsal root ganglia (DRG) and the spinal cord were collected (only L4 was assessed in this study) and placed in PFA/picric acid solution. Both complete hind limbs were collected and stored in PFA. After 24 hours, DRGs and the spinal cord were transferred to 30% sucrose solution and hind limbs were transferred to sterile PBS. Tissue samples were stored at 4°C continuously after harvesting.

After at least 72 hours, DRGs were removed from sucrose solution, embedded in optimal cutting temperature medium (OCT; Tissue-Tek®, Sakura, USA), and stored at -80°C. Hind limbs were decalcified using 10% EDTA (ethylenediaminetetraacetic acid, Merck, USA) at 4°C for 2-3 weeks. The grade of decalcification was monitored by plain x-ray (Fona X70, Fona, Italy). Once decalcified, the limbs were stored in 30% sucrose for at least 48 hours. The region surrounding the knee joint, including the distal femur and proximal tibia were embedded in OCT (Tissue-Tek®, Sakura, USA) and sectioned immediately.

Immunohistochemistry

Sectioning and Staining

The embedded tibia-femur tissue segment was sectioned along the longitudinal axis at 25 µm thickness and DRGs at 15 µm using a cryostat (Leica 1900, Leica Biosystems, Il, USA). Sections were mounted on gelatin-coated slides and dried at room temperature for at least 30-60 minutes before undergoing immunohistochemical staining (IHC) or long-term storage at -80°C. Tissue sections were washed three times with PBS and then incubated with blocking solution (3% normal donkey serum (NDS; Jackson ImmunoResearch, #017-000-121) and 0.3% Triton X100 (Sigma Aldrich, USA) in PBS) for 2 hours. Sections were incubated for 12 hours with primary antibodies in diluted blocking solution (1% NDS and 0.1% Triton X100 in PBS) at 4°C. To identify different nerve profiles, the following primary antibodies were selected: protein gene

product 9.5 (PGP 9.5, 1:3000; Cedarlane, #CL77556AP) is a pan-neuronal marker, calcitonin gene-related peptide (CGRP, polyclonal rabbit anti-mouse 1:3000; Sigma Aldrich, #C8198) is used to identify Aδ and C sensory nerve fibres, neurofilament 200 kDa (NF200, chicken anti-neurofilament 200 kDa; 1:3,000; Neuromics, #CH22104) is used to identify myelinated primary afferent sensory nerve fibres, tyrosine hydroxylase (TH, polyclonal rabbit anti-rat TH, 1:1,000; Merck Millipore, #AB152) is used to identify sympathetic nerve fibres, endomucin (EMCN, 1:100, Santa Cruz Biotechnology, #SC-65495) is used to detect the presence of blood vessels, and activating transcription factor 3 (ATF3, 1:500, Santa Cruz Biotechnology, #SC-188) is used as a marker of peripheral nerve damage. Tissue was washed with PBS (three times) and tissue was incubated for 3 hours with the respective secondary antibody in diluted blocking solution: Cy3 monoclonal donkey anti-rabbit, 1:600 (Jackson ImmunoResearch, #711−165-152), Cy2 monoclonal donkey anti-chicken, 1:400 (Jackson ImmunoResearch, #703−255-155), Cy3 monoclonal donkey anti-rat, 1:600 (Jackson ImmunoResearch, #712−165-150). Tissue was washed again with PBS and counterstained for 5 minutes with 4′,6-diamidino-2-phenylindole (DAPI; 1:20,000, Sigma Aldrich, #D21490) to detect cell nuclei. Tibia-femur tissue was dehydrated with serial ethanol and xylene gradients before being covered with DPX mounting medium (Sigma Aldrich, USA) and a coverslip. DRGs were covered with ProLong Gold antifade reagent (Invitrogen, USA).

DRG Neuronal Profiles and Axon Length Density Quantification

DRG tissue sections were separated by over 120 µm to prevent cell bodies and axons being counted more than once. Imaging was conducted using Zeiss LSM 800 confocal microscope (Zeiss, Germany), and confocal images from three different sections under a 20X objective lens were obtained from each animal. ImageJ (NIH, USA) was used to trace the TH-stained axons with the free-hand tool and the total length of axons was divided by the area of the cell body-rich area, which was determined by using the area selection tool. This number was multiplied by the thickness of the cut tissue (15 µm); results are expressed as the total axon length per unit of volume of DRG cell body-rich area (mm/mm^3).

To assess the proportion of ATF3-stained cells within the DRGs, three tissue sections from each animal were manually quantified using Zeiss HBO 100 epifluorescence microscope (Zeiss, Germany) at a 20x objective. DAPI imaging was used to quantify the total number of nuclei

within the tissue area of interest. The number of ATF3-positive cells was divided by the total number of nuclei then multiplied by 100 and reported as a percentage of cells stained with ATF3.

Semi-qualitative Analysis of Femur and Tibia

Nerve fibres, vasculature, and CD68+ cells were quantified in at least three sections per animal. Imaging was conducted using an epifluorescence microscope (Carl Zeiss HBO 100, Zeiss, Germany) with a 20X objective lens on the proximal tibia and distal femur regions. First, the bone tissue from control mice was assessed within the cortical bone and periosteum. The nerve fibres for each stain and the vasculature was assessed; the average observations were established and this was used for comparison against the FD bone tissue samples. If 2-6 nerve fibres were observed for CGRP, PGP9.5, TH, or NF200 within the FD lesion, then that was considered a 25% increase of that component. If 3-5 blood vessels stained with endomucin were observed in the FD lesion, then that was considered a 25% increase. The presence of CD68-positive cells within the FD lesion was considered substantially different from the cortical bone that normally occupies the region. Representative confocal images were obtained using the Z-stack and tile function at 40X magnification. The Z-stacked images were processed by an extended depth of focus and subsequently stitched by ZEN 3.6 (Zeiss, Germany) software.

Cell Culture and In Vitro Assays

Bone marrow stromal cells were extracted from six female mice (three FD mice, three control mice), approximately 8 weeks old according to a previously established protocol [26], and with the gene profile described in Table 1. Briefly, mice were euthanised by cervical dislocation and the femurs and tibias removed. Cleaned bones were placed in sterile PBS (4°C). The ends of the bones were cut off, placed in Eppendorff tubes (with culture media), and centrifuged at 10,000g for 15 seconds. The bones were removed and the pellets resuspended in culture media. FD cells were pooled together, as were control cells. Cells were passed through a sterile 70 μm cell sieve and counted using a haemocytometer. Cells were plated in sterile 12-well plates (10^5 cells per well; ThermoFisher Scientific, USA). Cells were cultured in Minimal Essential Medium alpha (MEM α; Gibco®), with 10% foetal bovine serum (Gibco®, USA), and 1% penicillin-streptomycin (Gibco®, USA) for 48 hours at 37°C with 5% CO_2. Afterwards, media was replaced twice a week until cells reached 80% confluence.

FD cells and control cells were treated with 10 μg/ml doxycycline for 24 hours, 15 ng/ml tumour necrosis factor alpha (TNF-α; positive control; from mouse, Sigma-Aldrich, USA) for 48 hours, and PBS (negative control) for 24 hours in 500 μl of culture media. All activating media was treated with 3-isobutyl-1-methylxanthine (IBMX) to prevent cAMP degradation. Conditioned media was removed and aliquoted. Cells were washed with PBS and lysed with RIPA (radioimmunoprecipitation assay) lysis and extraction buffer (Thermo Scientific ™, USA). Conditioned media and cell lysate were stored at -80°C.

cAMP Assay, Meso Scale Discovery Multiplex Assay, and Nerve Growth Factor ELISA

cAMP concentration assay (Cisbio GS Dynamic Kit, PerkinElmer, USA), Meso Scale Discovery Multiplex assay (U-PLEX; MSD, USA), and nerve growth factor (NGF) Enzyme-Linked Immunosorbent Assay (ELISA; NGF Rapid™ ELISA kit: mouse; avantor™, USA) were conducted according to manufacturer directions. The markers assessed in the multiplex assay were: TNF-α, interleukin-2 (IL-2), granulocyte-macrophage colony-stimulating factor (GM-CSF), monocyte chemoattractant protein 1 (MCP-1), stromal cell-derived factor 1 (SDF-1α), interleukin-1 beta (IL-1β), interleukin-6 (IL-6), vascular endothelial growth factor (VEGF-A), interferon gamma (IFN-γ), keratinocyte chemoattractant (KC)/human growth-regulated oncogene (GRO), interleukin-4 (IL-4), macrophage inflammatory protein alpha and beta (MIP-1α and MIP-1β), eotaxin, and interleukin-5 (IL-5). These markers were selected based on their prevalence in other painful bone disorders based on results from DisGeNET. All assays were optimised with different dilution factors. The cAMP assay was conducted on cell lysate (undiluted) and conditioned media (undiluted) and the multiplex assay and NGF ELISA were conducted on conditioned media only (undiluted).

Statistics

All statistical analysis was conducted using GraphPad Prism 9 (Version 9.0.4, USA). The group number of mice was calculated based on *a priori* sample size calculation using data from pilot experiments, power set at 80%, and p-value set at $p<0.05$ in G*Power (hhu, Germany). Statistical tests are defined for each experiment in the results, with statistical significance set at $p<0.05$.

Results

FD Mice Develop Pain-like Behaviour

When female and male mice were chronically treated with doxycycline, FD mice developed FD-like lesions as demonstrated by x-ray imaging (Supplementary Figure 2) and pain-like behaviours in contrast to the sex- and age-matched control mice that did not develop either. FD mice demonstrated significantly reduced burrowing (Figure 1A, 1B), grid hanging (Figure 1C, 1D), home cage activity (Figure 1G), and wheel running (Figure 1H) over time.

Due to the rapid FD-lesion and pain-like behaviour development in the male mice, female mice were used for intervention assessments. Female mice were treated with ibuprofen prior to burrowing and on a separate day they completed a grid hanging test before being treated with morphine and tested again. During the burrowing assessment, FD mice treated with ibuprofen maintained their burrowing behaviour over time, similar in magnitude compared to baseline and the control mice (Figure 1A). In contrast, FD mice treated with vehicle demonstrated reduced burrowing behaviour over time compared to both baseline and the other three groups. Likewise, morphine significantly improved the grid hanging time in FD mice as compared to FD mice treated with vehicle at D11 (Figure 1E). There was no significant difference between the groups at D18 (Figure 1F), but a majority of the mice in the morphine-treated group improved at post-treatment compared to the vehicle-treated group where a majority of the mice stayed the same or deteriorated.

Both male and female FD mice demonstrated reduced home cage activity over time (Figure 1G), indicating that they moved around their cages less as FD-lesions developed and in concert with reduced burrowing and grid hanging behaviour. Female control mice demonstrated significantly reduced home cage activity at one week on doxycycline, but there was no change between baseline and week 2 on doxycycline. Male control mice did not demonstrate significant changes in home cage activity over time. There was a significant reduction in wheel running distance in female and male FD mice after one week on doxycycline, getting worse as FD lesions developed (Figure 1H). In contrast, wheel running improved in female and male control mice over time (significantly in female control mice).

The diurnal behavioural patterns (Figure 1I-P) during the dark phase were similar to those observed in other studies, where C57Bl/6 mice demonstrate 2-3 activity peaks during the 12-

hour dark period for both home cage activity and wheel running [27, 28]. This suggests that the data obtained by the DVCs® is comparable to that obtained by previous studies using other home cage systems for behavioural assessment.

Mice Develop FD-like Bone Lesions that Corresponds to Pain-Like Behaviour

Haematoxylin and eosin staining of bone tissue confirmed the presence of fibrous tissue lesions in the FD mice, but not in the control mice (Figure 2A, 2B). End-stage micro-CT (Figure 2C-J) further supported that both male and female FD, but not control mice, developed FD pathology. Both female and male FD mice demonstrated significantly reduced BMD and BV/TV in the distal femur and proximal tibia compared to the control mice (Figure 2K-R), but the difference between these measures between the FD and control mice was more pronounced in the male mice than in the female mice. Furthermore, almost all other micro-CT measurements were significantly different between the male FD and control mice (Table 2; except Tb.Th (femur and tibia) and Tb.Sp (femur)). However, female mice had a slower progression of the lesions and primarily developed changes in the tibial trabecular bone (Figure 2G-H; Table 2). Similarly, x-ray analysis conducted throughout the study demonstrated faster progression in male FD mice, where pathological changes were evident in the calcaneus and tibia at D7 compared to the female mice, where pathological changes were evident only in the calcaneus. At D14, male FD mice demonstrated pathological changes and deformity in the calcaneus, tibia, fibula, and femur, whereas the female FD mice demonstrated pathological changes in the calcaneus, tibia, and fibula (Supplementary Figure 2).

Corresponding to the progression of the FD lesions, pain-like behaviour was observed in male FD mice one week earlier than in female FD mice in all pain assessments (Figure 1A, 1B, 1G, 1H). Furthermore, pain-like behaviour tended to become progressively worse as FD-lesions became more apparent in x-ray analysis. Comparison of the x-ray (Supplementary Figure 2) and micro-CT results (Figure 2C-J; Table 2) with the pain-like behaviour patterns (Figure 1) suggests that more advanced FD development corresponds with poorer pain-like behaviour.

Immunohistochemistry of the Bone Demonstrates Pathological Changes in Bone and Neurons

Confocal imaging of bones from FD mice revealed pathological changes that may contribute to pain. A majority of the bones demonstrated increased staining of CD68 within the FD lesions, which stains cells of the monocyte lineage (e.g. macrophages and osteoclasts) (Figure 3A-E).

Both mononuclear (e.g. macrophage/monocyte/pre-osteoclast) and multinuclear (e.g. osteoclast) cells were present in FD lesions (Figure 3A-C). Increased vascularisation is also observed in most of the bones within the FD lesions (Figure 3N, 3O). CGRP is a neuropeptide widely used as a sensory Aδ and C fibre label. Our results show that CGRP+ nerve axons were present in most femur samples within the FD lesion, but less commonly in the periosteum and in FD lesions within the tibia (Figure 3F, 3G; Table 3). TH+ (sympathetic) nerve fibres were also present in the FD lesion of two male and two female mice (Figure 3H, 3I; Table 3). PGP9.5, a pan-neuronal marker, stained a high density of nerve axons in the tibia of three female mice and two male mice, and in the femur of two female mice and one male mouse (Figure 3J, 3K). However, the myelinated nerve fibre marker NF200 was only present in three FD mice (two female, one male) and only in the tibia (Figure 3L, 3M).

Indication of Peripheral Nerve Damage Present in Male FD Mice

Increased expression of ATF3 in DRG cell bodies is a widely accepted sign of peripheral nerve damage, indicating a potential neuropathic state (Figure 4A, 4B) [29]. DRGs from male FD mice demonstrated significantly more cell bodies with positive ATF3 staining compared to control mice (Figure 4C). Similarly, increased presence of sympathetic nerve fibres (TH staining of axons) in the DRG is an indicator of neuropathic pain (Figure 4D,4E) [30]. There were significantly more TH-positive axons within the DRGs in male FD mice than control mice (Figure 4F). There were no significant differences between female FD and control mice (Figure 4C, 4F).

In Vitro Induction of FD Cells Generates Factors Associated with Pain

Having established the development of pain-like behaviour in FD mice when induced with doxycycline and the efficacy of anti-inflammatory analgesics to reverse this behaviour, it was necessary to determine whether FD cells express inflammatory factors that have been associated with painful conditions. FD cells (containing $GNAS^{R201C}$) and control cells isolated from mice were cultured *in vitro* and stimulated with doxycycline or vehicle, and then the conditioned media was analysed. FD cells stimulated with doxycycline produced significantly more cAMP than control cells stimulated with doxycycline, as well as both cell types that were treated with vehicle, thus confirming the *in vitro* induction of the *GNAS* mutation (Figure 5). Further analysis of the conditioned media showed significantly upregulated NGF expression in doxycycline-

stimulated FD cells compared to treatment and cell control conditions (Figure 5). The multiplex assay identified five factors that were significantly upregulated in FD cells stimulated with doxycycline: IL-6, VEGF, KC/GRO, TNF-α, and MCP-1 (Figure 5). However, the other factors analysed were either not detected, or not significantly different between cell types. TNF-α stimulation was employed to demonstrate that the cultured cells could express the chosen factors and to determine if there were differences between the FD and control cells. These results showed that the cells were capable of producing all 15 factors and there was no significant difference between the two cell types (Supplementary Figure 3).

Serum was taken from female mice at the experimental end stage and analysed using the multiplex assay. There was no significant difference between FD and control mouse serum for any of the markers assessed (Supplementary Figure 4).

Discussion

This study demonstrates for the first time that a pain-like phenotype develops in a mouse model of FD. Pain-like behaviour developed in FD mice when they were induced with doxycycline and corresponded to the development of FD. Additionally, more advanced FD pathology was coupled with worse pain-like behaviour. Previous studies reporting results from questionnaires on FD patients' pain experience showed that patients with polyostotic FD and more severe FD pathology typically reported greater prevalence of pain and higher pain scores than patients with monostotic FD [8, 10]. One challenge of this model and assessing pain-like behaviour is the bilateral development of FD which prevents the implementation of commonly used behavioural assessments such as gait analysis or weight bearing. As such, it was necessary to employ spontaneous behavioural tests that rely on welfare and functional assessments to determine the development of pain-like behaviour and subsequent relief from analgesics. Morphine treatment had a minor effect on grid hanging behaviour. This behaviour is typically utilised for muscle strength and mice may have difficulty gripping the grid. However, partial reversal was achieved in the morphine treated FD mice, demonstrating that pain-like development contributed to grid hanging deficiency, but this test and morphine treatment may not be suitable to assess pain-like development and analgesic treatment in this model. However, a robust change was observed in burrowing behaviour when FD was induced, which was reversed with ibuprofen treatment. This

strongly supports that the behavioural deficits observed in the FD mice were pain related and it further suggests an inflammatory component to the pain.

Four factors were identified that may contribute to pain-like development: inflammation, nerve sprouting in the FD lesion, acidosis due to osteoclast presence, and nerve damage (neuropathic-like pain). The presence of inflammatory chemokines (MCP-1, KC/GRO) and cytokines (IL-6, TNF-α), the efficacy of ibuprofen, presence of macrophages and/or monocytes, and presence of blood vessels (with increased expression of VEGF *in vitro*) in the lesion suggest that inflammation contributes to pain-like development [31-34]. However, the upregulated expression of these factors *in vitro* and not in the serum would suggest that these changes are local, rather than systemic. The expression of NGF, VEGF, cytokines, and chemokines by FD cells themselves suggests that they directly contribute to the FD pain-like pathology. Nerve sprouting of sensory nerve fibres and sympathetic neurons within the FD lesion, and NGF upregulation *in vitro* suggests increased peripheral sensitivity due to FD development [35, 36]. Furthermore, MCP-1 was upregulated in FD cells and previous research has demonstrated that MCP-1 can enhance transient receptor potential vanilloid 1 (TRPV1) density, which may contribute to pain [37]. MCP-1 may also contribute to the high presence of monocytes (osteoclast precursors) and macrophages in the FD lesion, due to its chemokine activity. Pain-like development in this model may be due to the pathological changes that occur in the FD lesion such as the increase of macrophages and osteoclasts that are associated with other painful bone disorders [19, 38, 39]. This high presence of osteoclasts may generate an acidic micro-environment that contributes to activation of acid-sensing ion channels in sensory nerve fibres [8, 40-42]. Lastly, two markers of peripheral nerve damage – ATF3 and TH – were upregulated in male mice that demonstrated more advanced FD, suggesting development of neuropathic-like pain in more advanced stages of FD [29, 30]. These four factors were somewhat variable across the mice; the complicated and individualistic nature of FD, as well as the difficulty of treating FD pain can suggest that these components variably contribute to pain in FD patients.

A limitation of the study is the lack of human samples with which to compare these results. FD is a rare disease and tissue samples are challenging to obtain. However, it would be highly beneficial to conduct histological and molecular assessments on FD lesions similar to those conducted here to determine the correlation strength. This would improve the validity and translatability of this model in studying FD pain and novel analgesic strategies. FD is a lifelong

condition, which is challenging to assess in this model that develops somewhat rapidly. A reduced and sustained doxycycline dose may allow for long-term *in vivo* assessment of pain-like development.

The confirmation of the development of a pain-like phenotype establishes this model as a tool to test novel analgesics to treat pain in FD patients, particularly novel antibody treatments targeting particular factors contributing to pain. Both TNF-α and NGF were upregulated *in vitro* in doxycycline-stimulated FD cells and analgesic treatments have been developed specifically targeting these two factors individually [43-45]. Both factors have adverse side-effects; recently however, novel research suggests that using a combination of the treatments maintains the analgesic effect with a lower dose of each drug and therefore producing fewer side-effects [46]. A proof-of-concept study applying this analgesic combination could be beneficial in further elucidating the underlying nociceptive mechanisms of FD and also testing novel analgesics for FD treatment. Further, the role of the central nervous system is yet to be explored, which may also yield information regarding the pain type in this model.

Here we established that this site-specific and inducible model developed FD with a corresponding pain-like phenotype. It can be further utilised to study novel and effective analgesics for FD patients, which are sorely needed.

Acknowledgement

Chelsea Hopkins and Anne-Marie Heegaard received funding for this project from the European Union's Horizon 2020 research and innovation programme under the Marie Skłodowska-Curie grant agreement No 814244.

References

1. Hartley, I., et al., *Fibrous Dysplasia of Bone and McCune-Albright Syndrome: A Bench to Bedside Review.* Calcif Tissue Int, 2019. **104**(5): p. 517-529.
2. Majoor, B.C.J., et al., *Illness Perceptions are Associated with Quality of Life in Patients with Fibrous Dysplasia.* Calcif Tissue Int, 2018. **102**(1): p. 23-31.
3. Hart, E.S., et al., *Onset, progression, and plateau of skeletal lesions in fibrous dysplasia and the relationship to functional outcome.* J Bone Miner Res, 2007. **22**(9): p. 1468-74.

4. Kelly, M.H., B. Brillante, and M.T. Collins, *Pain in fibrous dysplasia of bone: age-related changes and the anatomical distribution of skeletal lesions.* Osteoporos Int, 2008. **19**(1): p. 57-63.

5. Weinstein, L.S., *G(s)alpha mutations in fibrous dysplasia and McCune-Albright syndrome.* J Bone Miner Res, 2006. **21 Suppl 2**: p. P120-4.

6. Robinson, C., M.T. Collins, and A.M. Boyce, *Fibrous Dysplasia/McCune-Albright Syndrome: Clinical and Translational Perspectives.* Curr Osteoporos Rep, 2016. **14**(5): p. 178-86.

7. Javaid, M.K., et al., *Best practice management guidelines for fibrous dysplasia/McCune-Albright syndrome: a consensus statement from the FD/MAS international consortium.* Orphanet J Rare Dis, 2019. **14**(1): p. 139.

8. Spencer, T.L., et al., *Neuropathic-like Pain in Fibrous Dysplasia/McCune-Albright Syndrome.* J Clin Endocrinol Metab, 2022. **107**(6): p. e2258-e2266.

9. Kelly, M.H., et al., *Physical function is impaired but quality of life preserved in patients with fibrous dysplasia of bone.* Bone, 2005. **37**(3): p. 388-94.

10. Majoor, B.C.J., et al., *Pain in fibrous dysplasia: relationship with anatomical and clinical features.* Acta Orthop, 2019. **90**(4): p. 401-405.

11. Merrick, J. and M. Morad, *PAIN AND PAIN MANAGEMENT*, in *Pain Management: Recent International Research*. 2022. p. 1-6.

12. Thompson, A.L., T.M. Largent-Milnes, and T.W. Vanderah, *Animal models for the study of bone-derived pain*, in *Methods in Molecular Biology*. 2019. p. 391-407.

13. Chau, M.M. and D.R. Clohisy, *Mechanisms and management of bone cancer pain*, in *Bone Cancer: Bone Sarcomas and Bone Metastases - From Bench to Bedside*. 2021. p. 853-861.

14. Zhao, X.F., et al., *Expression of an active G alpha(s) mutant in skeletal stem cells is sufficient and necessary for fibrous dysplasia initiation and maintenance.* Proceedings of the National Academy of Sciences of the United States of America, 2018. **115**(3): p. E428-E437.

15. de Castro, L.F., et al., *Activation of RANK/RANKL/OPG Pathway Is Involved in the Pathophysiology of Fibrous Dysplasia and Associated With Disease Burden.* J Bone Miner Res, 2019. **34**(2): p. 290-294.

16. Hopkins, C., et al., *Fibrous dysplasia animal models: A systematic review.* Bone, 2022. **155**: p. 116270.

17. Iglesias-Bartolome, R., et al., *Inactivation of a Galpha(s)-PKA tumour suppressor pathway in skin stem cells initiates basal-cell carcinogenesis.* Nat Cell Biol, 2015. **17**(6): p. 793-803.

18. Logan, M., et al., *Expression of Cre recombinase in the developing mouse limb bud driven by a Prxl enhancer.* genesis, 2002. **33**(2): p. 77-80.

19. Domoto, R., et al., *Macrophage as a peripheral pain regulator.* Cells, 2021. **10**(8).

20. Falk, S., S. Gallego-Pedersen, and N.C. Petersen, *Grid-climbing Behaviour as a Pain Measure for Cancer-induced Bone Pain and Neuropathic Pain.* In Vivo, 2017. **31**(4): p. 619-623.

21. Deacon, R.M., *Measuring the strength of mice.* J Vis Exp, 2013(76).

22. Kondziella, W., *[a New Method for the Measurement of Muscle Relaxation in White Mice].* Arch Int Pharmacodyn Ther, 1964. **152**: p. 277-84.

23. Sliepen, S.H.J., et al., *Cancer-induced Bone Pain Impairs Burrowing Behaviour in Mouse and Rat.* In Vivo, 2019. **33**(4): p. 1125-1132.

24. Iannello, F., *Non-intrusive high throughput automated data collection from the home cage.* Heliyon, 2019. **5**(4): p. e01454.

25. Gage, G.J., D.R. Kipke, and W. Shain, *Whole animal perfusion fixation for rodents.* J Vis Exp, 2012(65).

26. Maridas, D.E., et al., *Isolation, Culture, and Differentiation of Bone Marrow Stromal Cells and Osteoclast Progenitors from Mice.* J Vis Exp, 2018(131).

27. Pernold, K., et al., *Towards large scale automated cage monitoring - Diurnal rhythm and impact of interventions on in-cage activity of C57BL/6J mice recorded*

24/7 with a non-disrupting capacitive-based technique. PLoS One, 2019. **14**(2): p. e0211063.

28. Urban, R., et al., *Behavioral indices of ongoing pain are largely unchanged in male mice with tissue or nerve injury-induced mechanical hypersensitivity.* Pain, 2011. **152**(5): p. 990-1000.

29. Matsuura, Y., et al., *Expression of activating transcription factor 3 (ATF3) in uninjured dorsal root ganglion neurons in a lower trunk avulsion pain model in rats.* Eur Spine J, 2013. **22**(8): p. 1794-9.

30. Atherton, M., et al., *Sympathetic modulation of tumor necrosis factor alpha-induced nociception in the presence of oral squamous cell carcinoma.* Pain, 2022.

31. Al-Mazidi, S., et al., *Association of Interleukin-6 and Other Cytokines with Self-Reported Pain in Prostate Cancer Patients Receiving Chemotherapy.* Pain Med, 2018. **19**(1526-4637 (Electronic)): p. 1058-1066.

32. Hu, X.M., et al., *Vascular Endothelial Growth Factor A Signaling Promotes Spinal Central Sensitization and Pain-related Behaviors in Female Rats with Bone Cancer.* Anesthesiology 2019. **131**(1528-1175 (Electronic)): p. 1125–1147.

33. Takano, S., et al., *Vascular Endothelial Growth Factor Is Regulated by the Canonical and Noncanonical Transforming Growth Factor-β Pathway in Synovial Fibroblasts Derived from Osteoarthritis Patients.* Biomed Res Int, 2019(2314-6141 (Electronic)).

34. Wyatt, L.A., et al., *Molecular expression patterns in the synovium and their association with advanced symptomatic knee osteoarthritis.* Osteoarthritis Cartilage, 2019. **27**(1522-9653 (Electronic)): p. 667-675.

35. Nencini, S., et al., *Mechanisms of nerve growth factor signaling in bone nociceptors and in an animal model of inflammatory bone pain.* Molecular Pain, 2017. **13**.

36. Morgan, M., et al., *TRPV1 activation alters the function of Aδ and C fiber sensory neurons that innervate bone.* Bone, 2019. **123**: p. 168-175.

37. Miller, R.E., et al., *CCR2 chemokine receptor signaling mediates pain in experimental osteoarthritis.* Proceedings of the National Academy of Sciences, 2012. **109**(50): p. 20602-20607.

38. Abe, Y., et al., *Inhibitory effect of bisphosphonate on osteoclast function contributes to improved skeletal pain in ovariectomized mice.* J Bone Miner Metab, 2015. **33**(2): p. 125-34.

39. Zhu, S., et al., *Subchondral bone osteoclasts induce sensory innervation and osteoarthritis pain.* J Clin Invest, 2019. **129**(3): p. 1076-1093.

40. Palmisano, B., et al., *RANKL Inhibition in Fibrous Dysplasia of Bone: A Preclinical Study in a Mouse Model of the Human Disease.* J Bone Miner Res, 2019.

41. Avnet, S., et al., *Cause and effect of microenvironmental acidosis on bone metastases.* Cancer and Metastasis Reviews, 2019. **38**(1-2): p. 133-147.

42. Julius, D. and A.I. Basbaum, *Molecular mechanisms of nociception.* Nature, 2001. **413**(6852): p. 203-210.

43. Katz, N., et al., *Efficacy and safety of tanezumab in the treatment of chronic low back pain.* PAIN, 2011. **152**(10).

44. Lane, N.E., et al., *Tanezumab for the treatment of pain from osteoarthritis of the knee.* N Engl J Med, 2010. **363**(16): p. 1521-31.

45. Li, J., et al., *Risk of Adverse Events After Anti-TNF Treatment for Inflammatory Rheumatological Disease. A Meta-Analysis.* Frontiers in Pharmacology, 2021. **12**.

46. AstraZeneca. *A Study of the Efficacy and Safety of MEDI7352 in Subjects With Painful Osteoarthritis of the Knee (BESPOKE)*. 2020 [cited 2022 22/12/2022]; Available from: https://clinicaltrials.gov/ct2/show/NCT04675034.

		Prrx1-Cre	Linker	GNAS	Reporter
Behavioural studies	FD mice	✓	✓	✓	Optional
	Control mice	✓	✓	X	Optional
In vitro studies	FD cells	✓	✓	✓	✓
	Control cells	✓	✓	X	✓

Table 1: Genotype of mice used in experimental studies. *Prrx1-Cre* represents the gene for Cre recombinase controlled by the Prrx1 promoter. Linker represents the *loxp-STOP-loxp-rtTA-IRES-GFP* gene controlling the expression of rtTA, which can only be expressed when Cre recombinase eliminates the *loxp-STOP-loxp* cassette. GNAS represents the $G\alpha_s^{R201C}$ gene that expresses the mutated FD gene. Reporter represents the *TetO-GLB1-Luc2* genes that expresses beta-galactosidase and luciferase. (FD: fibrous dysplasia; Prrx1: paired related homeobox 1; rtTA: reverse tetracycline transactivator; GFP: green fluorescent protein; $G\alpha_s^{R201C}$: mutated alpha subunit of G protein).

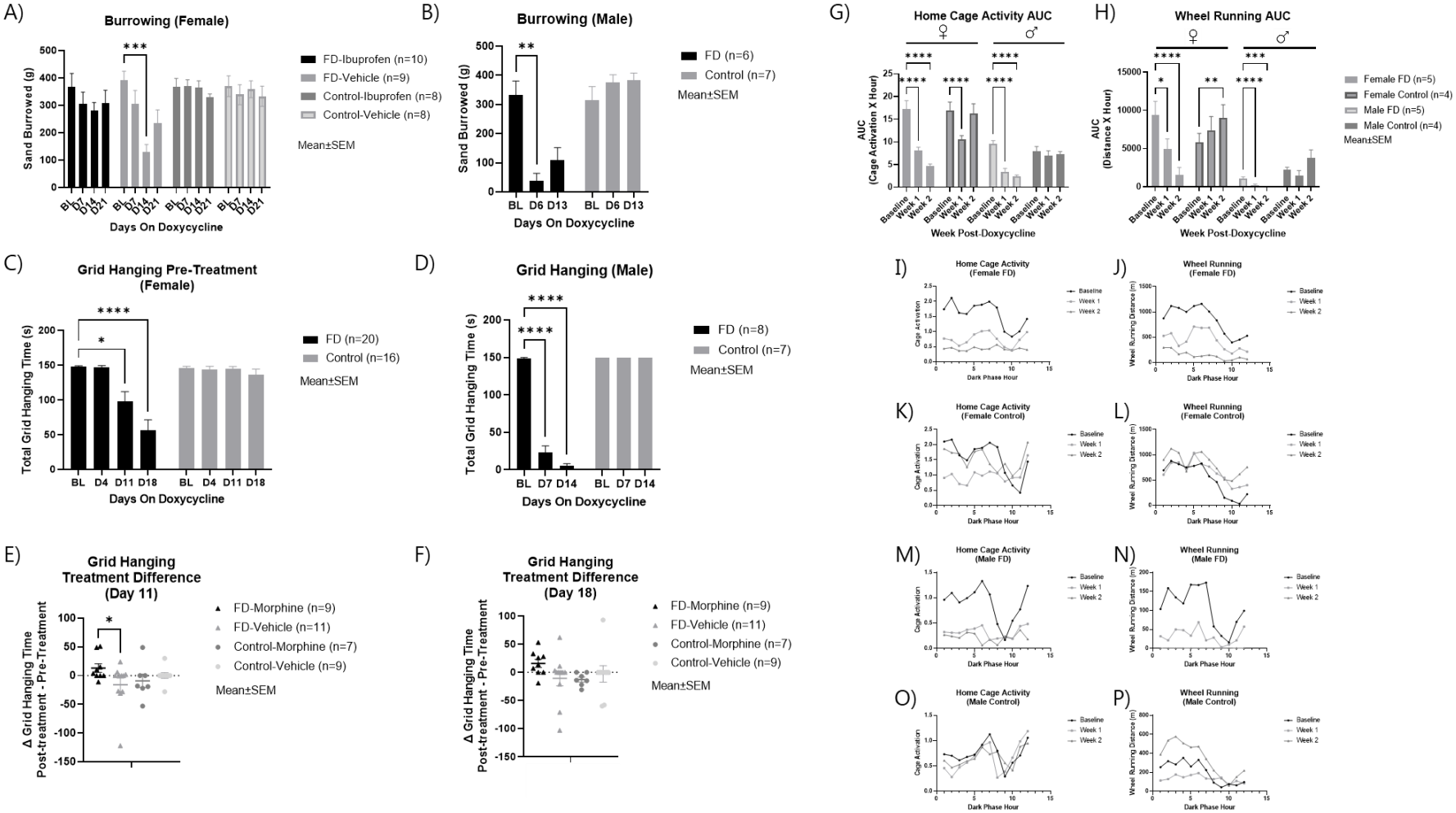
A)
Burrowing (Female)
Sand Burrowed (g)
Days On Doxycycline
FD-Ibuprofen (n=10)
FD-Vehicle (n=9)
Control-Ibuprofen (n=8)
Control-Vehicle (n=8)
Mean±SEM
B)
Burrowing (Male)
Sand Burrowed (g)
Days On Doxycycline
FD (n=6)
Control (n=7)
Mean±SEM
C)
Grid Hanging Pre-Treatment (Female)
Total Grid Hanging Time (s)
Days On Doxycycline
FD (n=20)
Control (n=16)
Mean±SEM
D)
Grid Hanging (Male)
Total Grid Hanging Time (s)
Days On Doxycycline
FD (n=8)
Control (n=7)
Mean±SEM
E)
Grid Hanging Treatment Difference (Day 11)
Δ Grid Hanging Time Post-treatment - Pre-Treatment
FD-Morphine (n=9)
FD-Vehicle (n=11)
Control-Morphine (n=7)
Control-Vehicle (n=9)
Mean±SEM
F)
Grid Hanging Treatment Difference (Day 18)
Δ Grid Hanging Time Post-treatment - Pre-Treatment
FD-Morphine (n=9)
FD-Vehicle (n=11)
Control-Morphine (n=7)
Control-Vehicle (n=9)
Mean±SEM
G)
Home Cage Activity AUC
AUC (Cage Activation X Hour)
Week Post-Doxycycline
H)
Wheel Running AUC
AUC (Distance X Hour)
Week Post-Doxycycline
Female FD (n=5)
Female Control (n=4)
Male FD (n=5)
Male Control (n=4)
Mean±SEM
I)
Home Cage Activity (Female FD)
J)
Wheel Running (Female FD)
K)
Home Cage Activity (Female Control)
L)
Wheel Running (Female Control)
M)
Home Cage Activity (Male FD)
N)
Wheel Running (Male FD)
O)
Home Cage Activity (Male Control)
P)
Wheel Running (Male Control)
Dark Phase Hour
Baseline
Week 1
Week 2

Figure 1: Behaviour changes in FD and Control Mice. A) Burrowing behaviour in female mice over time with ibuprofen (30mg/kg) and vehicle treatment (two-way ANOVA with Tukey's multiple comparison correction). B) Burrowing behaviour in male mice (two-way ANOVA with Tukey's multiple comparison correction). C) Grid climbing behaviour in female mice before treatment (two-way ANOVA with Tukey's multiple comparison correction). D) Grid climbing behaviour in male mice (two-way ANOVA with Tukey's multiple comparison correction). E) Grid climbing behaviour in female mice after morphine (10mg/kg) and vehicle treatment at D11 (one-way ANOVA). F) Grid climbing behaviour in female mice after morphine (10mg/kg) and vehicle treatment at D18 (one-way ANOVA). G) AUC of home cage activity in female and male mice over time (two-way ANOVA with Tukey's multiple comparison correction). H) AUC of wheel running distance in female and male mice over time (two-way ANOVA with Tukey's multiple comparison correction). I) Home cage activity of female FD mice. J) Wheel running distance of female FD mice. K) Home cage activity of female control mice. L) Wheel running distance of female control mice. M) Home cage activity of male FD mice. N) Wheel running distance of male FD mice. O) Home cage activity of male control mice. P) Wheel running distance of male control mice. (FD: fibrous dysplasia; BL: baseline; D: day; SEM: standard error mean; AUC: area under the curve; *: $p<0.05$; **: $p<0.01$; ***: $p<0.001$; ****: $p<0.0001$)

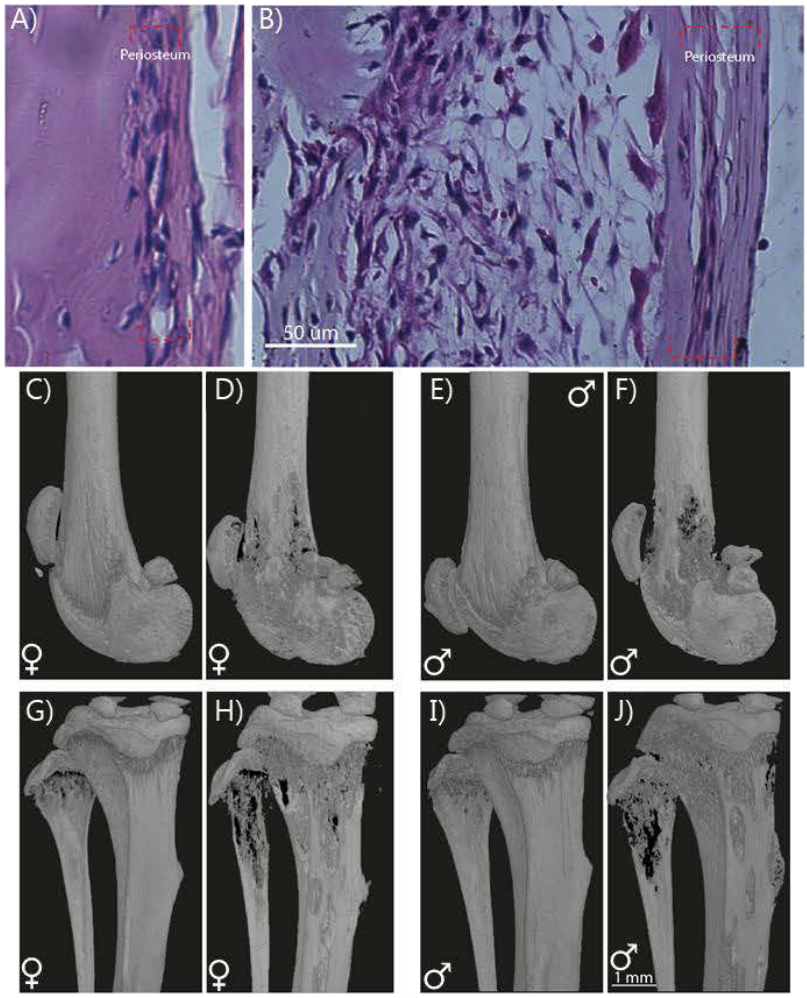
A)
Periosteum
B)
Periosteum
50 um
C)
D)
E)
F)
G)
H)
I)
J)
1 mm

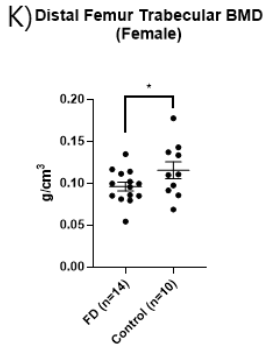
K) Distal Femur Trabecular BMD (Female)
g/cm3
FD (n=14)
Control (n=10)

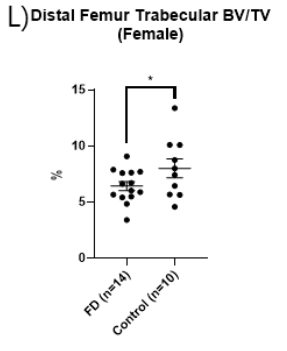
L) Distal Femur Trabecular BV/TV (Female)
%
FD (n=14)
Control (n=10)

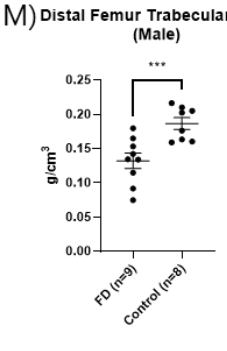
M) Distal Femur Trabecular BMD (Male)
g/cm3
FD (n=9)
Control (n=8)

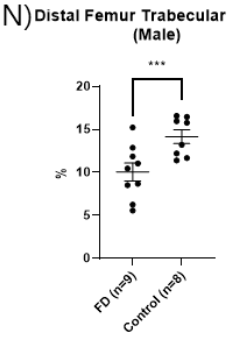
N) Distal Femur Trabecular BV/TV (Male)
%
FD (n=9)
Control (n=8)

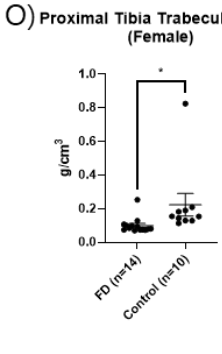
O) Proximal Tibia Trabecular BMD (Female)
g/cm3
FD (n=14)
Control (n=10)

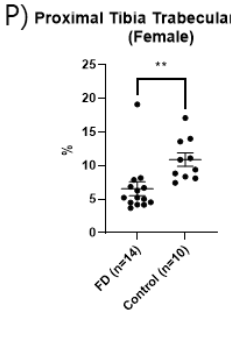
P) Proximal Tibia Trabecular BV/TV (Female)
%
FD (n=14)
Control (n=10)

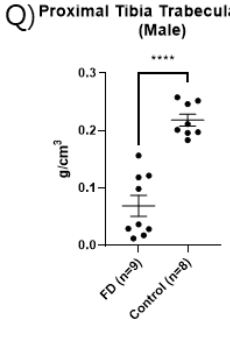
Q) Proximal Tibia Trabecular BMD (Male)
g/cm3
FD (n=9)
Control (n=8)

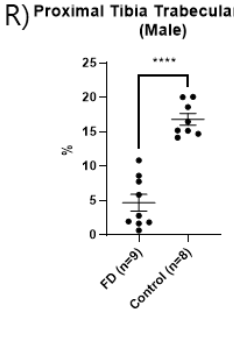
R) Proximal Tibia Trabecular BV/TV (Male)
%
FD (n=9)
Control (n=8)

Figure 2: Histological H&E staining (A, B) and micro-CT (C-R) in FD mice (B, D, F, H, J) compared to control mice (A, C, E, G, I). A, B) H&E histological staining of bone tissue. C-J) Representative micro-CT images of the distal femur (C-F) and proximal tibia and fibula (G-J) of FD (D, F, H, J) and control (C, E, G, I) mice, post-euthanasia. K-R) micro-CT analysis of BMD and BV/TV comparing FD mice and control mice. Unpaired student t-test used to compare groups. (FD: fibrous dysplasia; BMD: bone mineral density; BV/TV: bone volume fraction; CT: computed tomography; H&E: haematoxylin and eosin; *: $p<0.05$; **: $p<0.01$; ***: $p<0.001$; ****: $p<0.0001$)

			Female			Male		
			FD	Control	p-value	FD	Control	p-value
Trabecular Bone	Proximal Tibia	BMD (g/cm^3)	0.099±0.047	0.223±0.214	*0.0232*	0.069±0.055	0.218±0.029	*<0.0001*
		BV/TV (%)	6.550±3.880	10.90±3.130	*0.0040*	4.672±3.679	16.79±2.42	*<0.0001*
		Tb.Th (mm)	0.050±0.022	0.050±0.002	0.4598	0.053±0.016	0.047±0.002	0.1364
		Tb.N (mm^{-1})	1.290±0.247	2.160±0.591	*<0.0001*	0.938±0.765	3.560±0.396	*<0.0001*
		Tb.Sp (mm)	0.290±0.033	0.263±0.043	*0.0487*	0.334±0.137	0.178±0.011	*0.0030*
	Distal Femur	BMD (g/cm^3)	0.096±0.020	0.115±0.032	*0.0409*	0.132±0.034	0.187±0.024	*0.0009*
		BV/TV (%)	6.420±1.480	8.0±2.660	*0.0374*	10.10±3.120	14.20±2.250	*0.0039*
		Tb.Th (mm)	0.044±0.006	0.048±0.004	*0.0466*	0.046±0.005	0.046±0.002	0.4579
		Tb.N (mm^{-1})	1.460±0.268	1.670±0.515	0.0965	2.160±0.509	3.10±0.452	*0.0006*
		Tb.Sp (mm)	0.254±0.023	0.210±0.031	0.2547	0.217±0.041	0.193±0.012	0.0646
Cortical Bone	Proximal Tibia	BMD (g/cm^3)	1.130±0.038	1.120±0.028	0.267	1.010±0.051	1.10±0.017	*0.0002*
		Ct.Th (mm)	0.182±0.008	0.184±0.008	0.368	0.149±0.031	0.183±0.009	*0.0045*
		Ct.Ar (mm^{-1})	0.357±0.252	0.660±0.052	*0.0006*	0.042±0.025	0.737±0.058	*<0.0001*
	Distal Femur	BMD (g/cm^3)	1.218±0.042	1.213±0.029	0.362	1.090±0.660	1.180±0.034	*0.0025*
		Ct.Th (mm)	0.198±0.0	0.023±0.0	0.073	0.147±0.023	0.184±0.012	*0.0005*
		Ct.Ar (mm^{-1})	0.696±0.0	0.721±0.0	0.119	0.263±0.271	0.765±0.060	*<0.0001*

Table 2: micro-CT analysis and comparison between FD mice and control mice in both female and male mice. Italic values represent significant difference between the FD and control group based on the unpaired student t-test between the two values; no correction for multiple comparisons. (FD: fibrous dysplasia; BMD: bone mineral density; BV/TV: bone volume fraction; Tb.Th: trabecular thickness; Tb.N: trabecular number; Tb.Sp: trabecular spacing; Ct. Th: cortical thickness; Ct.Ar: cortical area)

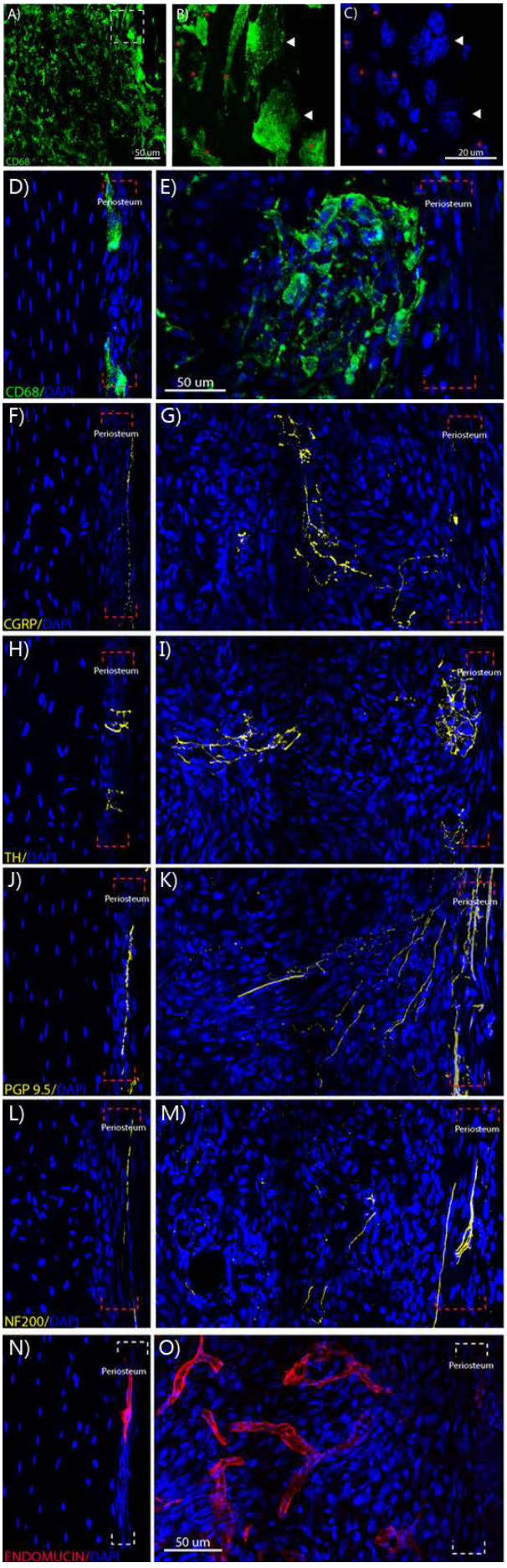
A)
B)
C)
50 um
CD68
20 um
D)
Periosteum
E)
Periosteum
CD68/DAPI
50 um
F)
Periosteum
G)
Periosteum
CGRP/DAPI
H)
Periosteum
I)
Periosteum
TH/DAPI
J)
Periosteum
K)
Periosteum
PGP 9.5/DAPI
L)
Periosteum
M)
Periosteum
NF200/DAPI
N)
Periosteum
O)
Periosteum
50 um
ENDOMUCIN/DAPI

Figure 3: Representative images of IHC staining of bone innervation and vascularity in FD mice (A, B, C, E, G, I, K, M, O) and control mice (D, F, H, J, L, N). A-E) CD68 and DAPI staining demonstrating cells from the monocyte-lineage. Red asterisk demonstrates mononuclear cells (e.g. monocytes, macrophages, pre-osteoclasts) and white arrowhead demonstrates multinuclear cells (e.g. osteoclasts); F,G) CGRP and DAPI staining; H,I) TH and DAPI staining; J,K) PGP9.5 and DAPI staining; L,M) NF200 and DAPI staining; N,O) Endomucin and DAPI staining. (IHC: immunohistochemistry; FD: fibrous dysplasia; CD68: cluster of differentiation 68; DAPI: 4',6-diamidino-2-phenylindole; PGP9.5: protein gene product 9.5; CGRP: calcitonin gene-related peptide; TH: tyrosine hydroxylase; NF200: neurofilament 200)

		Femur						Tibia					
		CD68	PGP9.5	CGRP	TH	NF200	Endomucin	CD68	PGP9.5	CGRP	TH	NF200	Endomucin
Female	FD Lesion	5/6	2/6	5/6	2/6	0/6	5/6	5/6	3/6	3/6	1/6	2/6	5/6
	Periosteum	N/A	0/6	2/6	0/6	N/A	N/A	N/A	0/6	0/6	0/6	N/A	N/A
Male	FD Lesion	6/6	1/6	6/6	2/6	0/6	5/6	6/6	2/6	2/6	0/6	1/6	6/6
	Periosteum	N/A	0/6	1/6	1/6	N/A	N/A	N/A	0/6	0/6	0/6	N/A	N/A

Table 3: Number of FD bone samples demonstrating staining of nerve fibres (PGP9.5, CGRP, TH, NF200), blood vessels (Endomucin), and CD68-positive cells in the fibrous tissue lesion and periosteum. (FD: fibrous dysplasia; CD68: cluster of differentiation 68; PGP9.5: protein gene product 9.5; CGRP: calcitonin gene-related peptide; TH: tyrosine hydroxylase; NF200: neurofilament 200)

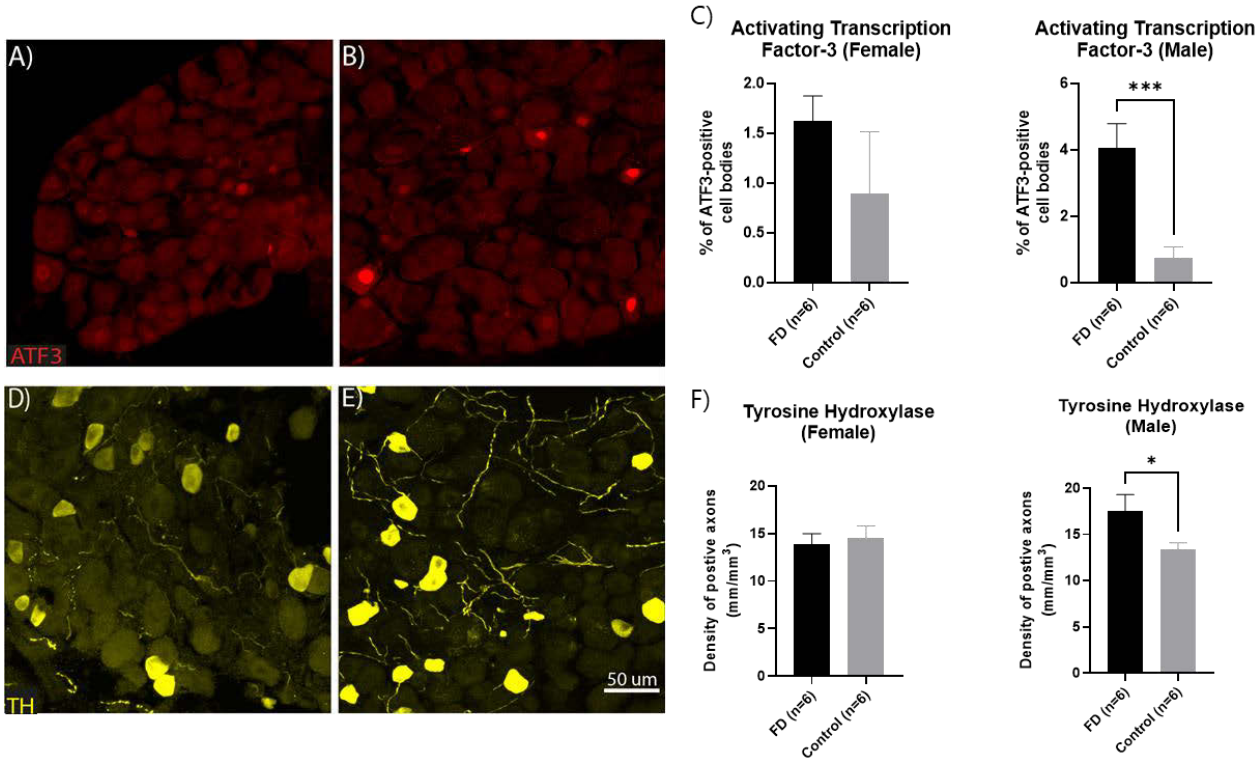

Figure 4: Protein expression change in DRGs from FD and control mice. Representative IHC images of DRGs from (A,D) control and (B,E) FD mice. A,B) ATF3 staining of DRGs; D,E) TH staining of DRGs; C) graphs demonstrating proportion of DRG cells bodies with ATF3 staining in female and male mice; F) graph demonstrating proportion of TH-positive axons in DRGs from female and male mice. Unpaired student t-test. (DRG: dorsal root ganglion; FD: fibrous dysplasia; ATF3: activating transcription factor 3; TH: tyrosine hydroxylase; *: $p<0.05$; ***: $p<0.001$)

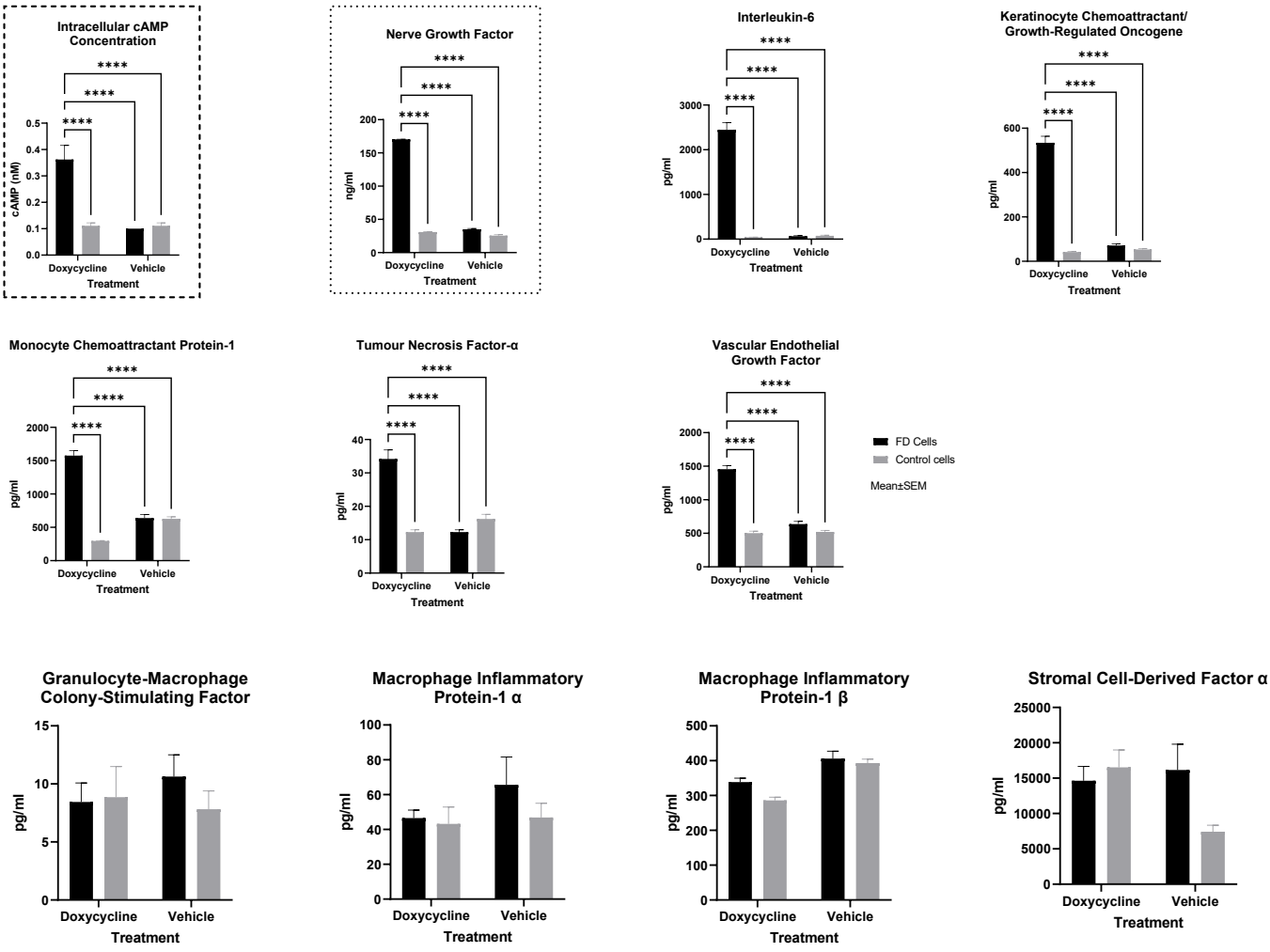

Figure 5: *In vitro* cAMP assay (dash border), NGF ELISA (dot border), and multiplex assay. FD cells (black) and control cells (grey) were activated with doxycycline (10µg/ml) or vehicle (phosphate buffered saline) for 24 hours. Intracellular cAMP assessed using cAMP Gs dynamic kit and protein factors assessed using MSD U-PLEX assay. Two-way ANOVA with Tukey's multiple comparison test. (FD: fibrous dysplasia; SEM: standard error mean; ****: $p<0.0001$)

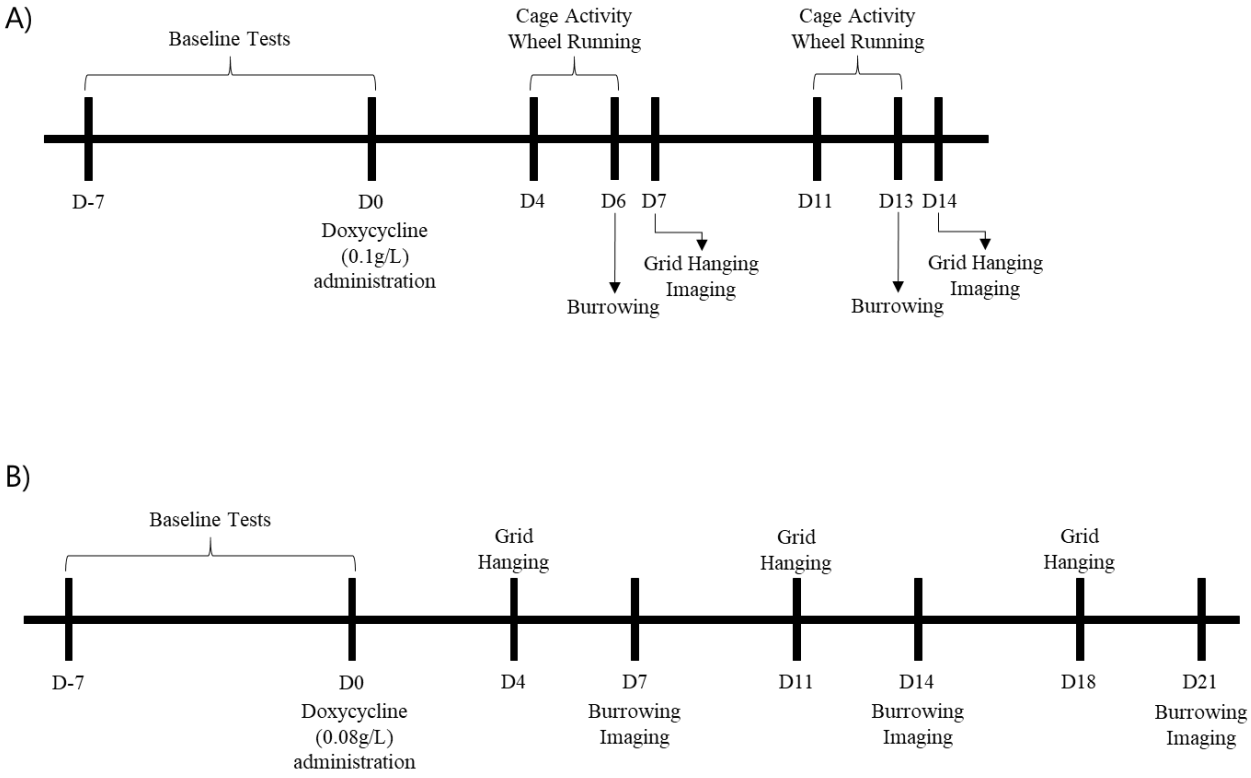

Supplementary Figure 1: Study designs of behavioural studies conducted. A) First behavioural study conducted on male and female mice to assess the development of pain-like behaviour in burrowing, grid hanging, home cage activity, and wheel running. B) Second behavioural study to assess the development of pain-like behaviour and efficacy of analgesics in female mice on burrowing and grid hanging.

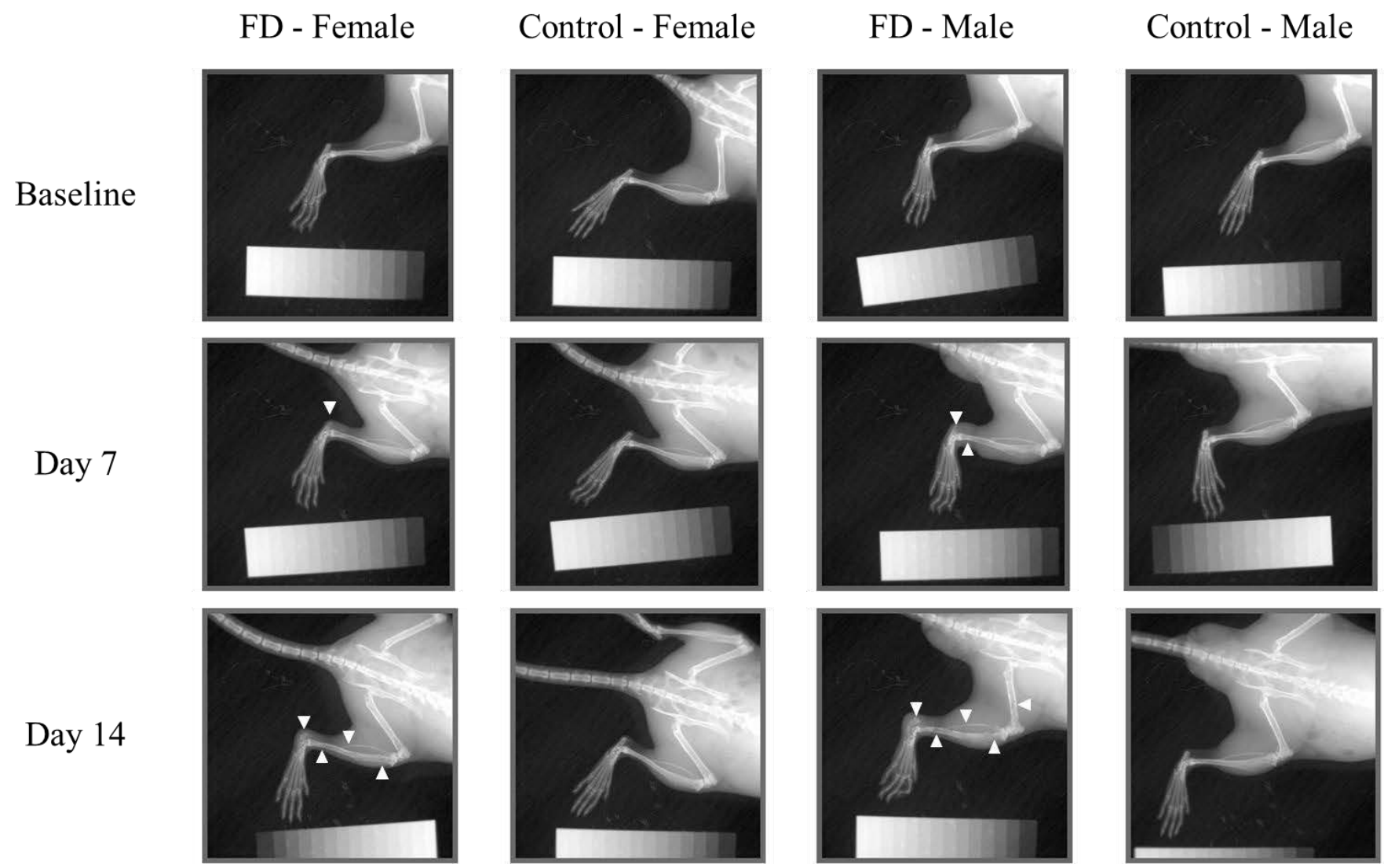
FD - Female
Control - Female
FD - Male
Control - Male
Baseline
Day 7
Day 14

Supplementary Figure 2: Representative x-ray images of right hind limbs in female and male mice for 14 days. White arrowheads represent areas of reduced calcification and pathological changes.

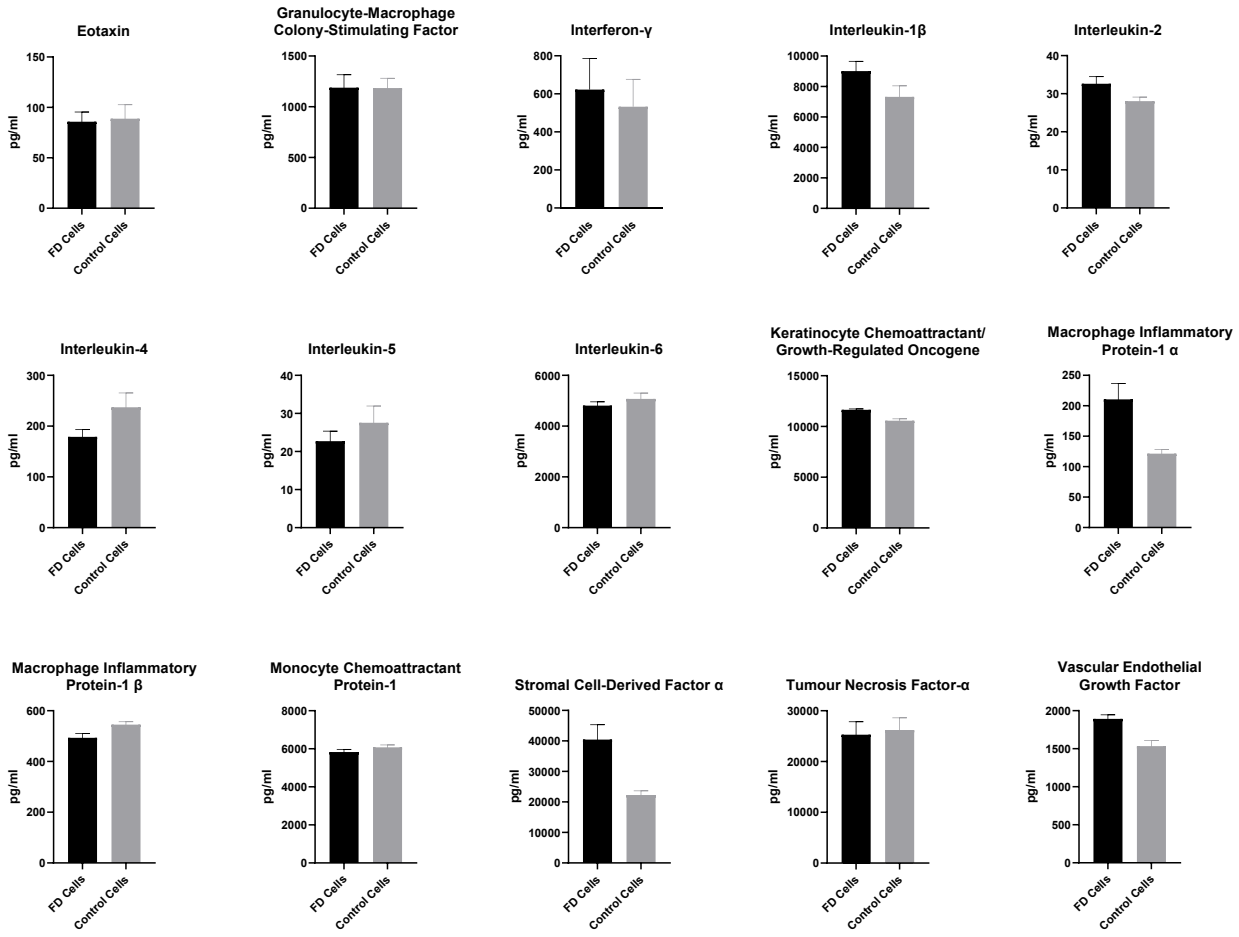

Supplementary Figure 3: *In vitro* conditioned medium assessed using a multiplex assay. FD cells and control cells were stimulated with TNF-α for 48 hours. Unpaired student t-test. (FD: fibrous dysplasia; TNF-α: tumour necrosis factor alpha)

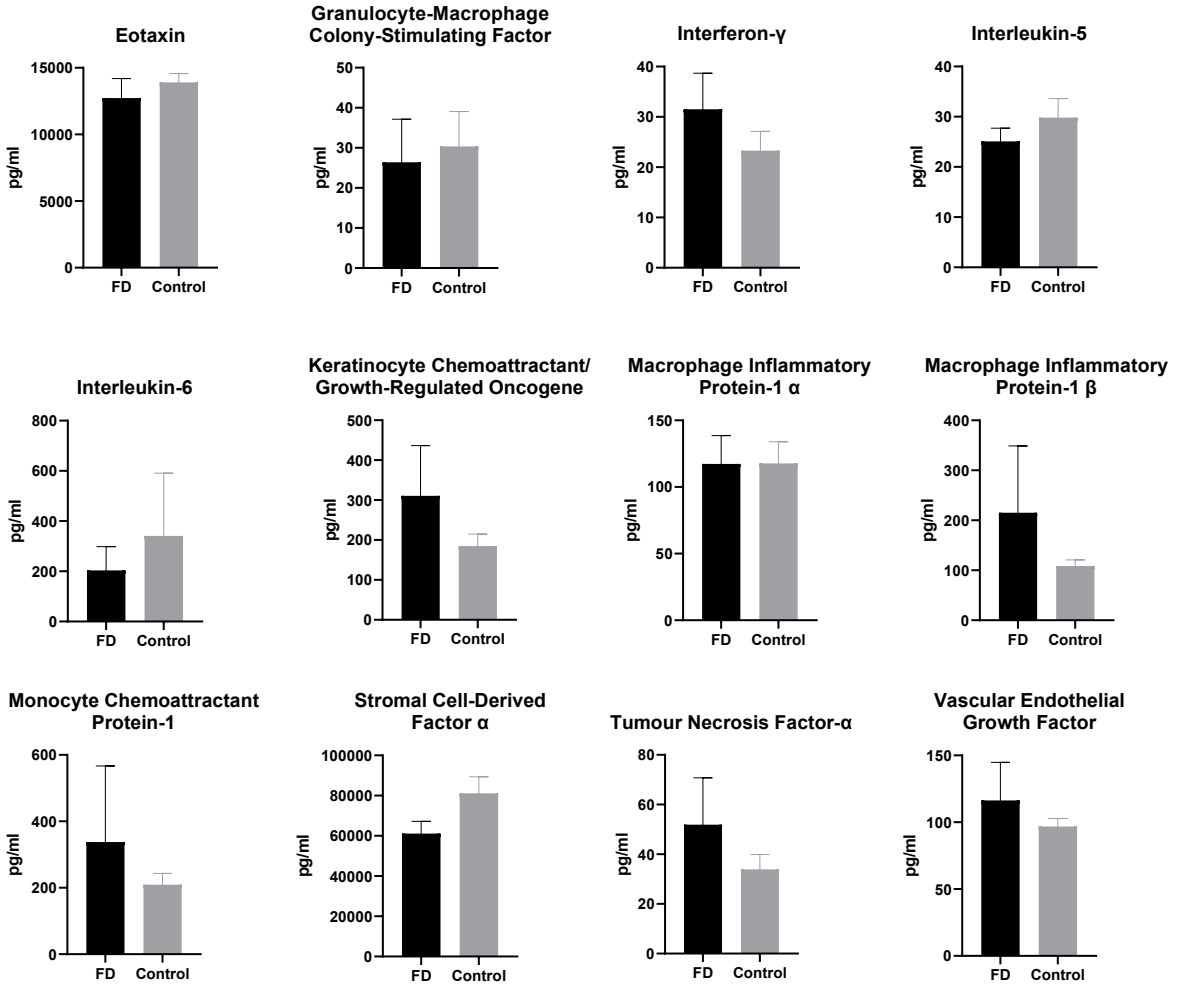

Supplementary Figure 4: Serum from FD and control mice assessed using a multiplex assay. Serum was collected from mice after three weeks of FD induction with doxycycline. Unpaired student t-test. (FD: fibrous dysplasia; TNF-α: tumour necrosis factor alpha)

Chapter 3

Cancer-Induced Bone Pain Model in Digital Ventilated Cages®

Introduction

Breast cancer patients often experience painful bone metastases [233]. Although patients are likely to experience pain relief when treated according to current guidelines, current medication and long-term treatments have side effects that impair quality of life [234]. Preclinical models have been established that are essential to test novel analgesics for use in cancer patients, and the tools to assess these models are quickly evolving [235].

Evoked stimuli (e.g. mechanical stimuli, thermal stimuli) are commonly used to assess pain in patients and pain-like behaviour in rodents [100, 172]. However, previous studies have questioned if these are reflexive rather than pain-like behaviours, and patients report that spontaneous and movement-evoked pain is more troublesome than evoked pain [236].

Indeed, Sadler et al. recently advocated for unbiased and prolonged behavioural assessments measuring spontaneous pain, citing both wheel running and home cage monitoring [236]. However, strain, sex, and model type can all affect these measures, thus behavioural patterns for specific experimental setups should be established prior to further studies involving treatments [181, 182, 186, 237].

DVCs® with home cage wheels provide the opportunity to assess spontaneous pain-like behaviour using home cage monitoring and wheel running, in a prolonged and unbiased manner [229]. The aim of this study was to develop a method to use DVCs® with in-cage wheels to assess pain-like behaviour in a defined cancer-induced bone pain model. In so doing, we may be able to confirm that these parameters are affected in a known model of pain-like development, supporting the behaviour observed in Manuscript 2.

Methodology

Twenty BALB/cAnHsd mice were used in this study. At baseline, mice were acclimatised and trained in group housing to establish wheel running behaviour. Mice were moved to single-housed DVCs® and baseline training and assessments were conducted for limb use and static weight bearing. Gait analysis was conducted using an established scoring technique assessing

normal gait (score = 4) to lack of use of the ipsilateral leg (score = 0). Static weight bearing was conducted by training mice to stand on two weight scale plates, which demonstrates if mice begin to favour the contralateral limb. On D0, 10 mice were inoculated with 4T1-Luc2 cells, mammary adenocarcinoma cells, in the right hind femur [228, 238]. The other 10 mice underwent sham surgery with no cell inoculation. The experimenter was blinded to group allocation until data analysis was complete. On D1-D4, mice underwent severity scoring and post-surgical care (Appendix 2). Every day from D5 until the humane endpoint was reached, mice were removed from the rack at 30-45 minute intervals and procedures were performed for tests lasting approximately 15 minutes. All mice were placed back in the DVC® rack before noon, to allow mice to return to baseline home cage behaviour before the dark phase from 7pm-7am. When mice reached the humane endpoint (limb use score = 0), mice underwent x-ray and bioluminescent imaging, and were euthanised by cervical dislocation. Statistical analysis was conducted using GraphPad Prism (9.3.1), with parametric data analysed using the mixed effect model, one-way ANOVA, or two-way ANOVA with correction for multiple comparisons. Non-parametric data (limb use) was analysed using the Friedman test and Mann-Whitney U test in SAS® and GraphPad Prism, respectively. Due to the loss of 4T1-inoculated mice throughout the course of the study, the last observation was carried forward to perform statistical analysis.

Results and Discussion

Mice that were inoculated with 4T1-Luc2 cells developed significant pain-like behaviour in both the limb use and weight bearing test from D12 and D10, respectively, but the sham group remained unchanged. Similarly, wheel running started to significantly decrease in the 4T1-inoculated mice from D12 and the sham group remained unchanged. When comparing wheel running decline to limb use decline, there was a significant difference between wheel running distance when mice scored a limb use score of 2 and 0 to baseline. When mice scored a limb use score of 1, they demonstrated decreased wheel running (similar to limb use score of 2), but this was not significant (most likely due to the data spread). Mice demonstrated a specific diurnal behavioural pattern, with high activity and wheel running in the first four hours, which then declined over the rest of the dark phase. Reduced wheel running due to the development of CIBP was particularly prevalent during this high-activity period. This same pattern was also observed in a different home cage system, highlighting that BALB/c mice demonstrate specific diurnal patterns reproducible in different systems [186]. The effect of CIBP on wheel running supports

results in past studies, but the primary benefit of this system over previously reported systems is the ability to assess wheel running behaviour over the full 12-hour dark phase.

There were no trends observed in home cage activity, which remained the same across the study – no trends or significant difference was observed. Previous studies have demonstrated that pain-like behaviour is related to reduced horizontal activity [181, 182, 239-241], but here and in the Urban et al. study (also used BALB/c strain) no difference was observed [186]. This may be strain or model dependent, but the process of testing two spontaneous behaviours in the same system may not be suitable.

A major limitation of this study is that analgesics were not assessed to reverse the effect of pain-like development on wheel running. Opioids are the standard treatment option for CIBP, as weaker analgesics such as NSAIDs and lower opioid doses are ineffective [242, 243]. However, opioids have effects on locomotion and activity that may affect its behaviour. A previous study demonstrated that a low dose of morphine (5mg/kg) demonstrated a significantly reduced wheel running in sham mice, but did partially recover wheel running in a model of inflammatory pain [181]. This suggests that opioids could feasibly be used to assess pain-like behaviour with wheel running as a behavioural outcome. However, morphine has a half-life of approximately 30 minutes in mice, which is not sufficient to provide analgesic relief over the first four active hours of the dark phase in this model [244, 245]. Buprenorphine hydrochloride with a 3-5 hour treatment period, or sustained release buprenorphine with a longer half-life may be better tolerated in this model, but further studies are required [246, 247].

Conclusion

This study is the first to demonstrate the potential of DVCs® as a tool to assess spontaneous pain-like behaviour in a mouse model. Here, the model used was of CIBP due to mammary adenocarcinoma inoculated in the femur, demonstrating an effect on wheel running but not home cage activity. This confirms that this system is capable of detecting the development of pain-like behaviour in an established model of pain-like development, which supports the observations in Manuscript 2 where the development of pain-like behaviour corresponded to a reduction in wheel running, and home cage activity as the disease progressed.

Wheel running, but not home cage activity in Digital Ventilated Cages® is impaired in a mouse model of breast cancer-induced bone pain

Chelsea Hopkins[1], Ida Buur Kanneworff[1], Birgitte Rahbek Kornum[2], Anne-Marie Heegaard[1]*

[1] Department of Drug Design and Pharmacology, University of Copenhagen, Copenhagen, Denmark

[2] Department of Neuroscience, University of Copenhagen, Copenhagen, Denmark

*Corresponding author: Department of Drug Design and Pharmacology, University of Copenhagen, Universitetsparken 2, 2100 Copenhagen, Denmark, amhe@sund.ku.dk

Abstract

Introduction: Cancer-induced bone pain (CIBP) due to metastatic breast cancer is common and debilitating. Effective, long-term treatment options have side effects that reduce patients' quality of life. Preclinical models are a valuable tool to test novel analgesics, but new methods that are translationally and clinically relevant are necessary. This study aimed to assess spontaneous pain-like behaviour of home cage activity and wheel running in Digital Ventilated Cages®.

Method: Twenty BALB/cAnNHsd mice were housed in Digital Ventilated Cages® from Tecniplast® with GYM500 home cage running wheels. Mice were assessed by limb use analysis and static weight bearing to determine the development of CIBP and this was compared to the dark-phase home cage activity and wheel running in the Digital Ventilated Cages®. Ten mice underwent 4T1-Luc2 mammary gland adenocarcinoma cell inoculation into the right femur to establish CIBP and another ten mice underwent a sham surgical procedure.

Results: The 4T1-inoculated mice displayed pain-like behaviour in limb use and weight bearing tests, demonstrating a preference for the contralateral limb. The limb use scores were compared with home cage activity and wheel running. A reduced wheel running distance corresponded to reduced limb use scores, with the shortest wheel running distances corresponding to the lowest limb use scores. However, this behavioural pattern was not observed in home cage activity, which remained consistent over the study period.

Discussion: Reduced wheel running corresponded with reduced limb use scores. This suggests that wheel running behaviour is affected by the development of metastatic breast cancer.

However, the home cage activity was not influenced by disease development. Digital Ventilated Cage® wheel running may be a useful behavioural assessment of spontaneous pain-like behaviour of CIBP and may be useful to assess analgesic efficacy.

Introduction

In patients with advanced breast cancer, 58% will experience bone metastases [1] and of those, 68% will experience bone pain [2]. These patients commonly experience worse pain and quality of life than patients with metastases in non-bone tissue. It has also been reported that of the patients with painful bone metastases, 97% are on analgesics; 55% taking opioids and 42% taking non-opioids [2]. However, long-term pain relief therapies (e.g. non-steroidal anti-inflammatory drugs, opioids) lead to an increase in side effects that impair quality of life [3]. Preclinical *in vivo* models are an essential tool to investigate nociceptive mechanisms and novel analgesics [4].

Evoked pain tests are common in pre-clinical settings to assess mechanical hypersensitivity (i.e. Von Frey test) and thermal hypersensitivity [5, 6]. However, spontaneous, ongoing pain is considered a more relevant issue for patients, and this is difficult to test *in vivo* [7]. Pain is not only a sensory condition, but may also encompass stress, anxiety, depression, and limit social interactions. The sensory and affective conditions should be assessed in combination to develop a well-rounded model of pain. Furthermore, *in vivo* tests often occur during the day over a short period, when rodents are least active, which means that a measure of spontaneous pain fluctuations may be difficult to gauge [8].

Tecniplast SpA has developed Digital Ventilated Cages® (DVCs®) that can track home cage activity and monitor wheel running. The DVC® rack is equipped with an electromagnetic sensing board with capacitance sensing technology to assess home cage activity; the board contains 12 electrodes that emit an electromagnetic field and when a mouse moves over these fields, it creates a disturbance that is recorded and measured. Readings are obtained continuously and unobtrusively when the cages are in the rack, allowing for continuous monitoring without handling interference during the 12-hour dark phase when mice are more active [9]. This provides the following benefits: evaluate ethologically relevant behaviour in a familiar home cage environment, minimise researcher interference, and reduce handling stress, thus mitigating common confounding factors in pain behavioural studies. DVCs® have been used in previous

studies to assess circadian rhythms [10-12], effect of standard procedures on cage activity [12, 13], severity monitoring [13, 14], and recently a novel treatment for osteoarthritis pain (rest disturbance metric only) [15]. Wheels with perpendicular magnets have been developed that can be placed in the cages, and their rotation, speed, and distance monitored automatically. However, wheel running in DVCs® has never been established or measured as a behavioural outcome.

A distinction should be made between home cage activity, horizontal activity, and vertical activity. Home cage activity describes the movement and activity around the home cage environment where a rodent is permanently housed. Horizontal activity describes movement in a two-dimensional testing area where a rodent is allowed to explore freely for a specified time. Vertical activity may be described as rearing, where the rodent stands only on its hind legs in order to extend vertically upwards. Reduced horizontal activity has been observed in fracture [16], arthritic [17], inflammatory [18, 19], neuropathic [19], and cancer-induced bone pain models [20]. These experiments were conducted over short (60-120 min) [17-19] and 20-hour periods [16, 20], but not in standard home cages. These experimental setups may introduce confounding stress and exploratory behaviours, and they require additional time to set up and carry out the experiment. Urban et al. [21] used a home cage monitoring system to demonstrate that a neuropathic pain model resulted in reduced cage activity in a neuropathic pain model in a BALB/c mouse strain compared to naïve mice. The system is similar to PhenoTyper® developed by Noldus®, which uses LED units and cameras to measure behaviour [22]. Wheel running (during a short period) has been used in previous studies to assess the development of pain-like behaviour in models of prostate cancer-induced bone pain [23], inflammation, and neuropathic pain [18, 19, 24].

The aim of this study is to determine if home cage activity and wheel running are affected by the development of breast CIBP. These metrics are compared to limb use behaviour, an established test of pain-like behaviour in this mouse model.

Method

Animals

Twenty 5-week-old female BALB/cAnNHsd mice were used in this study; ten mice were inoculated with 4T1-Luc2 cells and ten mice underwent sham surgery. All experiments were conducted according to the Danish Animal Experiments Inspectorate (Copenhagen, Denmark,

2020_15_0201_00439). Mice were purchased from Envigo (USA) and housed in a certified specific pathogen-free facility at the University of Copenhagen where all experiments were conducted. The research unit maintains a temperature of 22±2°C and humidity of 55±10% in housing and experimental rooms. The light/dark cycle was 12-hours and light was kept at 60% intensity (7am-7pm). During the acclimatisation period, mice were housed in GM500 individually ventilated cages with GYM500 cage wheels (Tecniplast®, Italy) and during the testing period, mice were housed in the DVCs® within the DVC® rack (Tecniplast®, Italy). All cages contained wood-chip bedding material (Tapvei 2HV, Brogaarden, Denmark), one transparent red housing unit (Polycarbonate Mouse Tunnel, Datesand, UK), a running wheel (DVC® GYM500, Tecniplast®, Italy), nesting material (paper shavings, Brogaarden, Denmark), and a wooden gnawing block (Aspe små klodser, Brogaarden, Denmark). Standard chow (Altromin 1324, Brogaarden, Denmark) and tap water were provided ad libitum. Fresh food and water was provided once per week and cages were changed every two weeks. Severity monitoring was conducted during the baseline experiments, D1-D4 after surgery, and every experimental day thereafter. Severity monitoring included weight loss/gain, coat condition, aggression, mobility, etc. A predefined scoring system was implemented to ensure that mice did not surpass the humane endpoint. The humane endpoint was a mouse reaching a pre-defined severity score of six or a limb use score zero. The experimental endpoint was defined as a 4T1-inoculated mouse reaching a limb use score of zero and control mice reached the experimental endpoint when all 4T1-inoculated mice had been euthanised. Mice were only handled using the tunnel handling method or scooping them with hands to minimise stress. All mice were euthanised by cervical dislocation.

Study Design

Mice were stratified into the 4T1-inoculated group and sham control group according to weight-bearing baseline data and body weight by the primary researcher (CH) to ensure that both groups had an equal average baseline behaviour and weight. The experimenter (IBK) was blinded throughout the experiment to the group allocation. Blinding was not possible during data analysis due to the nature of the experiment where group allocation is revealed during the course of the study. Each mouse acted as one experimental unit. Mice were excluded from the experiment if they demonstrated any indication of poor health prior to surgery, if they did not completely heal after surgery prior to D5, if they demonstrated symptoms of tendon

displacement (e.g. limping, unable to extend ipsilateral limb), or if they did not run on their cage wheel. All behavioural experiments that were conducted outside the cage were done in the morning (9am-12pm) at the same time for each mouse.

Experimental Timeline

Figure 1 demonstrates the timeline of the full experiment. Mice were introduced to the facilities at 5-weeks old. They acclimatised for one week prior to baseline experiments without interruption. At D-7 they were transferred to individually housed DVCs®. From D-7 to D-5, mice were trained and habituated to the static weight bearing procedure. On D-4, no behavioural or experimental procedures were conducted prior to the dark phase to obtain cage activity and wheel running data that is not influenced by experimenter handling. On D-3 and D-2, mice underwent limb use and weight bearing baseline tests. The following dark phases were used as baseline assessments to determine the effect of handling on cage activity and wheel running. Baseline x-ray images were collected on D-1 and surgery was conducted on D0. Post-surgical care was conducted from D1-D4. From D5 onwards, limb use and weight bearing were conducted every day during the light phase and cage activity and wheel running were only assessed in the dark phase. Imaging was conducted on D8 and prior to euthanasia when mice reached the experimental or humane endpoint.

Cell Culture

Mouse mammary gland adenocarcinoma cells (Bioware Ultra Cell Line 4T1-luc2; Caliper Life Sciences, Teralfene, Belgium; ATCC (CRL-2539^{TM}) parental line) were cultured as previously described [25, 26]. Cells were cultured in vented sterile cell culture flasks (75cm^2; Cellstar®, Greiner, Austria) in a sterile environment. Cells were maintained in RPMI 1640 cell culture media without phenol red (Gibco®, USA), supplemented with 10% heat-inactivated foetal bovine serum (Gibco®, USA) and 1% penicillin-streptomycin-glutamine (Gibco®, USA). Prior to surgery, cells were cultured for two weeks and then split two days before to ensure log-phase growth. To split and harvest the cells, 0.5% trypsin-EDTA (Gibco®, USA) was applied to the cells for 5 minutes. Trypsin was inactivated with regular cell media, the solution was centrifuged, supernatant discarded, and cells resuspended in Hank Balanced Salt Solution (HBSS; Gibco®, USA) to a concentration of 10^6 cells/ml. Cells were kept on ice thereafter.

Cancer Cell Inoculation in Femur

Surgery was conducted as previously described, with minor modification [26]. Mice were anaesthetised with an intraperitoneal xylazine/ketamine cocktail (43 mg/kg ketamine, MSD Animal Health, AN Boxmeer, the Netherlands; 6mg/kg xylazine, Rompun vet, Bayer, Germany). Mice were maintained on 1-1.2% isoflurane (1000mg/g isoflurane, Attane vet, ScanVet, UK) throughout surgery. Eye ointment (Ophtha A/S, Activis Group, Gentofte, Denmark) was applied to the eyes, 0.9% saline was injected subcutaneously to prevent post-surgical dehydration, and 5 mg/kg carprofen (Carprosan Vet, Dechra, the Netherlands) was injected subcutaneously. Mice were placed on a heated surgery table in a supine position. A small incision was made over the patella tendon and in the connective tissue on the medial side of the tendon. The tendon was positioned to the lateral side of the knee. A 30-G needle was used to manually drill a hole into the femoral epiphysis until the medullary cavity was reached. Using a 0.3 ml insulin syringe (BD, USA), 10 µl of 4T1-luc2 cells (4T1-inoculated group) or HBSS was injected into the cavity and incubated for 1 minute. The hole was filled with bone wax (Harvard Apparatus, USA) and the patella tendon moved back to the central position. The region was thoroughly rinsed with 0.9% saline and the incision closed with two medical clips (Michel Suture Clips, Agnthos, Sweden). Mice were maintained in a prone position on a heat map until they regained mobility. On D1, mice were administered 5 mg/kg carprofen subcutaneously for post-surgical analgesia.

Digital Ventilated Cage® - Home Cage Activity and Wheel Running

The electromagnetic wheels (GYM500, Tecniplast, Italy) were secured to the inner side of the DVCs®. When the wheel spins, the electromagnetic field produced by the magnets can be detected and tracked. The cumulative distance during the dark phase was assessed. Mice are acclimatised for one week in group housing (5 mice per cage) with a cage wheel in the Individual Ventilated Cages®. This is an essential training and habituation step for the mice. Mice without wheel habituation may not use the running wheel during the testing period. After the acclimatisation period, mice were single housed in the DVCs® and rack. Assessments conducted outside of the cages were conducted during the same time in the morning, for the same period. This arrangement was practiced to ensure that dark phase behaviour was not influenced by behaviour experiments and handling during the light phase. When mice were removed from their cages during the behavioural experiments, bedding material was moved

away from the wheel; bedding can interfere with the wheel mechanism and magnets, preventing accurate readings. The rack was placed in the housing room away from the entrance door to prevent excess interference and in a position with minimal human traffic. The mice were housed with half the mice from each group at the top and bottom of the rack to determine if position in the rack was a confounding factor. Analysis was conducted on data collected from the dark phase (7pm-7am). Mice with a peak hourly distance of less than 500 m were excluded from the experiment.

Home cage activity metrics and the associated calculations have been described previously [9] and shown to be comparable to manually analysed video analysis of mouse behaviour in the cage. When the emitted electromagnetic field is disturbed, it will be detected and recorded. The calculated activity density is calculated every minute (four recordings per minute) and the average home cage activity per hour was assessed.

When comparing data from different tests, the cage activity and wheel running data collected from the dark phase prior to the limb use and weight bearing tests were matched.

Limb Use

Mice were placed in an empty transparent box for ten minutes to habituate. Thereafter, mice were transferred to an identical testing arena where they were monitored for three minutes. Mice were scored according to the following scale:

4 – Normal gait

3 – Insignificant limping

2 – Significant limping and shift in bodyweight towards the healthy limb

1 – Significant limping and partial lack of use of the ipsilateral leg

0 – Total lack of use of the ipsilateral leg

Different boxes were used for each mouse.

Static Weight Bearing

Static weight bearing was assessed using the Incapacitance Tester (Version 5.2, Linton, UK). Mice were habituated and trained to maintain a testing position (hind paws individually placed

on two weight plates) prior to baseline measurements. Triplicate measures of 3-second readings were obtained for every mouse and the ratio of weight distribution was calculated.

X-ray and Bioluminescent Imaging

Mice underwent imaging on D8 and when the mice reached their experimental or humane endpoint. Mice were injected intraperitoneally with 150mg/kg D-Luciferin (PerkinElmer, Inc., USA) nine minutes prior to imaging. Mice were sedated with 2.5% isoflurane (1000 mg/g isoflurane, Attane vet, ScanVet, UK) and maintained throughout the imaging procedure. Lumina XR apparatus (Caliper Life Sciences, Teralfene, Belgium) was used to obtain both x-ray and bioluminescent images in triplicate for 4T1-inoculated mice. One x-ray image was obtained for the sham control mice.

Statistics

The *a priori* sample size calculation was based on previous studies conducted on the same model, with power set at 80% and statistical significance set at $p<0.05$. Calculated group size was increased by 20% to account for possible exclusion.

Data collected by the DVC® system was extracted with data summarised for every hour. Home cage activity data was presented as previously described [9]. Wheel running was presented as cumulative running distance per hour.

Due to the experimental design of mice euthanised during the course of the study, the last observation was carried forward to account for missing measures at later time points.

All graphs and plots presented were generated with GraphPad Prism 9.3.1 (GraphPad Software, United States). The parametric data (weight bearing, home cage activity, wheel running) was analysed using the mixed-effects model, one-way ANOVA, or two-way ANOVA with appropriate corrections for multiple comparison (see specific information in figure legends) in GraphPad Prism. The non-parametric data (limb use) was analysed by the Friedman test in SAS® 9.4 (SAS Institute, United States) with pairwise Mann-Whitney U tests in Graphpad Prism.

Results

Mice in the sham group did not demonstrate significantly decreased behaviour in any of the tests over the course of the experiment. Mice that were inoculated with 4T1-Luc2 cells in the right femur were evaluated daily by activity monitoring in DVCs®, limb use, and weight bearing. Presence of pain-like behaviour in the 4T1-inoculated mice was confirmed by a significant decrease in limb use score compared to baseline from D12 (Figure 2A) and weight bearing ratio from D10 (Figure 2B) after inoculation.

4T1-inoculated mice showed significantly decreased wheel running from D12 (Figure 2C) compared to baseline. Horizontal activity did not change within the experimental timeframe (Figure 2D). Tumour growth in the ipsilateral femur was confirmed by *in vivo* luciferase imaging on D8 and upon reaching the humane and experimental endpoint (Figure 2E), which showed that all 4T1-inoculated mice that developed pain-like behaviour, developed a tumour in their inoculated limb.

To evaluate the relationship between activity measures and an established measure of pain-like behaviour, the DVC®-data from the dark phases were matched to the limb use score obtained the following study day (Figure 3A, 3B). 4T1-inoculated mice reaching a limb use score of 2 (significant limping) or 0 (complete lack of use of the ipsilateral limb) showed significantly lower wheel running distance compared to baseline throughout the whole dark phase (Figure 3A, 3C). The horizontal activity did not differ between any limb use scores (Figure 3B). Sham mice assessed during days that corresponded to a mean limb use score of 4, 2, and 0 in the 4T1-inoculated sham group were plotted, demonstrating no significant change in wheel running over time (Figure 3D).

Discussion

For the first time, DVCs® were used to assess spontaneous pain-like behaviour in a mouse model of breast CIBP. Wheel running was significantly reduced over time and reduced in concert with the reduction of limb use and static weight bearing. However, horizontal cage activity did not demonstrate a significant change over time or show any relationship with limb use or weight bearing.

Three measures of spontaneous pain-like development were reduced in this study as CIBP developed: limb use, weight bearing, and wheel running. Limb use and weight bearing are non-

evoked behaviours, but they are performed during the light phase when mice are less active over a short period of time (total of 15 minutes to perform both tests). Previous studies on this model, using the same techniques have demonstrated that a decrease in limb use can be reversed with 10mg/kg morphine [27]. The reduction of wheel running occurred in parallel with the reduction of the limb use score. The first significant difference from baseline was observed on D12 in both limb use and wheel running (Figure 2A and 2C); also, wheel running significantly decreased comparably with limb use scores, demonstrating lower wheel running when mice scored lower in gait analysis. This suggests that wheel running is affected by the development of a malignant tumour and the associated nociceptive pathology. However, wheel running within this system holds the significant advantage of occurring during the more active dark phase, over the entire 12-hour period.

Wheel running has previously been performed in other models [18, 19, 23, 24]. However, these tests were performed during the light hours over a short period. Even so, similar to previous studies on prostate CIBP [23], inflammatory [18, 19], and chronic constriction injury models [19], this model also demonstrated significantly reduced wheel running behaviour. However, there are no previous studies demonstrating long-period wheel running and not in a home cage environment; this data suggests that this is a robust system capable of detecting the development of pain-like activity. There is evidence to suggest that these tests may be sex [24] and model [19] dependent. Care should be taken to understand the sex and strain constraints in this system, prior to implementing further studies. There is a legitimate concern that wheel running constitutes a stereotypic behaviour, defined as a repetitive behaviour with no goal or function [28] and it is to be avoided. However, a previous study demonstrates that wheel running is performed voluntarily by wild mice [29] and may be a rewarding and motivating activity [30].

In this study, there was no effect of CIBP on home cage activity. The only other comparable study on home cage systems was performed by Urban et al. [21] where a reduction of home cage activity was only observed in BALB/c mice with a chronic constriction injury. Home cage activity was not impacted in an inflammatory or spared nerve injury model [21]. Horizontal activity may be considered similar to home cage activity, which was affected in several models of bone pain [16-20]. However, home cage assessment offers an advantage of assessing pain-like behaviour over an extended period, instead of in an experimental system confounded by external

factors. Again, sex and model within the DVC® system should be taken into account prior to using the system for further studies.

Analgesics are necessary to assess whether change of behaviour is due to pain-like development or other factors associated with stress or illness. However, spontaneous behaviour is constrained by the use of analgesics due the effect on overall behaviour. For example, previous studies on burrowing (also a spontaneous behaviour) demonstrated that most analgesics adversely affect the procedure. High doses of opioids (e.g. 10-30mg/kg morphine) are necessary to treat mouse models of CIBP, as weak analgesics are ineffective [27, 31]. Cobos et al. [18] have tested the use of analgesics in short-term wheel running assessments. In sham mice, a low dose of morphine (5mg/kg) significantly reduced wheel running. In mice with inflammatory-like pain, wheel running is partially reduce, but not significantly so, suggesting that morphine moderately restores wheel running behaviour in a pain-like model. This suggests that at least low doses of morphine could be used in intervention studies using wheel running as a behavioural outcome. However, an analgesic with a long half-life is required to span the 12-hour dark phase, or at least in this model, the first four hours when mice are most active. Morphine has a half-life of approximately 30 minutes, which would not work in this study design [32, 33], but buprenorphine hydrochloride with a 3-5 hour half-life or sustained release buprenorphine which lasts longer, may be more suitable alternatives [34, 35].

DVCs® also offer an advantage over other commercially available home cage systems. If Tecniplast® Individually Ventilated Cages are being used in a facility, DVCs® can be integrated easily, because their service and cleaning is similar to individually ventilated cages. They do not take up a lot of space, allowing 64 cages to be placed in a vertical rack, contrary to other systems that are larger and require more space for fewer cages. However, DVCs® are expensive (not compared to other home cage systems) relative to smaller, non-home cage experimental systems and they do not currently offer adaptability.

The first limitation of this study is that it was not possible to directly test the effect of analgesics as described above, as morphine would likely decrease wheel running and weaker analgesics have poor efficacy in models of CIBP [31]. Secondly, there was no difference observed in horizontal home cage activity and use of this system only for wheel running may not be a cost-effective.

This study demonstrates that DVCs® can be an exciting tool to assess pain-like behaviour in different models of pain-like development. It facilitates the simultaneous study of two measures of spontaneous pain-like behaviour over a long period, while reducing the introduction of confounding factors.

To conclude, this is the first study that uses DVC® home cage activity and wheel running to assess pain-like behaviour, here in a model of breast CIBP. This method can be implemented to assess characteristics of other mouse models of painful diseases and perhaps test novel analgesics.

Acknowledgement

Chelsea Hopkins and Anne-Marie Heegaard received funding for this project from the European Union's Horizon 2020 research and innovation programme under the Marie Skłodowska-Curie grant agreement No 814244.

References

1. Body, J.-J., et al., *Systematic review and meta-analysis on the proportion of patients with breast cancer who develop bone metastases.* Critical Reviews in Oncology/Hematology, 2017. **115**: p. 67-80.
2. von Moos, R., et al., *Bone-targeted agent treatment patterns and the impact of bone metastases on patients with advanced breast cancer in real-world practice in six European countries.* Journal of Bone Oncology, 2018. **11**: p. 1-9.
3. Meuser, T., et al., *Symptoms during cancer pain treatment following WHO-guidelines: a longitudinal follow-up study of symptom prevalence, severity and etiology.* Pain, 2001. **93**(3): p. 247-257.
4. Currie, G.L., et al., *Animal models of bone cancer pain: systematic review and meta-analyses.* Pain, 2013. **154**(6): p. 917-26.
5. Tena, B., et al., *Reproducibility of electronic von Frey and von Frey monofilaments testing.* Clinical Journal of Pain, 2012. **28**(4): p. 318-323.
6. Shahidi, B. and K.S. Maluf, *Adaptations in evoked pain sensitivity and conditioned pain modulation after development of chronic neck pain.* BioMed Research International, 2017. **2017**.

7. Sadler, K.E., J.S. Mogil, and C.L. Stucky, *Innovations and advances in modelling and measuring pain in animals.* Nat Rev Neurosci, 2022. **23**(2): p. 70-85.
8. Tappe-Theodor, A. and R. Kuner, *Studying ongoing and spontaneous pain in rodents – challenges and opportunities.* European Journal of Neuroscience, 2014. **39**(11): p. 1881-1890.
9. Iannello, F., *Non-intrusive high throughput automated data collection from the home cage.* Heliyon, 2019. **5**(4): p. e01454.
10. Fuochi, S., et al., *Phenotyping spontaneous locomotor activity in inbred and outbred mouse strains by using Digital Ventilated Cages.* Lab Anim (NY), 2021. **50**(8): p. 215-223.
11. Golini, E., et al., *A Non-invasive Digital Biomarker for the Detection of Rest Disturbances in the SOD1G93A Mouse Model of ALS.* Front Neurosci, 2020. **14**: p. 896.
12. Pernold, K., et al., *Towards large scale automated cage monitoring - Diurnal rhythm and impact of interventions on in-cage activity of C57BL/6J mice recorded 24/7 with a non-disrupting capacitive-based technique.* PLoS One, 2019. **14**(2): p. e0211063.
13. Zentrich, E., et al., *Automated Home-Cage Monitoring During Acute Experimental Colitis in Mice.* Front Neurosci, 2021. **15**: p. 760606.
14. Shenk, J., et al., *Automated Analysis of Stroke Mouse Trajectory Data With Traja.* Front Neurosci, 2020. **14**: p. 518.
15. Ai, M., et al., *Human mesenchymal stem cells and derived extracellular vesicles reduce sensory neuron hyperexcitability and pain behaviors in murine osteoarthritis.* Arthritis Rheumatol, 2022.
16. Majuta, L.A., et al., *Anti-nerve growth factor does not change physical activity in normal young or aging mice but does increase activity in mice with skeletal pain.* Pain, 2018. **159**(11): p. 2285-2295.
17. Sluka, K.A., et al., *Acid-sensing ion channel 3 deficiency increases inflammation but decreases pain behavior in murine arthritis.* Arthritis Rheum, 2013. **65**(5): p. 1194-202.
18. Cobos, E.J., et al., *Inflammation-induced decrease in voluntary wheel running in mice: a nonreflexive test for evaluating inflammatory pain and analgesia.* Pain, 2012. **153**(4): p. 876-884.

19. Contreras, K.M., et al., *Deficit in voluntary wheel running in chronic inflammatory and neuropathic pain models in mice: Impact of sex and genotype.* Behav Brain Res, 2021. **399**: p. 113009.
20. Majuta, L.A., et al., *Mice with cancer-induced bone pain show a marked decline in day/night activity.* Pain Rep, 2017. **2**(5): p. e614.
21. Urban, R., et al., *Behavioral indices of ongoing pain are largely unchanged in male mice with tissue or nerve injury-induced mechanical hypersensitivity.* Pain, 2011. **152**(5): p. 990-1000.
22. Jankovic, M.J., P.P. Kapadia, and V. Krishnan, *Home-cage monitoring ascertains signatures of ictal and interictal behavior in mouse models of generalized seizures.* PLoS ONE, 2019. **14**(11).
23. Martha Beatriz Ramirez-Rosas, S.H.P., Matt Eber, Carol Kittel, Thomas Martin, Enriqueta Munoz-Islas, Juan Miguel Jimenez-Andrade, Yusuke Shiozawa, Renee Parker, Christopher Peters, *Pain related behaviors and disease related outcomes in an immunocompetent mouse model of prostate cancer induced bone pain.* The Journal of Pain, 2021. **22**(5): p. 584.
24. Sheahan, T.D., et al., *Inflammation and nerve injury minimally affect mouse voluntary behaviors proposed as indicators of pain.* Neurobiol Pain, 2017. **2**: p. 1-12.
25. Falk, S., et al., *Influence of sex differences on the progression of cancer-induced bone pain.* Anticancer Res, 2013. **33**(5): p. 1963-9.
26. Sliepen, S.H.J., et al., *Cancer-induced Bone Pain Impairs Burrowing Behaviour in Mouse and Rat.* In Vivo, 2019. **33**(4): p. 1125-1132.
27. Falk, S., S. Gallego-Pedersen, and N.C. Petersen, *Grid-climbing Behaviour as a Pain Measure for Cancer-induced Bone Pain and Neuropathic Pain.* In Vivo, 2017. **31**(4): p. 619-623.
28. J.Mason, G., *Stereotypies: a critical review.* Animal Behaviour, 1991. **41**(6): p. 1015-1037.
29. Meijer, J.H. and Y. Robbers, *Wheel running in the wild.* Proc Biol Sci, 2014. **281**(1786).
30. Novak, C.M., P.R. Burghardt, and J.A. Levine, *The use of a running wheel to measure activity in rodents: relationship to energy balance, general activity, and reward.* Neurosci Biobehav Rev, 2012. **36**(3): p. 1001-1014.

31. Luger, N.M., et al., *Efficacy of systemic morphine suggests a fundamental difference in the mechanisms that generate bone cancer vs. inflammatory pain.* PAIN, 2002. **99**(3).
32. Gabel, F., et al., *Unveiling the Impact of Morphine on Tamoxifen Metabolism in Mice in vivo.* Frontiers in Oncology, 2020. **10**.
33. Gabel, F., et al., *Central metabolism as a potential origin of sex differences in morphine analgesia but not in the induction of analgesic tolerance in mice.* bioRxiv, 2020: p. 2020.12.07.414185.
34. Carbone, E.T., et al., *Duration of Action of Sustained-Release Buprenorphine in 2 Strains of Mice.* Journal of the American Association for Laboratory Animal Science, 2012. **51**(6): p. 815-819.
35. Saenz, M., et al., *Pharmacokinetics of Sustained-release and Extended-release Buprenorphine in Mice after Surgical Catheterization.* Journal of the American Association for Laboratory Animal Science, 2022. **61**(5): p. 468-474.

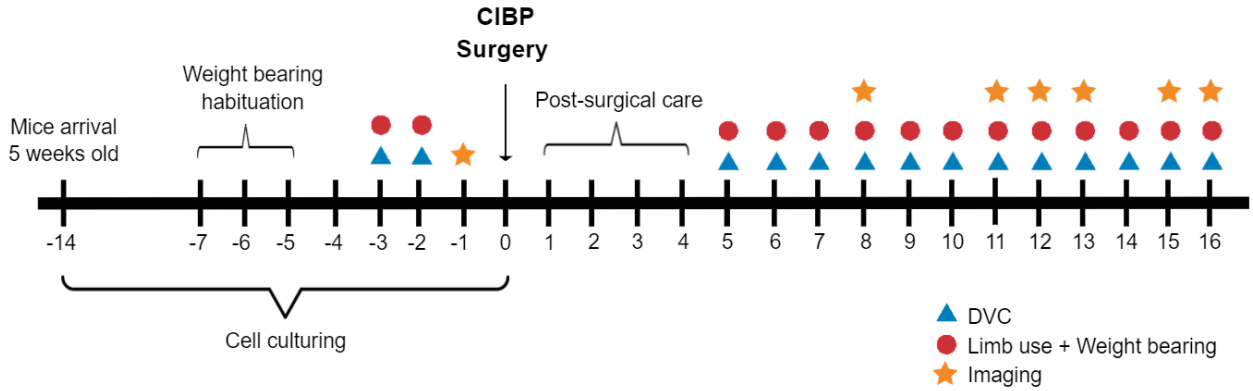

Figure 1: Experimental timeline demonstrating animal behaviour and cell culture procedures over the course of the experiment. (CIBP: cancer-induced bone pain, DVC: Digital Ventilated Cage®)

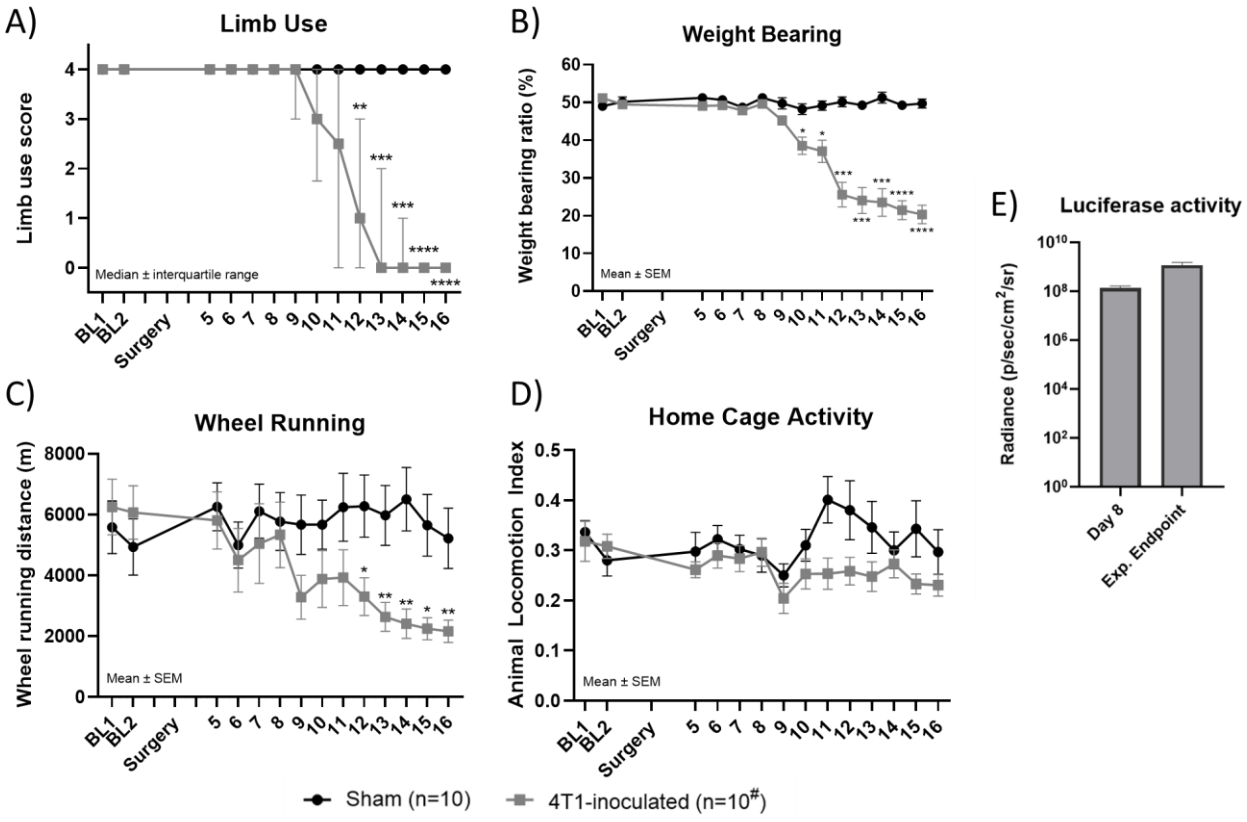

Figure 2: Effect of intrafemoral inoculation of 4T1-Luc2 cells on A) limb use, B) weight bearing, C) wheel running, D) home cage activity, E) luciferase activity. Cumulative wheel running distance and average animal locomotion index data is hourly DVC®-data from the dark phase (7pm-7am) preceding a study day. Statistics are performed with (A) Friedman test with pairwise Mann-Whitney U tests or (B, C, D, E) mixed-effects model with Sidak multiple comparisons test. #Data analyses at last observation carried forward to account for animals euthanised during the study and comparisons were made to BL. (BL: baseline; *: $p<0.05$; **: $p<0.01$; ***: $p<0.001$, ****: $p<0.0001$; #: last observation carried forward)

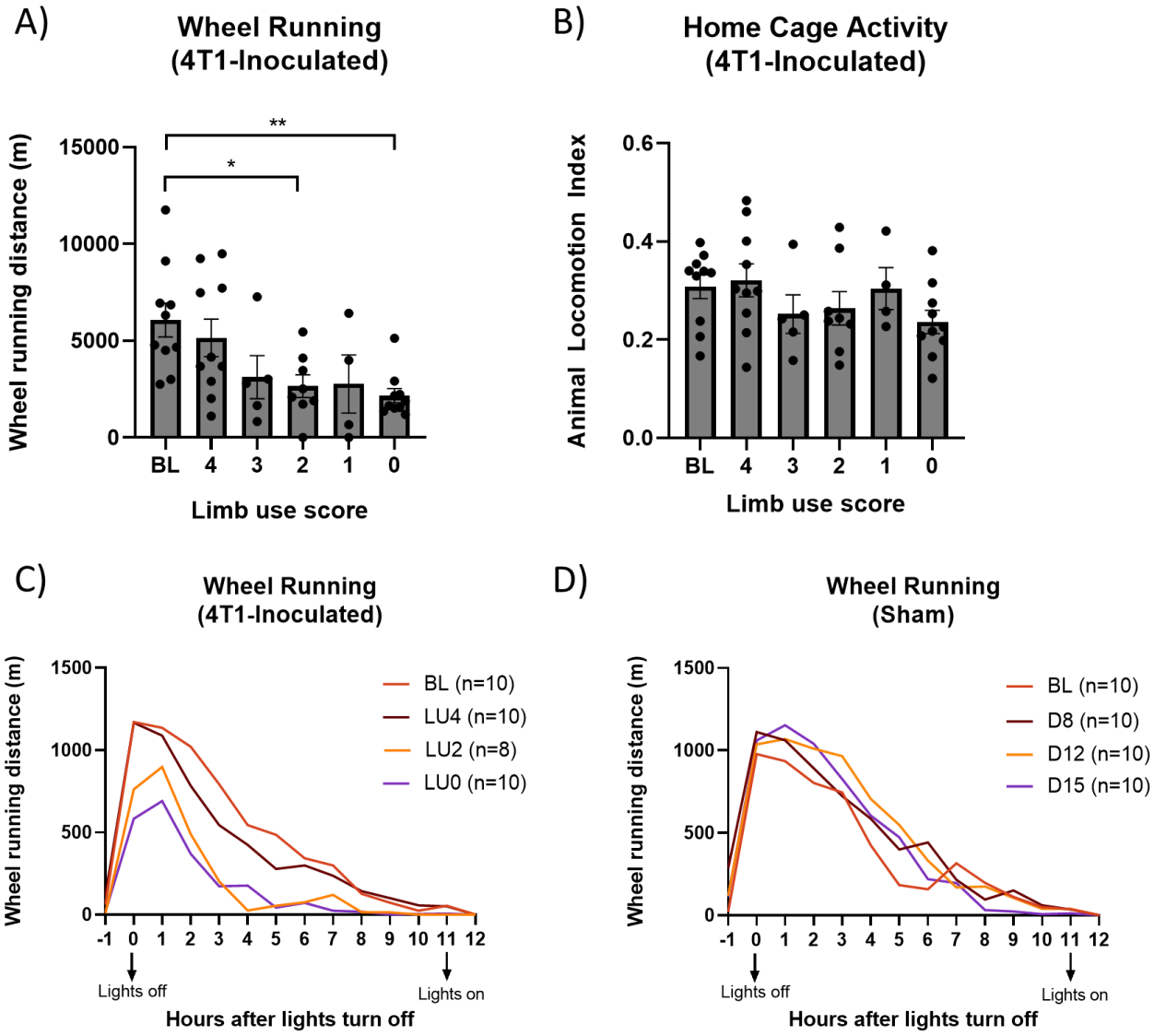

Figure 3: Relationship between limb use score and wheel running. A) Cumulative wheel running distance and B) home cage activity in 4T1-inoculated mice during the dark phase preceding the day the limb use was acquired for each mouse. C) Diurnal pattern of wheel running in 4T1-inoculated mice during the dark phase preceding the indicated limb use score. D) Diurnal pattern of wheel running in sham mice during the dark phase on days corresponding to an average limb use score of 4, 2, 0 within the 4T1-inoculated group.

Statistics are performed with one-way ANOVA with Tukey's test for multiple comparisons. Data is shown as mean±SEM (A, B) and mean (C, D).

Overall Discussion and Conclusion

Fibrous Dysplasia Bone Pain

Overall Discussion

FD commonly causes bone pain, but the underlying mechanisms are unknown and pain treatment is often ineffective [22, 24, 25]. These studies sought to determine which available animal model of FD is most suitable to study pain, identify nociceptive mechanisms of FD *in vivo* and *in vitro*, and establish a novel behavioural technique which could be used to measure spontaneous pain-like development.

Through a systematic review, three animal models were identified that demonstrated good face validity of FD [7, 51, 56, 58, 59]. In particular, the Prrx1-Gutkind model demonstrated good construct validity and promising predictive validity, having been used to assess the efficacy and mechanisms of anti-RANKL treatment for FD [53, 55, 58]. This model develops quickly, only in the bone, with a mosaic-like phenotype, and it is inducible, allowing it to be experimentally flexible (e.g. induction at different ages, administering doxycycline and then removing it) [58]. However, a limitation of this model is that it cannot develop MAS and allow for studies on the more complex nature of FD/MAS. Although there are no studies to demonstrate the influence of endocrinopathies (and their associated treatments) on FD, studies have demonstrated the effect of these endocrinopathies on bone in isolation. The impact of endocrinopathies on FD developed in tandem is worth addressing. In order to do so, the EF1α-Riminucci model may develop MAS due to ubiquitous expression of the $G\alpha s^{R201C}$ gene [56]. However, this needs to be established and characterised before further studies can be conducted. Alternatively, mouse models of endocrinopathies have been developed by artificially increasing specific hormone levels. Using the Prrx1-Gutkind model, one can induce FD, while simultaneously increasing specific hormone levels. For example, hypercortisol models have been developed through specific feed diets [248]. It is essential to ensure necessary ethical standards when inducing two diseases in the same animal.

Having identified a suitable animal model of FD, several mechanisms were identified that could indicate the development of a pain-like phenotype. First, behavioural assessments were conducted to determine the development of pain-like behaviour. Four behavioural tests were conducted, for which burrowing and grid hanging demonstrated reduced activity, which was

recovered by ibuprofen and morphine, respectively. The use of DVCs® to assess the change in home cage activity and wheel running has not yet been reported. As such, it was pertinent to determine if this system would demonstrate similar changes in an established model of bone pain. Wheel running was reduced as a tumour developed in the inoculated femur and the limb use score decreased. As such, this system is sensitive enough to detect pain-like behaviour in an established model, and we may infer that the reduced wheel running and home cage activity in the FD mice was due to – at least in part – pain-like development. This system may be used in future experiments on this model to determine the efficacy of analgesic treatments. Finally, for the first time, DVCs® were used to detect pain-like behaviour in two models of bone pain, which offers the benefit of assessing two spontaneous behaviours over a long period, during the dark phase when mice are most active. This system may also be useful for other models of painful conditions.

The underlying mechanisms that may contribute to FD were assessed in this study in a translationally relevant model. While these observations are novel and provide information about pain-like development in FD that may help to establish novel pain treatments, there are parallels that can be drawn between FD and other painful bone disorders. Increased osteoclastogenesis is observed in FD [2, 23, 24, 33], OA (subchondral bone) [86, 96, 97], and cancer in the bone [77, 84]; the large number of osteoclasts has been theorised to lead to an acidic micro-environment that could act on ASIC receptors on nociceptive neurons [118]. Cancer cells secrete factors (e.g. VEGF, IL-6, TNF-α) [78] and OA is influenced by inflammatory mediators (e.g. IL-1β, IL-6, TNF-α) [87-90]; this study has now demonstrated that FD cells cultured *in vitro*, similarly, secrete factors that may contribute to pain-like development. Notably, MCP-1 was upregulated in FD cells, and has been implicated in pain-like development in OA due to its ability to enhance TRPV1 density [91]. Finally, NGF expression has been implicated in both OA pain [91, 92] and CIBP [83]. This study similarly demonstrated that FD cells express NGF, which could influence the development of bone pain, yet may also be a treatment target. Although FD is rare, identification of similar pain mechanisms in relatively common painful bone disorders could provide insight into effective treatment mechanisms. Unfortunately, if one is to draw inspiration for FD treatment from studies on other painful bone disorders, the results may be disappointing as effective analgesic treatments remain elusive. Although, if there are treatment breakthroughs in other painful bone disorders, these may be applicable to treating FD as well.

In mid-2022, the International Consortium for FD/MAS released a consolidated list of top priorities for FD/MAS research. Pain treatment was top of the list, followed by local and international research collaboration [249]. The information presented in this thesis demonstrates fulfilment of these research priorities, having investigated pain and its underlying mechanisms in a mouse model of FD using novel and high-quality research techniques. The studies were conducted in collaboration with international academic, clinical, and industrial partners, bringing together experts in FD/MAS, bone, pain, and biomarker assays. Advanced procedures including multiplex assays, tissue staining and imaging techniques, and novel behavioural equipment (DVCs®) were utilised to conduct these studies. Although rare, FD/MAS patients deserve high-quality research that deciphers underlying mechanisms of their disease, which may elucidate methods of treatment.

Perspectives for Future Studies

The results of these studies present novel research opportunities. Research on the role of the CNS is ongoing; spinal cords were harvested from mice after behavioural studies (in addition to bone and DRG tissue samples) and those are currently being processed to assess the presence of neuropeptides and glial cells. Previous studies have demonstrated altered expression in different pain phenotypes (e.g. neuropathic, inflammatory, cancer pain) [121]. The results of this study on the CNS will provide additional information about the type of pain that develops in FD and if central sensitisation may occur.

Having identified increased expression of TNF-α and NGF in FD cells, future studies will aim to assess the efficacy of anti-TNF-α with anti-NGF treatments. Anti-TNF-α is used to treat RA, psoriatic arthritis, and ankylosing spondylitis, but there is an increased risk of developing severe infections and malignancy [250]. Anti-NGF is effective in treating OA and lower back pain [251, 252]; however, serious adverse effects include advanced OA and development of osteonecrosis [253, 254], as well as headaches, myalgia, and hyperesthesia [251, 252]. Preliminary studies have demonstrated that when combined, the dose of both drugs may be reduced while maintaining the overall analgesic effect and reducing adverse effects [255]. Clinical trials are ongoing, although a proof-of-concept study on this treatment plan in this mouse model of FD may prove advantageous.

As previously mentioned, a limitation of this study is not having human tissue with which to reference the results. Given the rarity of the disease, it is challenging to identify patients with FD and, further, surgical debridement of FD lesions is not a first-line solution, restraining access to tissue samples. However, should tissue samples become available, it would be beneficial to conduct IHC for CD68 (e.g. osteoclasts, macrophage, monocyte, etc.), vascularity, and sensory nerve fibres. It would also be beneficial to culture FD cells from patients and assess the cell secretome for inflammatory markers.

Conclusion

FD pain is a concern for patients and clinicians that has no clear mechanisms or treatment options. These studies have aimed to identify a suitable mouse model of FD that develops a pain-like phenotype and investigate the underlying nociceptive mechanisms. By way of a systematic review, none of the studies described pain-like development in their model, thereby demonstrating a knowledge gap in the field. A suitable site-specific, inducible model was selected with good face and construct validity that could be generated to further investigate the presence and mechanisms of FD pain. Having developed this model, pain-like behaviour was observed, with underlying inflammatory and perhaps neuropathic contributions. Finally, novel spontaneous pain-like behaviour methods were developed that showed changes in the FD model, as well as a model of CIBP that is known to develop a pain-like phenotype. Further studies are necessary to develop novel and effective treatment strategies for FD pain and the research presented here provides the foundation on which to do so.

"A rare disorder, yes; an unimportant one, never." – Angelo M. DiGeorge (on Albright syndrome)

References

1. Boyce, A.M. and M.T. Collins, *Fibrous Dysplasia/McCune-Albright Syndrome: A Rare, Mosaic Disease of Galpha s Activation.* Endocr Rev, 2020. **41**(2): p. 345-70.
2. Hartley, I., et al., *Fibrous Dysplasia of Bone and McCune-Albright Syndrome: A Bench to Bedside Review.* Calcif Tissue Int, 2019. **104**(5): p. 517-529.
3. Riminucci, M., et al., *A novel GNAS1 mutation, R201G, in McCune-albright syndrome.* J Bone Miner Res, 1999. **14**(11): p. 1987-9.
4. Chau, M.M. and D.R. Clohisy, *Mechanisms and management of bone cancer pain*, in *Bone Cancer: Bone Sarcomas and Bone Metastases - From Bench to Bedside*. 2021. p. 853-861.
5. Happle, R., *The McCune-Albright syndrome: a lethal gene surviving by mosaicism.* Clin Genet, 1986. **29**(4): p. 321-4.
6. Bianco, P., et al., *Reproduction of human fibrous dysplasia of bone in immunocompromised mice by transplanted mosaics of normal and Gsalpha-mutated skeletal progenitor cells.* J Clin Invest, 1998. **101**(8): p. 1737-44.
7. Khan, S.K., et al., *Induced Gnas(R201H) expression from the endogenous Gnas locus causes fibrous dysplasia by up-regulating Wnt/beta-catenin signaling.* Proc Natl Acad Sci U S A, 2018. **115**(3): p. E418-E427.
8. Remoli, C., et al., *Osteoblast-specific expression of the fibrous dysplasia (FD)-causing mutation Gs(R201C) produces a high bone mass phenotype but does not reproduce FD in the mouse.* Journal of Bone and Mineral Research, 2015. **30**(6): p. 1030-1043.
9. Riminucci, M., et al., *Fibrous dysplasia as a stem cell disease.* Journal of Bone and Mineral Research, 2006. **21**: p. P125-P131.
10. Sadana, R. and C.W. Dessauer, *Physiological roles for G protein-regulated adenylyl cyclase isoforms: insights from knockout and overexpression studies.* Neurosignals, 2009. **17**(1): p. 5-22.
11. Kamato, D., et al., *Structure, Function, Pharmacology, and Therapeutic Potential of the G Protein, Galpha/q,11.* Front Cardiovasc Med, 2015. **2**: p. 14.
12. Hilger, D., M. Masureel, and B.K. Kobilka, *Structure and dynamics of GPCR signaling complexes.* Nat Struct Mol Biol, 2018. **25**(1): p. 4-12.

13. Hu, Q. and K.M. Shokat, *Disease-Causing Mutations in the G Protein Galphas Subvert the Roles of GDP and GTP.* Cell, 2018. **173**(5): p. 1254-1264 e11.
14. Skroblin, P., et al., *Mechanisms of Protein Kinase A Anchoring*, in *International Review of Cell and Molecular Biology*. 2010. p. 235-330.
15. Tascau, L., et al., *Activation of Protein Kinase A in Mature Osteoblasts Promotes a Major Bone Anabolic Response.* Endocrinology, 2016. **157**(1): p. 112-26.
16. Tsang, K.M., et al., *Alternate protein kinase A activity identifies a unique population of stromal cells in adult bone.* Proc Natl Acad Sci U S A, 2010. **107**(19): p. 8683-8.
17. Liu, S., et al., *Bone Abnormalities in Mice with Protein Kinase A (PKA) Defects Reveal a Role of Cyclic AMP Signaling in Bone Stromal Cell-Dependent Tumor Development.* Horm Metab Res, 2016. **48**(11): p. 714-725.
18. Saloustros, E., et al., *Celecoxib treatment of fibrous dysplasia (FD) in a human FD cell line and FD-like lesions in mice with protein kinase A (PKA) defects.* Mol Cell Endocrinol, 2017. **439**: p. 165-174.
19. Liu, S., et al., *Haploinsufficiency for either one of the type-II regulatory subunits of protein kinase A improves the bone phenotype of Prkar1a+/- mice.* Hum Mol Genet, 2015. **24**(21): p. 6080-92.
20. Espiard, S., et al., *PRKACB variants in skeletal disease or adrenocortical hyperplasia: effects on protein kinase A.* Endocr Relat Cancer, 2020. **27**(11): p. 647-656.
21. Benhamou, J., et al., *Prognostic Factors From an Epidemiologic Evaluation of Fibrous Dysplasia of Bone in a Modern Cohort: The FRANCEDYS Study.* J Bone Miner Res, 2016. **31**(12): p. 2167-2172.
22. Kelly, M.H., et al., *Physical function is impaired but quality of life preserved in patients with fibrous dysplasia of bone.* Bone, 2005. **37**(3): p. 388-94.
23. Spencer, T.L., et al., *Neuropathic-like Pain in Fibrous Dysplasia/McCune-Albright Syndrome.* J Clin Endocrinol Metab, 2022. **107**(6): p. e2258-e2266.
24. Kelly, M.H., B. Brillante, and M.T. Collins, *Pain in fibrous dysplasia of bone: age-related changes and the anatomical distribution of skeletal lesions.* Osteoporos Int, 2008. **19**(1): p. 57-63.
25. Hart, E.S., et al., *Onset, progression, and plateau of skeletal lesions in fibrous dysplasia and the relationship to functional outcome.* J Bone Miner Res, 2007. **22**(9): p. 1468-74.

26. Munns, C.F. and A.M. Boot, *Chapter 9 - Bone Health*, in *Practical Pediatric Endocrinology in a Limited Resource Setting*, M. Zacharin, Editor. 2013, Academic Press: San Diego. p. 205-221.
27. Marchiori, D.M., *Chapter 13 - Bone Tumors and Related Diseases*, in *Clinical Imaging (Third Edition)*, D.M. Marchiori, Editor. 2014, Mosby: Saint Louis. p. 811-924.
28. Majoor, B.C.J., et al., *Pain in fibrous dysplasia: relationship with anatomical and clinical features.* Acta Orthop, 2019. **90**(4): p. 401-405.
29. Javaid, M.K., et al., *Best practice management guidelines for fibrous dysplasia/McCune-Albright syndrome: a consensus statement from the FD/MAS international consortium.* Orphanet J Rare Dis, 2019. **14**(1): p. 139.
30. Kushchayeva, Y.S., et al., *Fibrous dysplasia for radiologists: beyond ground glass bone matrix.* Insights Imaging, 2018. **9**(6): p. 1035-1056.
31. Chapurlat, R.D. and P.J. Meunier, *Fibrous dysplasia of bone.* Baillieres Best Pract Res Clin Rheumatol, 2000. **14**(2): p. 385-98.
32. Jour, G., et al., *GNAS Mutations in Fibrous Dysplasia: A Comparative Study of Standard Sequencing and Locked Nucleic Acid PCR Sequencing on Decalcified and Nondecalcified Formalin-fixed Paraffin-embedded Tissues.* Appl Immunohistochem Mol Morphol, 2016. **24**(9): p. 660-667.
33. de Castro, L.F., et al., *RANKL inhibition with denosumab improves fibrous dysplasia by decreasing lesional cell proliferation and increasing osteogenesis.* medRxiv, 2022: p. 2022.10.24.22281375.
34. Collins, M.T., et al., *Renal Phosphate Wasting in Fibrous Dysplasia of Bone Is Part of a Generalized Renal Tubular Dysfunction Similar to That Seen in Tumor-Induced Osteomalacia.* Journal of Bone and Mineral Research, 2001. **16**(5): p. 806-813.
35. Jreige, M., et al., *A novel approach for fibrous dysplasia assessment using combined planar and quantitative SPECT/CT analysis of Tc-99m-diphosphonate bone scan in correlation with biological bone turnover markers of disease activity.* Frontiers in Medicine, 2022. **9**.
36. Yamamoto, T., et al., *Increased IL-6-production by cells isolated from the fibrous bone dysplasia tissues in patients with McCune-Albright syndrome.* J Clin Invest, 1996. **98**(1): p. 30-5.

37. Chapurlat, R.D., et al., *Pathophysiology and medical treatment of pain in fibrous dysplasia of bone.* Orphanet J Rare Dis, 2012. **7 Suppl 1**: p. S3.
38. Grob, F. and M. Zacharin, *McCune Albright Syndrome: Gastrointestinal Polyps and Platelet Dysfunction over 12 Years.* Horm Res Paediatr, 2020. **93**(1): p. 40-45.
39. Majoor, B.C., et al., *Increased Risk of Breast Cancer at a Young Age in Women with Fibrous Dysplasia.* J Bone Miner Res, 2018. **33**(1): p. 84-90.
40. Zacharin, M., et al., *Gastrointestinal polyps in McCune Albright syndrome.* J Med Genet, 2011. **48**(7): p. 458-61.
41. Riggs, B.L., S. Khosla, and L.J. Melton, 3rd, *Sex steroids and the construction and conservation of the adult skeleton.* Endocr Rev, 2002. **23**(3): p. 279-302.
42. Sagsveen, M., et al., *Gonadotrophin-releasing hormone analogues for endometriosis: bone mineral density.* Cochrane Database Syst Rev, 2003. **2003**(4): p. CD001297.
43. Smith, M.R., et al., *Gonadotropin-Releasing Hormone Agonists and Fracture Risk: A Claims-Based Cohort Study of Men With Nonmetastatic Prostate Cancer.* Journal of Clinical Oncology, 2005. **23**(31): p. 7897-7903.
44. Duncan Bassett, J.H. and G.R. Williams, *Role of thyroid hormones in skeletal development and bone maintenance.* Endocrine Reviews, 2016. **37**(2): p. 135-187.
45. Nicolaisen, P., et al., *Consequences of Hyperthyroidism and Its Treatment for Bone Microarchitecture Assessed by High-Resolution Peripheral Quantitative Computed Tomography.* Thyroid, 2021. **31**(2): p. 208-216.
46. Rutkowski, M.J., et al., *Acromegaly due to McCune-Albright syndrome.* US Endocrinology, 2020. **16**(1): p. 47-50.
47. Duan, L., et al., *The Negative Impacts of Acromegaly on Bone Microstructure Not Fully Reversible.* Frontiers in Endocrinology, 2021. **12**.
48. van Trigt, V.R., et al., *Low prevalence of neuropathic-like pain symptoms in long-term controlled acromegaly.* Pituitary, 2022. **25**(2): p. 229-237.
49. Guo, W., et al., *Effect of hypercortisolism on bone mineral density and bone metabolism: A potential protective effect of adrenocorticotropic hormone in patients with Cushing's disease.* Journal of International Medical Research, 2018. **46**(1): p. 492-503.
50. Pereira, R.M.R., A.M. Delany, and E. Canalis, *Cortisol inhibits the differentiation and apoptosis of osteoblasts in culture.* Bone, 2001. **28**(5): p. 484-490.

51. Denayer, T., T. Stöhr, and M. Van Roy, *Animal models in translational medicine: Validation and prediction.* New Horizons in Translational Medicine, 2014. **2**(1): p. 5-11.
52. Hopkins, C., et al., *Fibrous dysplasia animal models: A systematic review.* Bone, 2022. **155**: p. 116270.
53. de Castro, L.F., et al., *Activation of RANK/RANKL/OPG Pathway Is Involved in the Pathophysiology of Fibrous Dysplasia and Associated With Disease Burden.* J Bone Miner Res, 2019. **34**(2): p. 290-294.
54. Palmisano, B., et al., *RANKL Inhibition in Fibrous Dysplasia of Bone: A Preclinical Study in a Mouse Model of the Human Disease.* J Bone Miner Res, 2019.
55. Liu, Z., et al., *RANKL inhibition halts lesion progression and promotes bone remineralization in mice with fibrous dysplasia.* Bone, 2022. **156**: p. 116301.
56. Saggio, I., et al., *Constitutive expression of Gsalpha(R201C) in mice produces a heritable, direct replica of human fibrous dysplasia bone pathology and demonstrates its natural history.* J Bone Miner Res, 2014. **29**(11): p. 2357-68.
57. Karaca, A., et al., *Constitutive stimulatory G protein activity in limb mesenchyme impairs bone growth.* Bone, 2018. **110**: p. 230-237.
58. Zhao, X.F., et al., *Expression of an active G alpha(s) mutant in skeletal stem cells is sufficient and necessary for fibrous dysplasia initiation and maintenance.* Proceedings of the National Academy of Sciences of the United States of America, 2018. **115**(3): p. E428-E437.
59. Xu, R.S., et al., *G alpha(s) signaling controls intramembranous ossification during cranial bone development by regulating both Hedgehog and Wnt/beta-catenin signaling.* Bone Research, 2018. **6**.
60. McNamara, L.M., *2.10 Bone as a material*, in *Comprehensive Biomaterials II*. 2017. p. 202-227.
61. Evans, S.F., H. Chang, and M.L. Knothe Tate, *Elucidating multiscale periosteal mechanobiology: A key to unlocking the smart properties and regenerative capacity of the periosteum?* Tissue Engineering - Part B: Reviews, 2013. **19**(2): p. 147-159.
62. Hadjidakis, D.J. and I.I. Androulakis. *Bone remodeling*. in *Annals of the New York Academy of Sciences*. 2006.

63. Ardura, J.A., et al., *Chapter 6 - Linking bone cells, aging, and oxidative stress: Osteoblasts, osteoclasts, osteocytes, and bone marrow cells*, in *Aging (Second Edition)*, V.R. Preedy and V.B. Patel, Editors. 2020, Academic Press. p. 61-71.
64. Milovanovic, P., et al., *Osteocytic canalicular networks: Morphological implications for altered mechanosensitivity.* ACS Nano, 2013. **7**(9): p. 7542-7551.
65. Lane, N.E., et al., *Acute changes in trabecular bone connectivity and osteoclast activity in the ovariectomized rat in vivo.* Journal of Bone and Mineral Research, 1998. **13**(2): p. 229-236.
66. Kim, Y., et al., *MicroCT for Scanning and Analysis of Mouse Bones.* Methods Mol Biol, 2021. **2230**: p. 169-198.
67. Aerts-Kaya, F., et al., *Neurological Regulation of the Bone Marrow Niche*, in *Advances in Experimental Medicine and Biology*. 2020. p. 127-153.
68. Travlos, G.S., *Normal Structure, Function, and Histology of the Bone Marrow.* Toxicologic Pathology, 2006. **34**(5): p. 548-565.
69. Boyle, W.J., W.S. Simonet, and D.L. Lacey, *Osteoclast differentiation and activation.* Nature, 2003. **423**(6937): p. 337-342.
70. Boyce, B.F. and L. Xing, *Functions of RANKL/RANK/OPG in bone modeling and remodeling.* Archives of Biochemistry and Biophysics, 2008. **473**(2): p. 139-146.
71. Yao, Y., et al., *The Macrophage-Osteoclast Axis in Osteoimmunity and Osteo-Related Diseases.* Frontiers in Immunology, 2021. **12**.
72. Aerts-Kaya, F., et al., *Neurological Regulation of the Bone Marrow Niche.* Adv Exp Med Biol, 2020. **1212**: p. 127-153.
73. Artico, M., et al., *Noradrenergic and cholinergic innervation of the bone marrow.* Int J Mol Med, 2002. **10**(1): p. 77-80.
74. Jung, W.C., J.P. Levesque, and M.J. Ruitenberg, *It takes nerve to fight back: The significance of neural innervation of the bone marrow and spleen for immune function.* Semin Cell Dev Biol, 2017. **61**: p. 60-70.
75. Jimenez-Andrade, J.M., et al., *A phenotypically restricted set of primary afferent nerve fibers innervate the bone versus skin: therapeutic opportunity for treating skeletal pain.* Bone, 2010. **46**(2): p. 306-13.

76. Steverink, J.G., et al., *Sensory Innervation of Human Bone: An Immunohistochemical Study to Further Understand Bone Pain.* The Journal of Pain, 2021. **22**(11): p. 1385-1395.
77. Tahara, R.K., et al., *Bone Metastasis of Breast Cancer*, in *Breast Cancer Metastasis and Drug Resistance: Challenges and Progress*, A. Ahmad, Editor. 2019, Springer International Publishing: Cham. p. 105-129.
78. Cappariello, A. and M. Capulli, *The Vicious Cycle of Breast Cancer-Induced Bone Metastases, a Complex Biological and Therapeutic Target.* Current Molecular Biology Reports, 2018. **4**(3): p. 123-131.
79. Wu, X., et al., *RANKL/RANK System-Based Mechanism for Breast Cancer Bone Metastasis and Related Therapeutic Strategies.* Front Cell Dev Biol, 2020. **8**(2296-634X (Print)).
80. Jones, D.H., et al., *Regulation of cancer cell migration and bone metastasis by RANKL.* Nature, 2006. **440**(1476-4687 (Electronic)): p. 692-696.
81. Mantyh, W.G., et al., *Blockade of nerve sprouting and neuroma formation markedly attenuates the development of late stage cancer pain.* Neuroscience, 2010. **171**(1873-7544 (Electronic)): p. 588-598.
82. Falk, S. and A.H. Dickenson, *Pain and Nociception: Mechanisms of Cancer-Induced Bone Pain.* Journal of Clinical Oncology, 2014. **32**(16): p. 1647-1654.
83. Mazaki, A., et al., *Nerve Growth Factor in Breast Cancer Cells Promotes Axonal Growth and Expression of Calcitonin Gene-related Peptide in a Rat Model of Spinal Metastasis.* Anticancer Research, 2022. **42**(1): p. 581-587.
84. Cleeland, C.S., et al., *Pain outcomes in patients with advanced breast cancer and bone metastases.* Cancer, 2013. **119**(4): p. 832-838.
85. Eitner, A., G.O. Hofmann, and H.-G. Schaible, *Mechanisms of Osteoarthritic Pain. Studies in Humans and Experimental Models.* Frontiers in Molecular Neuroscience, 2017. **10**.
86. Hu, Y., et al., *Subchondral bone microenvironment in osteoarthritis and pain.* Bone Research, 2021. **9**(1): p. 20.

87. Orita, S., et al., *Associations between proinflammatory cytokines in the synovial fluid and radiographic grading and pain-related scores in 47 consecutive patients with osteoarthritis of the knee.* BMC Musculoskeletal Disorders, 2011. **12**(1): p. 144.
88. Orita, S., et al., *Pain-related sensory innervation in monoiodoacetate-induced osteoarthritis in rat knees that gradually develops neuronal injury in addition to inflammatory pain.* BMC Musculoskeletal Disorders, 2011. **12**(1): p. 134.
89. Harkey, M.S., et al., *Osteoarthritis-related biomarkers following anterior cruciate ligament injury and reconstruction: a systematic review.* Osteoarthritis and Cartilage, 2015. **23**(1): p. 1-12.
90. Larsson, S., et al., *Interleukin-6 and tumor necrosis factor alpha in synovial fluid are associated with progression of radiographic knee osteoarthritis in subjects with previous meniscectomy.* Osteoarthritis and Cartilage, 2015. **23**(11): p. 1906-1914.
91. Miller, R.E., et al., *CCR2 chemokine receptor signaling mediates pain in experimental osteoarthritis.* Proceedings of the National Academy of Sciences, 2012. **109**(50): p. 20602-20607.
92. McNamee, K.E., et al., *Treatment of murine osteoarthritis with TrkAd5 reveals a pivotal role for nerve growth factor in non-inflammatory joint pain.* PAIN, 2010. **149**(2).
93. Obeidat, A.M., et al., *The nociceptive innervation of the normal and osteoarthritic mouse knee.* Osteoarthritis and Cartilage, 2019. **27**(11): p. 1669-1679.
94. Ivanavicius, S.P., et al., *Structural pathology in a rodent model of osteoarthritis is associated with neuropathic pain: Increased expression of ATF-3 and pharmacological characterisation.* PAIN, 2007. **128**(3).
95. Arendt-Nielsen, L., et al., *Sensitization in patients with painful knee osteoarthritis.* PAIN, 2010. **149**(3).
96. Martínez-Calatrava, M.J., et al., *RANKL synthesized by articular chondrocytes contributes to juxta-articular bone loss in chronic arthritis.* Arthritis Research & Therapy, 2012. **14**(3): p. R149.
97. Kwan Tat, S., et al., *Modulation of OPG, RANK and RANKL by human chondrocytes and their implication during osteoarthritis.* Rheumatology, 2009. **48**(12): p. 1482-1490.

98. *IASP Announces Revised Definition of Pain*. 2020 [cited 2022 16/12/2022]; Available from: https://www.iasp-pain.org/publications/iasp-news/iasp-announces-revised-definition-of-pain/.
99. Blackburn-Munro, G., *Pain-like behaviours in animals – how human are they?* Trends in Pharmacological Sciences, 2004. **25**(6): p. 299-305.
100. Deuis, J.R., L.S. Dvorakova, and I. Vetter, *Methods Used to Evaluate Pain Behaviors in Rodents.* Frontiers in Molecular Neuroscience, 2017. **10**(284).
101. IASP. *Terminology*. 2011 [cited 2022 27/12/2022]; Available from: https://www.iasp-pain.org/resources/terminology/.
102. Prescott, S.A. and S. Ratté, *Chapter 23 - Somatosensation and Pain*, in *Conn's Translational Neuroscience*, P.M. Conn, Editor. 2017, Academic Press: San Diego. p. 517-539.
103. Vardeh, D., R.J. Mannion, and C.J. Woolf, *Toward a Mechanism-Based Approach to Pain Diagnosis.* The Journal of Pain, 2016. **17**(9, Supplement): p. T50-T69.
104. Szok, D.A.-O., et al., *Therapeutic Approaches for Peripheral and Central Neuropathic Pain.* Behav Neurol, 2019(1875-8584 (Electronic)).
105. Chan, S.F., S.M. Hayek, and E. Veizi, *Mechanisms of Physiologic Pain*, in *Fundamentals of Pain Medicine*, J. Cheng and R.W. Rosenquist, Editors. 2018, Springer International Publishing: Cham. p. 13-20.
106. Kwon, M., et al., *The Role of Descending Inhibitory Pathways on Chronic Pain Modulation and Clinical Implications.* Pain Practice, 2014. **14**(7): p. 656-667.
107. Basbaum, A.I., *Chapter 3 - Basic Mechanisms*, in *Pain Management Secrets (Third Edition)*, C.E. Argoff and G. McCleane, Editors. 2009, Mosby: Philadelphia. p. 19-26.
108. Varga, I. and B. Mravec, *Chapter 8 - Nerve Fiber Types*, in *Nerves and Nerve Injuries*, R.S. Tubbs, et al., Editors. 2015, Academic Press: San Diego. p. 107-113.
109. Basbaum, A.I., et al., *Cellular and Molecular Mechanisms of Pain.* Cell, 2009. **139**(2): p. 267-284.
110. Julius, D. and A.I. Basbaum, *Molecular mechanisms of nociception.* Nature, 2001. **413**(6852): p. 203-210.

111. Tsujino, H., et al., *Activating Transcription Factor 3 (ATF3) Induction by Axotomy in Sensory and Motoneurons: A Novel Neuronal Marker of Nerve Injury.* Molecular and Cellular Neuroscience, 2000. **15**(2): p. 170-182.
112. Peters, C.M., et al., *Tumor-induced injury of primary afferent sensory nerve fibers in bone cancer pain.* Experimental Neurology, 2005. **193**(1): p. 85-100.
113. Coronel, M.F., et al., *Differential galanin upregulation in dorsal root ganglia and spinal cord after graded single ligature nerve constriction of the rat sciatic nerve.* Journal of Chemical Neuroanatomy, 2008. **35**(1): p. 94-100.
114. Atherton, M., et al., *Sympathetic modulation of tumor necrosis factor alpha-induced nociception in the presence of oral squamous cell carcinoma.* Pain, 2022.
115. Morgan, M., et al., *TRPV1 activation alters the function of Aδ and C fiber sensory neurons that innervate bone.* Bone, 2019. **123**: p. 168-175.
116. Liu, Q., et al., *The TRPA1 Channel Mediates Mechanical Allodynia and Thermal Hyperalgesia in a Rat Bone Cancer Pain Model.* Frontiers in Pain Research, 2021. **2**.
117. de Almeida, A.S., et al., *Role of transient receptor potential ankyrin 1 (TRPA1) on nociception caused by a murine model of breast carcinoma.* Pharmacological Research, 2020. **152**: p. 104576.
118. Avnet, S., et al., *Cause and effect of microenvironmental acidosis on bone metastases.* Cancer and Metastasis Reviews, 2019. **38**(1-2): p. 133-147.
119. Aso, K., et al., *Associations of Symptomatic Knee Osteoarthritis With Histopathologic Features in Subchondral Bone.* Arthritis & Rheumatology, 2019. **71**(6): p. 916-924.
120. Delay, L., et al., *Tyrosine kinase type A-specific signalling pathways are critical for mechanical allodynia development and bone alterations in a mouse model of rheumatoid arthritis.* Pain, 2022. **163**(7): p. e837-e849.
121. Honore, P., et al., *Murine models of inflammatory, neuropathic and cancer pain each generates a unique set of neurochemical changes in the spinal cord and sensory neurons.* Neuroscience, 2000. **98**(3): p. 585-98.
122. Coull, J.A.M., et al., *BDNF from microglia causes the shift in neuronal anion gradient underlying neuropathic pain.* Nature, 2005. **438**(7070): p. 1017-1021.

123. Ji, R.-R., et al., *Possible role of spinal astrocytes in maintaining chronic pain sensitization: review of current evidence with focus on bFGF/JNK pathway.* Neuron Glia Biology, 2006. **2**(4): p. 259-269.
124. Wang, C., et al., *A critical role of the cAMP sensor Epac in switching protein kinase signalling in prostaglandin E2-induced potentiation of P2X3 receptor currents in inflamed rats.* The Journal of Physiology, 2007. **584**(1): p. 191-203.
125. Chen, L., G. Yang, and T. Grosser, *Prostanoids and inflammatory pain.* Prostaglandins & Other Lipid Mediators, 2013. **104-105**: p. 58-66.
126. Monastero, R.A.-O. and S. Pentyala, *Cytokines as Biomarkers and Their Respective Clinical Cutoff Levels.* Int J Inflam, 2017(2090-8040 (Print)).
127. Oi, K., et al., *Tumour necrosis factor alpha augments the inhibitory effects of CTLA-4-Ig on osteoclast generation from human monocytes via induction of CD80 expression.* Clin Exp Immunol, 2019. **196**(3): p. 392-402.
128. Yoshitaka, T., et al., *Etanercept administration to neonatal SH3BP2 knock-in cherubism mice prevents TNF-alpha-induced inflammation and bone loss.* J Bone Miner Res, 2014. **29**(5): p. 1170-82.
129. Tsubaki, M., et al., *Inhibition of the tumour necrosis factor-alpha autocrine loop enhances the sensitivity of multiple myeloma cells to anticancer drugs.* Eur J Cancer, 2013. **49**(17): p. 3708-17.
130. Marahleh, A., et al., *TNF-alpha Directly Enhances Osteocyte RANKL Expression and Promotes Osteoclast Formation.* Front Immunol, 2019. **10**: p. 2925.
131. Luo, G., et al., *TNF-α and RANKL promote osteoclastogenesis by upregulating RANK via the NF-κB pathway.* Mol Med Rep, 2018. **17**(5): p. 6605-6611.
132. Houssiau, F.A., et al., *Interleukin-6 in synovial fluid and serum of patients with rheumatoid arthritis and other inflammatory arthritides.* Arthritis Rheum, 1988. **31**(6): p. 784-8.
133. Chapurlat, R., et al., *Inhibition of IL-6 in the treatment of fibrous dysplasia of bone: The randomized double-blind placebo-controlled TOCIDYS trial.* Bone, 2022. **157**: p. 116343.

134. Yang, L., et al., *High glucose inhibits proliferation and differentiation of osteoblast in alveolar bone by inducing pyroptosis.* Biochem Biophys Res Commun, 2020. **522**(1090-2104 (Electronic)): p. 471-478.
135. Lee, Y.M., et al., *IL-1 plays an important role in the bone metabolism under physiological conditions.* Int Immunol, 2010. **22**(1460-2377 (Electronic)): p. 805-816.
136. Gao, Y., et al., *IFN-gamma stimulates osteoclast formation and bone loss in vivo via antigen-driven T cell activation.* J Clin Invest, 2007. **117**(0021-9738 (Print)): p. 122-32.
137. Jiang, F.A.-O., et al., *Deficient invariant natural killer T cells had impaired regulation on osteoclastogenesis in myeloma bone disease.* J Cell Mol Med, 2018. **22**(1582-4934 (Electronic)): p. 2706-2716.
138. Jeong, J.S., et al., *Increased expression of the Cbl family of E3 ubiquitin ligases decreases Interleukin-2 production in a rat model of peripheral neuropathy.* BMC Anesthesiol, 2018. **18**(1471-2253 (Electronic)).
139. Chatterjee, P., et al., *Regulation of the Anti-Inflammatory Cytokines Interleukin-4 and Interleukin-10 during Pregnancy.* Frontiers in Immunology, 2014. **5**.
140. Nie, B., et al., *AKAP150 involved in paclitaxel-induced neuropathic pain via inhibiting CN/NFAT2 pathway and downregulating IL-4.* Brain Behav Immun, 2018. **68**(1090-2139 (Electronic)): p. 158-168.
141. Wadley Al Fau - Kamerman, P.R., et al., *A polymorphism in IL4 may associate with sensory neuropathy in African HIV patients.* Mol Immunol, 2013. **55**(1872-9142 (Electronic)): p. 197-199.
142. Cook, A.D., et al., *TNF and granulocyte macrophage-colony stimulating factor interdependence mediates inflammation via CCL17.* JCI Insight, 2018. **22**(2379-3708 (Electronic)).
143. Miyagawa, K., et al., *Frequent expression of receptors for granulocyte-macrophage colony-stimulating factor on human nonhematopoietic tumor cell lines.* J Cell Physiol, 1990. **143**(0021-9541 (Print)): p. 483-487.
144. Zhang, F., et al., *Transcriptional Regulation of Voltage-Gated Sodium Channels Contributes to GM-CSF-Induced Pain.* J Neurosci, 2019. **39**(1529-2401 (Electronic)): p. 5222-5233.

145. Nicol, L.S.C., et al., *Central inhibition of granulocyte-macrophage colony-stimulating factor is analgesic in experimental neuropathic pain.* Pain, 2018. **159**(1872-6623 (Electronic)): p. 550-559.
146. Deshmane, S.L., et al., *Monocyte chemoattractant protein-1 (MCP-1): an overview.* J Interferon Cytokine Res, 2009. **29**(1557-7465 (Electronic)): p. 313-326.
147. Wang, Y., et al., *Nuclear factor kappa B regulated monocyte chemoattractant protein-1/chemokine CC motif receptor-2 expressing in spinal cord contributes to the maintenance of cancer-induced bone pain in rats.* Mol Pain, 2018. **14**(1744-8069 (Electronic)).
148. He, Z., et al., *MAPK11 in breast cancer cells enhances osteoclastogenesis and bone resorption.* Biochimie, 2014. **106**(1638-6183 (Electronic)).
149. Jiang, Z.Y., et al., *Downregulation of miR-223 and miR-19a induces differentiation and promotes recruitment of osteoclast cells in giant-cell tumor of the bone via the Runx2/TWIST-RANK/RANKL pathway.* Biochem Biophys Res Commun, 2018. **505**(1090-2104 (Electronic)): p. 1003-1009.
150. Mulholland, B.S., M.R. Forwood, and N.A. Morrison, *Monocyte Chemoattractant Protein-1 (MCP-1/CCL2) Drives Activation of Bone Remodelling and Skeletal Metastasis.* Curr Osteoporos Rep, 2019. **17**(1544-2241 (Electronic)): p. 538-547.
151. Jung, H., et al., *Monocyte chemoattractant protein-1 functions as a neuromodulator in dorsal root ganglia neurons.* Journal of Neurochemistry, 2008. **104**(1): p. 254-263.
152. O'Grady, N.P., et al., *Detection of Macrophage Inflammatory Protein (MIP)-1α and MIP-β during Experimental Endotoxemia and Human Sepsis.* The Journal of Infectious Diseases, 1999. **179**(1): p. 136-141.
153. Teodorczyk-Injeyan, J.A., et al., *Elevated Production of Nociceptive CC Chemokines and sE-Selectin in Patients With Low Back Pain and the Effects of Spinal Manipulation: A Nonrandomized Clinical Trial.* Clin J Pain, 2018. **34**(1536-5409 (Electronic)): p. 68-75.
154. Zhang, J., et al., *TGF-β1 suppresses CCL3/4 expression through the ERK signaling pathway and inhibits intervertebral disc degeneration and inflammation-related pain in a rat model.* Exp Mol Med, 2017. **49**(2092-6413 (Electronic)).

155. Kim, H.R., et al., *Reciprocal activation of CD4+ T cells and synovial fibroblasts by stromal cell-derived factor 1 promotes RANKL expression and osteoclastogenesis in rheumatoid arthritis.* Arthritis Rheumatol, 2014. **66**(2326-5205 (Electronic)): p. 538-548.
156. Zannettino, A.C., et al., *Elevated serum levels of stromal-derived factor-1alpha are associated with increased osteoclast activity and osteolytic bone disease in multiple myeloma patients.* Cancer Res, 2005. **65**(0008-5472 (Print)): p. 1700-1709.
157. Li, T., et al., *Annexin 1 inhibits remifentanil-induced hyperalgesia and NMDA receptor phosphorylation via regulating spinal CXCL12/CXCR4 in rats.* Neurosci Res, 2019. **144**(1872-8111 (Electronic)): p. 48-55.
158. Ni, H., et al., *Crosstalk between NFκB-dependent astrocytic CXCL1 and neuron CXCR2 plays a role in descending pain facilitation.* J Neuroinflammation, 2019. **16**(1742-2094 (Electronic)).
159. Silva, R.L., et al., *CXCL1/CXCR2 signaling in pathological pain: Role in peripheral and central sensitization.* Neurobiol Dis, 2017. **105**(1095-953X (Electronic)): p. 109-116.
160. Wang, W., et al., *Serum C-C Motif Ligand 11/eotaxin-1 May Serve as a Candidate Biomarker for Postmenopausal Osteoporosis.* J Med Biochem, 2019. **38**(1452-8258 (Print)): p. 353-360.
161. Al-Mazidi, S., et al., *Association of Interleukin-6 and Other Cytokines with Self-Reported Pain in Prostate Cancer Patients Receiving Chemotherapy.* Pain Med, 2018. **19**(1526-4637 (Electronic)): p. 1058-1066.
162. Stucker, S., et al., *Bone Angiogenesis and Vascular Niche Remodeling in Stress, Aging, and Diseases.* Front Cell Dev Biol, 2020. **8**: p. 602269.
163. Wyatt, L.A., et al., *Molecular expression patterns in the synovium and their association with advanced symptomatic knee osteoarthritis.* Osteoarthritis Cartilage, 2019. **27**(1522-9653 (Electronic)): p. 667-675.
164. Takano, S., et al., *Vascular Endothelial Growth Factor Is Regulated by the Canonical and Noncanonical Transforming Growth Factor-β Pathway in Synovial Fibroblasts Derived from Osteoarthritis Patients.* Biomed Res Int, 2019(2314-6141 (Electronic)).
165. Xu, J., et al., *Efficacy of wIRA in the treatment of sacroiliitis in male patients with ankylosing spondylitis and its effect on serum VEGF levels.* J Orthop Surg Res, 2019. **14**(1749-799X (Electronic)).

166. Hu, X.M., et al., *Vascular Endothelial Growth Factor A Signaling Promotes Spinal Central Sensitization and Pain-related Behaviors in Female Rats with Bone Cancer.* Anesthesiology 2019. **131**(1528-1175 (Electronic)): p. 1125–1147.
167. Dixon, W.J., *The up-and-down Method for Small Samples.* Journal of the American Statistical Association, 1965. **60**(312): p. 967-978.
168. Chaplan, S.R., et al., *Quantitative assessment of tactile allodynia in the rat paw.* Journal of Neuroscience Methods, 1994. **53**(1): p. 55-63.
169. Randall Lo Fau - Selitto, J.J. and J.J. Selitto, *A method for measurement of analgesic activity on inflamed tissue.* Arch Int Pharmacodyn Ther, 1957. **111**(0003-9780 (Print)): p. 409-419.
170. Hargreaves, K., et al., *A new and sensitive method for measuring thermal nociception in cutaneous hyperalgesia.* PAIN, 1988. **32**(1).
171. Woolfe, G. and A.D. Macdonald, *THE EVALUATION OF THE ANALGESIC ACTION OF PETHIDINE HYDROCHLORIDE (DEMEROL).* Journal of Pharmacology and Experimental Therapeutics, 1944. **80**(3): p. 300.
172. Deuis, J.R. and I. Vetter, *The thermal probe test: A novel behavioral assay to quantify thermal paw withdrawal thresholds in mice.* Temperature, 2016. **3**(2): p. 199-207.
173. Yoon, C., et al., *Behavioral signs of ongoing pain and cold allodynia in a rat model of neuropathic pain.* PAIN, 1994. **59**(3).
174. King, T. and F. Porreca, *Preclinical Assessment of Pain: Improving Models in Discovery Research*, in *Behavioral Neurobiology of Chronic Pain*, B.K. Taylor and D.P. Finn, Editors. 2014, Springer Berlin Heidelberg: Berlin, Heidelberg. p. 101-120.
175. Deacon, R.M.J., *Burrowing in rodents: a sensitive method for detecting behavioral dysfunction.* Nature Protocols, 2006. **1**(1): p. 118-121.
176. Zhang, X.Y., et al., *Systematic review and meta-analysis of studies in which burrowing behaviour was assessed in rodent models of disease-associated persistent pain.* Pain, 2022.
177. Schött, E., et al., *Weight bearing as an objective measure of arthritic pain in the rat.* Journal of Pharmacological and Toxicological Methods, 1994. **31**(2): p. 79-83.

178. Lakes, E.H. and K.D. Allen, *Gait analysis methods for rodent models of arthritic disorders: reviews and recommendations.* Osteoarthritis and Cartilage, 2016. **24**(11): p. 1837-1849.
179. Griffioen, M.A., et al., *Evaluation of Dynamic Weight Bearing for Measuring Nonevoked Inflammatory Hyperalgesia in Mice.* Nursing Research, 2015. **64**(2).
180. King, T., et al., *Unmasking the tonic-aversive state in neuropathic pain.* Nature Neuroscience, 2009. **12**(11): p. 1364-1366.
181. Cobos, E.J., et al., *Inflammation-induced decrease in voluntary wheel running in mice: a nonreflexive test for evaluating inflammatory pain and analgesia.* Pain, 2012. **153**(4): p. 876-884.
182. Contreras, K.M., et al., *Deficit in voluntary wheel running in chronic inflammatory and neuropathic pain models in mice: Impact of sex and genotype.* Behav Brain Res, 2021. **399**: p. 113009.
183. Martha Beatriz Ramirez-Rosas, S.H.P., Matt Eber, Carol Kittel, Thomas Martin, Enriqueta Munoz-Islas, Juan Miguel Jimenez-Andrade, Yusuke Shiozawa, Renee Parker, Christopher Peters, *Pain related behaviors and disease related outcomes in an immunocompetent mouse model of prostate cancer induced bone pain.* The Journal of Pain, 2021. **22**(5): p. 584.
184. Meijer, J.H. and Y. Robbers, *Wheel running in the wild.* Proc Biol Sci, 2014. **281**(1786).
185. Sheahan, T.D., et al., *Inflammation and nerve injury minimally affect mouse voluntary behaviors proposed as indicators of pain.* Neurobiol Pain, 2017. **2**: p. 1-12.
186. Urban, R., et al., *Behavioral indices of ongoing pain are largely unchanged in male mice with tissue or nerve injury-induced mechanical hypersensitivity.* Pain, 2011. **152**(5): p. 990-1000.
187. Research, N.C.f.t.R.R.R.o.A.i. *The 3Rs*. 2017 17/12/2022]; Available from: https://nc3rs.org.uk/who-we-are/3rs.
188. Percie du Sert, N., et al., *The ARRIVE guidelines 2.0: Updated guidelines for reporting animal research.* PLOS Biology, 2020. **18**(7): p. e3000410.
189. Florenzano, P., et al., *Age-Related Changes and Effects of Bisphosphonates on Bone Turnover and Disease Progression in Fibrous Dysplasia of Bone.* J Bone Miner Res, 2019. **34**(4): p. 653-660.

190. Sakamoto, A., et al., *A comparative study of fibrous dysplasia and osteofibrous dysplasia with regard to Gsalpha mutation at the Arg201 codon: polymerase chain reaction-restriction fragment length polymorphism analysis of paraffin-embedded tissues.* J Mol Diagn, 2000. **2**(2): p. 67-72.
191. Majoor, B.C.J., et al., *Determinants of impaired quality of life in patients with fibrous dysplasia.* Orphanet J Rare Dis, 2017. **12**(1): p. 80.
192. Riddle, N.D. and M.M. Bui, *Fibrous Dysplasia.* Archives of Pathology & Laboratory Medicine, 2013. **137**(1): p. 134-138.
193. Chapurlat, R.D. and P. Orcel, *Fibrous dysplasia of bone and McCune-Albright syndrome.* Best Pract Res Clin Rheumatol, 2008. **22**(1): p. 55-69.
194. DiCaprio, M.R. and W.F. Enneking, *Fibrous Dysplasia: Pathophysiology, Evaluation, and Treatment.* JBJS, 2005. **87**(8): p. 1848-1864.
195. Riminucci, M., et al., *The histopathology of fibrous dysplasia of bone in patients with activating mutations of the Gs alpha gene: site-specific patterns and recurrent histological hallmarks.* J Pathol, 1999. **187**(2): p. 249-58.
196. Fitzpatrick, K.A., et al., *Imaging findings of fibrous dysplasia with histopathologic and intraoperative correlation.* AJR Am J Roentgenol, 2004. **182**(6): p. 1389-98.
197. Weinstein, R.S., *Long-term aminobisphosphonate treatment of fibrous dysplasia: spectacular increase in bone density.* J Bone Miner Res, 1997. **12**(8): p. 1314-5.
198. Bhattacharyya, N., et al., *Mechanism of FGF23 processing in fibrous dysplasia.* J Bone Miner Res, 2012. **27**(5): p. 1132-41.
199. Toyosawa, S., et al., *Ossifying fibroma vs fibrous dysplasia of the jaw: molecular and immunological characterization.* Mod Pathol, 2007. **20**(3): p. 389-96.
200. Corsi, A., et al., *Osteomalacic and hyperparathyroid changes in fibrous dysplasia of bone: core biopsy studies and clinical correlations.* J Bone Miner Res, 2003. **18**(7): p. 1235-46.
201. Guerin Lemaire, H., et al., *Serum periostin levels and severity of fibrous dysplasia of bone.* Bone, 2019. **121**: p. 68-71.
202. Regard, J.B., et al., *Wnt/beta-catenin signaling is differentially regulated by Galpha proteins and contributes to fibrous dysplasia.* Proc Natl Acad Sci U S A, 2011. **108**(50): p. 20101-6.

203. Page, M.J., et al., *The PRISMA 2020 statement: an updated guideline for reporting systematic reviews.* Rev Esp Cardiol (Engl Ed), 2021. **74**(9): p. 790-799.
204. Hooijmans, C.R., et al., *SYRCLE's risk of bias tool for animal studies.* BMC Med Res Methodol, 2014. **14**: p. 43.
205. Corsi, A., et al., *Zoledronic Acid in a Mouse Model of Human Fibrous Dysplasia: Ineffectiveness on Tissue Pathology, Formation of "Giant Osteoclasts" and Pathogenetic Implications.* Calcif Tissue Int, 2020. **107**(6): p. 603-610.
206. Zhu, F., et al., *Humanising the mouse genome piece by piece.* Nat Commun, 2019. **10**(1): p. 1845.
207. Schepers, K., et al., *Activated Gs signaling in osteoblastic cells alters the hematopoietic stem cell niche in mice.* Blood, 2012. **120**(17): p. 3425-35.
208. Akil, O., et al., *Disrupted bone remodeling leads to cochlear overgrowth and hearing loss in a mouse model of fibrous dysplasia.* PLoS One, 2014. **9**(5): p. e94989.
209. Hsiao, E.C., et al., *Gs G protein-coupled receptor signaling in osteoblasts elicits age-dependent effects on bone formation.* J Bone Miner Res, 2010. **25**(3): p. 584-93.
210. Hsiao, E.C., et al., *Ligand-mediated activation of an engineered gs g protein-coupled receptor in osteoblasts increases trabecular bone formation.* Mol Endocrinol, 2010. **24**(3): p. 621-31.
211. Kazakia, G.J., et al., *Mineral Composition is Altered by Osteoblast Expression of an Engineered G(s)-Coupled Receptor.* Calcified Tissue International, 2011. **89**(1): p. 10-20.
212. Hsiao, E.C., et al., *Osteoblast expression of an engineered Gs-coupled receptor dramatically increases bone mass.* Proc Natl Acad Sci U S A, 2008. **105**(4): p. 1209-14.
213. Liu, S., et al., *Haploinsufficiency for either one of the type-II regulatory subunits of protein kinase A improves the bone phenotype of Prkar1a(+/-) mice.* Human Molecular Genetics, 2015. **24**(21): p. 6080-6092.
214. Calvi, L.M., et al., *Activated parathyroid hormone/parathyroid hormone-related protein receptor in osteoblastic cells differentially affects cortical and trabecular bone.* J Clin Invest, 2001. **107**(3): p. 277-86.
215. Kuznetsov, S.A., et al., *The interplay of osteogenesis and hematopoiesis: expression of a constitutively active PTH/PTHrP receptor in osteogenic cells perturbs the establishment*

of hematopoiesis in bone and of skeletal stem cells in the bone marrow. J Cell Biol, 2004. **167**(6): p. 1113-22.

216. Yu, J., et al., *Bone marrow fibrosis with fibrocytic and immunoregulatory responses induced by beta-catenin activation in osteoprogenitors.* Bone, 2016. **84**: p. 38-46.
217. Regard, J.B., et al., *Wnt/beta-catenin signaling is differentially regulated by G alpha proteins and contributes to fibrous dysplasia.* Proceedings of the National Academy of Sciences of the United States of America, 2011. **108**(50): p. 20101-20106.
218. Ruther, U., et al., *Deregulated C-Fos Expression Interferes with Normal Bone-Development in Transgenic Mice.* Nature, 1987. **325**(6103): p. 412-416.
219. Kashimaa, T.G., et al., *Periostin, a novel marker of intramembranous ossification, is expressed in fibrous dysplasia and in c-Fos-overexpressing bone lesions.* Human Pathology, 2009. **40**(2): p. 226-237.
220. Kuznetsov, S.A., et al., *Age-dependent demise of GNAS-mutated skeletal stem cells and "normalization" of fibrous dysplasia of bone.* J Bone Miner Res, 2008. **23**(11): p. 1731-40.
221. Fan, Q.M., et al., *The CREB-Smad6-Runx2 axis contributes to the impaired osteogenesis potential of bone marrow stromal cells in fibrous dysplasia of bone.* J Pathol, 2012. **228**(1): p. 45-55.
222. Riminucci, M., et al., *Gnathodiaphyseal dysplasia: a syndrome of fibro-osseous lesions of jawbones, bone fragility, and long bone bowing.* J Bone Miner Res, 2001. **16**(9): p. 1710-8.
223. Xiao, T., et al., *HDAC8, A Potential Therapeutic Target, Regulates Proliferation and Differentiation of Bone Marrow Stromal Cells in Fibrous Dysplasia.* Stem Cells Transl Med, 2019. **8**(2): p. 148-161.
224. Piersanti, S., et al., *Transfer, analysis, and reversion of the fibrous dysplasia cellular phenotype in human skeletal progenitors.* J Bone Miner Res, 2010. **25**(5): p. 1103-16.
225. Majoor, B.C.J., et al., *Illness Perceptions are Associated with Quality of Life in Patients with Fibrous Dysplasia.* Calcif Tissue Int, 2018. **102**(1): p. 23-31.
226. Falk, S., S. Gallego-Pedersen, and N.C. Petersen, *Grid-climbing Behaviour as a Pain Measure for Cancer-induced Bone Pain and Neuropathic Pain.* In Vivo, 2017. **31**(4): p. 619-623.

227. Deacon, R.M., *Measuring the strength of mice.* J Vis Exp, 2013(76).
228. Sliepen, S.H.J., et al., *Cancer-induced Bone Pain Impairs Burrowing Behaviour in Mouse and Rat.* In Vivo, 2019. **33**(4): p. 1125-1132.
229. Iannello, F., *Non-intrusive high throughput automated data collection from the home cage.* Heliyon, 2019. **5**(4): p. e01454.
230. Gage, G.J., D.R. Kipke, and W. Shain, *Whole animal perfusion fixation for rodents.* J Vis Exp, 2012(65).
231. Matsuura, Y., et al., *Expression of activating transcription factor 3 (ATF3) in uninjured dorsal root ganglion neurons in a lower trunk avulsion pain model in rats.* Eur Spine J, 2013. **22**(8): p. 1794-9.
232. Maridas, D.E., et al., *Isolation, Culture, and Differentiation of Bone Marrow Stromal Cells and Osteoclast Progenitors from Mice.* J Vis Exp, 2018(131).
233. Caraceni, A., R.K. Portenoy, and I.T.F.o.C.P. a working group of the, *An international survey of cancer pain characteristics and syndromes. IASP Task Force on Cancer Pain. International Association for the Study of Pain.* Pain, 1999. **82**(3): p. 263-274.
234. Meuser, T., et al., *Symptoms during cancer pain treatment following WHO-guidelines: a longitudinal follow-up study of symptom prevalence, severity and etiology.* Pain, 2001. **93**(3): p. 247-257.
235. Currie, G.L., et al., *Animal models of bone cancer pain: systematic review and meta-analyses.* Pain, 2013. **154**(6): p. 917-26.
236. Sadler, K.E., J.S. Mogil, and C.L. Stucky, *Innovations and advances in modelling and measuring pain in animals.* Nat Rev Neurosci, 2022. **23**(2): p. 70-85.
237. Fuochi, S., et al., *Phenotyping spontaneous locomotor activity in inbred and outbred mouse strains by using Digital Ventilated Cages.* Lab Anim (NY), 2021. **50**(8): p. 215-223.
238. Falk, S., et al., *Influence of sex differences on the progression of cancer-induced bone pain.* Anticancer Res, 2013. **33**(5): p. 1963-9.
239. Majuta, L.A., et al., *Mice with cancer-induced bone pain show a marked decline in day/night activity.* Pain Rep, 2017. **2**(5): p. e614.

240. Majuta, L.A., et al., *Anti-nerve growth factor does not change physical activity in normal young or aging mice but does increase activity in mice with skeletal pain.* Pain, 2018. **159**(11): p. 2285-2295.
241. Sluka, K.A., et al., *Acid-sensing ion channel 3 deficiency increases inflammation but decreases pain behavior in murine arthritis.* Arthritis Rheum, 2013. **65**(5): p. 1194-202.
242. Schneider, G., R. Voltz, and J. Gaertner, *Cancer Pain Management and Bone Metastases: An Update for the Clinician.* Breast Care (Basel), 2012. **7**(2): p. 113-120.
243. Luger, N.M., et al., *Efficacy of systemic morphine suggests a fundamental difference in the mechanisms that generate bone cancer vs. inflammatory pain.* PAIN, 2002. **99**(3).
244. Gabel, F., et al., *Unveiling the Impact of Morphine on Tamoxifen Metabolism in Mice in vivo.* Frontiers in Oncology, 2020. **10**.
245. Gabel, F., et al., *Central metabolism as a potential origin of sex differences in morphine antinociception but not induction of antinociceptive tolerance in mice.* British Journal of Pharmacology, 2022. **n/a**(n/a).
246. Saenz, M., et al., *Pharmacokinetics of Sustained-release and Extended-release Buprenorphine in Mice after Surgical Catheterization.* Journal of the American Association for Laboratory Animal Science, 2022. **61**(5): p. 468-474.
247. Carbone, E.T., et al., *Duration of Action of Sustained-Release Buprenorphine in 2 Strains of Mice.* Journal of the American Association for Laboratory Animal Science, 2012. **51**(6): p. 815-819.
248. Nishiyama, M., Y. Iwasaki, and S. Makino, *Animal Models of Cushing's Syndrome.* Endocrinology, 2022. **163**(12): p. bqac173.
249. FD/MAS Alliance, I.C.f.F.M. *International FD/MAS Patient Groups Release Top Priorities for FD/MAS research*. 2022 [cited 2022 22/12/2022]; Available from: https://fdmasalliance.org/patient-priorities-for-research-2022/.
250. Li, J., et al., *Risk of Adverse Events After Anti-TNF Treatment for Inflammatory Rheumatological Disease. A Meta-Analysis.* Frontiers in Pharmacology, 2021. **12**.
251. Lane, N.E., et al., *Tanezumab for the treatment of pain from osteoarthritis of the knee.* N Engl J Med, 2010. **363**(16): p. 1521-31.
252. Katz, N., et al., *Efficacy and safety of tanezumab in the treatment of chronic low back pain.* PAIN, 2011. **152**(10).

253. Hochberg, M.C., *Serious joint-related adverse events in randomized controlled trials of anti-nerve growth factor monoclonal antibodies.* Osteoarthritis and Cartilage, 2015. **23**: p. S18-S21.
254. Hochberg, M.C., et al., *When Is Osteonecrosis Not Osteonecrosis?: Adjudication of Reported Serious Adverse Joint Events in the Tanezumab Clinical Development Program.* Arthritis & Rheumatology, 2016. **68**(2): p. 382-391.
255. AstraZeneca. *A Study of the Efficacy and Safety of MEDI7352 in Subjects With Painful Osteoarthritis of the Knee (BESPOKE)*. 2020 [cited 2022 22/12/2022]; Available from: https://clinicaltrials.gov/ct2/show/NCT04675034.

Appendices

Appendix 1:
Figure Reuse Permission

SPRINGER NATURE LICENSE
TERMS AND CONDITIONS

Dec 16, 2022

This Agreement between University of Copenhagen -- Chelsea Hopkins ("You") and Springer Nature ("Springer Nature") consists of your license details and the terms and conditions provided by Springer Nature and Copyright Clearance Center.

License Number	5450740377355
License date	Dec 16, 2022
Licensed Content Publisher	Springer Nature
Licensed Content Publication	Calcified Tissue International
Licensed Content Title	Fibrous Dysplasia of Bone and McCune–Albright Syndrome: A Bench to Bedside Review
Licensed Content Author	Iris Hartley et al
Licensed Content Date	Apr 29, 2019
Type of Use	Thesis/Dissertation
Requestor type	academic/university or research institute
Format	print and electronic
Portion	figures/tables/illustrations
Number of figures/tables/illustrations	2
Will you be translating?	no
Circulation/distribution	30 - 99

Author of this Springer Nature content	no
Title	Ms
Institution name	University of Copenhagen
Expected presentation date	Dec 2022
Portions	Figure 4A and whole of Figure 5.
Requestor Location	University of Copenhagen Jagtvej 160, Building 22, C421 København Ø, 2100 Denmark Attn: University of Copenhagen
Total	0.00 EUR

Terms and Conditions

Springer Nature Customer Service Centre GmbH Terms and Conditions

The following terms and conditions ("Terms and Conditions") together with the terms specified in your [RightsLink] constitute the License ("License") between you as Licensee and Springer Nature Customer Service Centre GmbH as Licensor. By clicking 'accept' and completing the transaction for your use of the material ("Licensed Material"), you confirm your acceptance of and obligation to be bound by these Terms and Conditions.

1. Grant and Scope of License

1. 1. The Licensor grants you a personal, non-exclusive, non-transferable, non-sublicensable, revocable, world-wide License to reproduce, distribute, communicate to the public, make available, broadcast, electronically transmit or create derivative works using the Licensed Material for the purpose(s) specified in your RightsLink Licence Details only. Licenses are granted for the specific use requested in the order and for no other use, subject to these Terms and Conditions. You acknowledge and agree that the rights granted to you under this License do not include the right to modify, edit, translate, include in collective works, or create derivative works of the Licensed Material in whole or in part unless expressly stated in your RightsLink Licence Details. You may use the Licensed Material only as permitted under this Agreement and will not reproduce, distribute, display, perform, or otherwise use or exploit any Licensed Material in any way, in whole or in part, except as expressly permitted by this License.

1. 2. You may only use the Licensed Content in the manner and to the extent permitted by these Terms and Conditions, by your RightsLink Licence Details and by any

applicable laws.

1. 3. A separate license may be required for any additional use of the Licensed Material, e.g. where a license has been purchased for print use only, separate permission must be obtained for electronic re-use. Similarly, a License is only valid in the language selected and does not apply for editions in other languages unless additional translation rights have been granted separately in the License.

1. 4. Any content within the Licensed Material that is owned by third parties is expressly excluded from the License.

1. 5. Rights for additional reuses such as custom editions, computer/mobile applications, film or TV reuses and/or any other derivative rights requests require additional permission and may be subject to an additional fee. Please apply to journalpermissions@springernature.com or bookpermissions@springernature.com for these rights.

2. Reservation of Rights

Licensor reserves all rights not expressly granted to you under this License. You acknowledge and agree that nothing in this License limits or restricts Licensor's rights in or use of the Licensed Material in any way. Neither this License, nor any act, omission, or statement by Licensor or you, conveys any ownership right to you in any Licensed Material, or to any element or portion thereof. As between Licensor and you, Licensor owns and retains all right, title, and interest in and to the Licensed Material subject to the license granted in Section 1.1. Your permission to use the Licensed Material is expressly conditioned on you not impairing Licensor's or the applicable copyright owner's rights in the Licensed Material in any way.

3. Restrictions on use

3. 1. Minor editing privileges are allowed for adaptations for stylistic purposes or formatting purposes provided such alterations do not alter the original meaning or intention of the Licensed Material and the new figure(s) are still accurate and representative of the Licensed Material. Any other changes including but not limited to, cropping, adapting, and/or omitting material that affect the meaning, intention or moral rights of the author(s) are strictly prohibited.

3. 2. You must not use any Licensed Material as part of any design or trademark.

3. 3. Licensed Material may be used in Open Access Publications (OAP), but any such reuse must include a clear acknowledgment of this permission visible at the same time as the figures/tables/illustration or abstract and which must indicate that the Licensed Material is not part of the governing OA license but has been reproduced with permission. This may be indicated according to any standard referencing system but must include at a minimum 'Book/Journal title, Author, Journal Name (if applicable), Volume (if applicable), Publisher, Year, reproduced with permission from SNCSC'.

4. STM Permission Guidelines

4. 1. An alternative scope of license may apply to signatories of the STM Permissions Guidelines ("STM PG") as amended from time to time and made available at https://www.stm-assoc.org/intellectual-property/permissions/permissions-guidelines/.

4. 2. For content reuse requests that qualify for permission under the STM PG, and which may be updated from time to time, the STM PG supersede the terms and conditions contained in this License.

4. 3. If a License has been granted under the STM PG, but the STM PG no longer apply at the time of publication, further permission must be sought from the Rightsholder. Contact journalpermissions@springernature.com or bookpermissions@springernature.com for these rights.

5. Duration of License

5. 1. Unless otherwise indicated on your License, a License is valid from the date of purchase ("License Date") until the end of the relevant period in the below table:

Reuse in a medical communications project	Reuse up to distribution or time period indicated in License
Reuse in a dissertation/thesis	Lifetime of thesis
Reuse in a journal/magazine	Lifetime of journal/magazine
Reuse in a book/textbook	Lifetime of edition
Reuse on a website	1 year unless otherwise specified in the License
Reuse in a presentation/slide kit/poster	Lifetime of presentation/slide kit/poster. Note: publication whether electronic or in print of presentation/slide kit/poster may require further permission.
Reuse in conference proceedings	Lifetime of conference proceedings
Reuse in an annual report	Lifetime of annual report
Reuse in training/CME materials	Reuse up to distribution or time period indicated in License
Reuse in newsmedia	Lifetime of newsmedia
Reuse in coursepack/classroom materials	Reuse up to distribution and/or time period indicated in license

6. Acknowledgement

6. 1. The Licensor's permission must be acknowledged next to the Licensed Material in print. In electronic form, this acknowledgement must be visible at the same time as the figures/tables/illustrations or abstract and must be hyperlinked to the journal/book's homepage.

6. 2. Acknowledgement may be provided according to any standard referencing system and at a minimum should include "Author, Article/Book Title, Journal name/Book imprint, volume, page number, year, Springer Nature".

7. Reuse in a dissertation or thesis

7. 1. Where 'reuse in a dissertation/thesis' has been selected, the following terms apply: Print rights of the Version of Record are provided for; electronic rights for use only on institutional repository as defined by the Sherpa guideline (www.sherpa.ac.uk/romeo/) and only up to what is required by the awarding institution.

7. 2. For theses published under an ISBN or ISSN, separate permission is required. Please contact journalpermissions@springernature.com or bookpermissions@springernature.com for these rights.

7. 3. Authors must properly cite the published manuscript in their thesis according to current citation standards and include the following acknowledgement: '*Reproduced with permission from Springer Nature*'.

8. License Fee

You must pay the fee set forth in the License Agreement (the "License Fees"). All amounts payable by you under this License are exclusive of any sales, use, withholding, value added or similar taxes, government fees or levies or other assessments. Collection and/or remittance of such taxes to the relevant tax authority shall be the responsibility of the party who has the legal obligation to do so.

9. Warranty

9. 1. The Licensor warrants that it has, to the best of its knowledge, the rights to license reuse of the Licensed Material. **You are solely responsible for ensuring that the material you wish to license is original to the Licensor and does not carry the copyright of another entity or third party (as credited in the published version).** If the credit line on any part of the Licensed Material indicates that it was reprinted or adapted with permission from another source, then you should seek additional permission from that source to reuse the material.

9. 2. EXCEPT FOR THE EXPRESS WARRANTY STATED HEREIN AND TO THE EXTENT PERMITTED BY APPLICABLE LAW, LICENSOR PROVIDES THE LICENSED MATERIAL "AS IS" AND MAKES NO OTHER REPRESENTATION OR WARRANTY. LICENSOR EXPRESSLY DISCLAIMS ANY LIABILITY FOR ANY CLAIM ARISING FROM OR OUT OF THE CONTENT, INCLUDING BUT NOT LIMITED TO ANY ERRORS, INACCURACIES, OMISSIONS, OR DEFECTS CONTAINED THEREIN, AND ANY IMPLIED OR EXPRESS WARRANTY AS TO MERCHANTABILITY OR FITNESS FOR A PARTICULAR PURPOSE. IN NO EVENT SHALL LICENSOR BE LIABLE TO YOU OR ANY OTHER PARTY OR ANY OTHER PERSON OR FOR ANY SPECIAL, CONSEQUENTIAL, INCIDENTAL, INDIRECT, PUNITIVE, OR EXEMPLARY DAMAGES, HOWEVER CAUSED, ARISING OUT OF OR IN CONNECTION WITH THE DOWNLOADING, VIEWING OR USE OF THE LICENSED MATERIAL REGARDLESS OF THE FORM OF ACTION, WHETHER FOR BREACH OF CONTRACT, BREACH OF WARRANTY, TORT, NEGLIGENCE, INFRINGEMENT OR OTHERWISE (INCLUDING, WITHOUT LIMITATION, DAMAGES BASED ON LOSS OF PROFITS, DATA, FILES, USE, BUSINESS OPPORTUNITY OR CLAIMS OF THIRD PARTIES), AND WHETHER OR NOT THE PARTY HAS BEEN ADVISED OF THE POSSIBILITY OF SUCH DAMAGES. THIS LIMITATION APPLIES NOTWITHSTANDING ANY FAILURE OF ESSENTIAL PURPOSE OF ANY LIMITED REMEDY PROVIDED HEREIN.

10. Termination and Cancellation

10. 1. The License and all rights granted hereunder will continue until the end of the applicable period shown in Clause 5.1 above. Thereafter, this license will be terminated and all rights granted hereunder will cease.

10. 2. Licensor reserves the right to terminate the License in the event that payment is not received in full or if you breach the terms of this License.

11. General

11. 1. The License and the rights and obligations of the parties hereto shall be construed, interpreted and determined in accordance with the laws of the Federal Republic of Germany without reference to the stipulations of the CISG (United

Nations Convention on Contracts for the International Sale of Goods) or to Germany´s choice-of-law principle.

11. 2. The parties acknowledge and agree that any controversies and disputes arising out of this License shall be decided exclusively by the courts of or having jurisdiction for Heidelberg, Germany, as far as legally permissible.

11. 3. This License is solely for Licensor's and Licensee's benefit. It is not for the benefit of any other person or entity.

Questions? For questions on Copyright Clearance Center accounts or website issues please contact springernaturesupport@copyright.com or +1-855-239-3415 (toll free in the US) or +1-978-646-2777. For questions on Springer Nature licensing please visit https://www.springernature.com/gp/partners/rights-permissions-third-party-distribution

Other Conditions:

Version 1.4 - Dec 2022

Questions? customercare@copyright.com or +1-855-239-3415 (toll free in the US) or +1-978-646-2777.

Appendix 2:
Severity Score Sheets

Severity monitoring for experiment: Mice inoculated with FD cells and induced with doxycycline to develop localised fibrous dysplasia

Animal no.			
Date			
Appearance			
Body weight			
Coat condition			
Facial expression			
Body function			
Dyspnoea and/or tachypnoea			
Environment			
Loose stools or diarrhoea			
Blood in diarrhoea			
Behaviours			
Handling Aggression			
Locomotion/posture			
Stereotypical behaviours**			
Total Score			
Any other observations			

ACTIONS	
Score 1 (mild)	Review frequency of monitoring
Score 2 (moderate)	Consider supplementary care, e.g. extra fluid increase monitoring
Score 4	-Consult veterinarian (Henrik Bo Hansen 21474905)
Score 6 (severe)	Implement humane end point (HEP)

*Body weight compared to transgenic background strain without doxycycline

**stereotypical behaviour can be anything from licking the fur to repeated movements and score from mild to HEP

Clinical scores Appearance	Score
Bodyweight*	
5-10 % weight loss	1
11-15 % weight loss	2
16-20 % Weight loss	3
20+% weight loss	HEP
Coat condition	
Coat slightly unkempt/slight piloerection	1
Marked piloerection	3
Facial expression	
Eyes narrow, ears back in combination with at least one other factor	3
Body function	
Tachypnoea (fast breathing)	1
Dyspnoea (difficult breathing)	3
Environment	
Loose stools or diarrhoea	1
Blood in diarrhoea	HEP
Behaviour	
Tense and nervous on handling	1
Markedly distressed on handling, e.g. shaking, vocalizing, aggressive	3
Locomotion	
Slightly abnormal gait/posture	1
markedly abnormal gait/posture	2
Significant mobility problems	3
Immobility	HEP

Severity monitoring for experiment: cancer-induced bone pain in mice/rats

Animal no.

Date			

Appearance

Body weight			
Porfyrin (rats only)			
coat condition			

Body function

Dyspnoea and/or tachypnoea			

Environment

Loose stools or diarrhoea			
Blood in diarrhoea			

Behaviours

Handling Aggression			
Abnormal posture			
Stereotypical behaviours			
Reluctance to move			

Procedure-specific indicators

Procedure-specific limb use			

Total Score			
Any other observations			

ACTIONS	
Score 1 (mild)	Review frequency of monitoring
Score 2 (moderate)	Consider supplementary care, e.g. extra fluid increase monitoring
Score 4 (moderate/severe)	-Consult veterinarian (Henrik Bo Hansen 21474905) -Also reconsider experimental setup
Score 6 (severe)	Implement humane end point (HEP)

Procedure-specific limb use: Score for the affected limb 0=Normal use of the leg. 1 = Mild or insignificant limping. 2=-significant limp 3=Severe limp and partial lack of use. 6= lack of use of the affected limb (HEP)

Examples of clinical scores

Appearance	Score
Bodyweight	
5-10 % weight loss	1
11-15 % weight loss	2
16-20 % Weight loss	3
20+% weight loss	HEP
Porfyrin (rats only)	
Visible around the eyes	1
Clearly visible around eyes and in the fur	2
Coat condition	
Coat slightly unkempt/slight piloerection	1
Marked piloerection	3
Body function	
Tachypnoea (fast breathing)	1
Dyspnoea (difficult breathing)	3
Environment	
Loose stools or diarrhoea	1
Blood in diarrhoea	HEP
Behaviour	
Tense and nervous on handling	1
Markedly distressed on handling, e.g. shaking, vocalizing, aggressive	3
Locomotion	
Slightly abnormal gait/posture	1
markedly abnormal gait/posture	2
Significant mobility problems	3
Immobility >24h	HEP